

From Golgi body movement to cellulose microfibril alignment

Miriam Akkerman

Thesis committee

Thesis supervisor

Prof. dr. A.M.C. Emons
Professor of Plant Cell Biology
Wageningen University

Thesis co-supervisor

Dr. ir. M.J. Ketelaar
Assistant professor, Laboratory of Cell Biology
Wageningen University

Other members

Prof. dr. J.T.M. Elzenga, University of Groningen
Prof. dr. G.C. Angenent, Wageningen University
Dr. L.M. Trindade, Wageningen University
Dr. H.J.G.M. Franssen, Wageningen University

This research was conducted under the auspices of the Graduate School of
Experimental Plant Sciences

From Golgi body movement to cellulose microfibril alignment

Miriam Akkerman

Thesis

submitted in fulfilment of the requirements for the degree of doctor
at Wageningen University
by the authority of the Rector Magnificus
Prof. dr. M.J. Kropff,
in the presence of the
Thesis Committee appointed by the Academic Board
to be defended in public
on Monday 17 September 2012
at 11 a.m. in the Aula.

Miriam Akkerman
From Golgi body movement to cellulose microfibril alignment
122 pages

Thesis Wageningen University, Wageningen, The Netherlands (2012)
With references, with summaries in English and Dutch

ISBN: 978-94-6173-303-0

Contents

Chapter 1	Introduction and outline	7
Chapter 2	Golgi body motility in the plant cell cortex correlates with actin cytoskeleton organization	23
Chapter 3	Cellulose synthase complex, cortical microtubule, and cellulose microfibril alignment in <i>Arabidopsis</i> root epidermal cells	49
Chapter 4	Texture of cellulose microfibrils of root hair cell walls of <i>Arabidopsis thaliana</i> , <i>Medicago</i> <i>truncatula</i> and <i>Vicia sativa</i>	73
Chapter 5	General discussion: Aspects of the mechanism behind the highly ordered textures of cellulose microfibrils in plant cell walls	93
Summaries and Acknowledgements		109
	Summary	110
	Samenvatting	113
	Dankwoord/acknowledgements	116
About the author		117
	<i>Curriculum vitae</i>	118
	List of publications	119
	Education Statement	120

Chapter 1

Introduction and outline

Miriam Akkerman, Tijs Ketelaar, Anne Mie C. Emons

*Laboratory of Plant Cell Biology, Wageningen University, Droevendaalsesteeg 1,
6708 PB Wageningen, The Netherlands*

The role of an organized cell wall texture

Plant cells owe their shape and strength to a combination of turgor pressure and constraining cell wall (Carpita and Gibeaut 1993, Liepman et al. 2010). During growth, driven by turgor pressure, the cell wall expands in determined directions (Cosgrove 2005). The main load bearing structures in the wall are the cellulose microfibrils (CMFs), the most abundant biopolymer on earth. CMFs are cable like structures with high tensile strength. They are embedded in a matrix of complex proteins and polysaccharides. Cell wall proteins are involved in modifications of cell wall components, wall structure, signalling, and interactions with plasma membrane proteins at the cell surface (Jamet et al. 2006). Cell wall polysaccharides can be classified in hemicelluloses and pectins (Cosgrove 2005). The hemicelluloses cover and connect the CMFs to form a strong and extensible network. The pectins form hydrated gels that keep CMFs apart during cell growth and hold them in place when growth ceases (Cosgrove 2005). By this constitution the cell wall is able to provide resistance against the osmotic pressure, which is comparable to the air pressure in a car tire (Somerville 2006). This turgor mechanism provides stiffness and allows plants to stay upright.

CMFs are deposited in highly organized cell wall textures (Emons et al. 1992). CMFs deposited during cell elongation around axially (also called diffuse or intercalary) growing cells of *Arabidopsis* roots and inner cells of hypocotyls have a transverse orientation, i.e. perpendicular to the growth axis of the cell. It is generally thought that the orientation of the CMFs determines the cell elongation direction, which is perpendicular to the orientation of the CMFs (Baskin 2005). In CMF layers deposited after cell growth in those cells the CMF orientation shifts towards helical / longitudinal.

The key role of an organized texture of CMFs in controlling shape has been inferred from cellulose deficient mutants (Arioli et al. 1998, Williamson et al. 2001, Fagard et al. 2000), antisense constructs for cellulose synthases (CESA's) (Burn et al. 2002) and cellulose synthesis disturbing agents like isoxaben (Scheible et al. 2001, Desprez et al. 2002) and thiazolidinone (Scheible et al. 2001). The most pronounced effect during disturbance of

cellulose synthesis is that elongating root and shoot cells grow more isotropic, they swell, while severe reduction of cellulose production is lethal (Gillmor et al. 2002).

Cellulose synthase complexes, their transport to the plasma membrane

CMFs are produced by cellulose synthase complexes that move through the plasma membrane. By electron microscopy of freeze-fractured plasma membranes the complex is seen as a 'rosette' with six lobes and a diameter of 25-30 nm in the plasmatic fracture face of the plasma membrane (Mueller and Brown 1980, Emons 1985, Kimura et al. 1999). Cellulose synthase complexes are transported through the cytoplasm towards the plasma membrane in Golgi bodies. Haigler and Brown (1986) visualized a rosette in a Golgi body with freeze-fracture electron microscopy. Furthermore in plants expressing XFP-CESA3 or XFP-CESA6, Golgi bodies have been shown to contain these fusion proteins, which are part of functional CESA complexes (Paredes 2006, Desprez et al. 2007, Crowell et al. 2009, Gutierrez et al., 2009, Chan et al., 2010). The CESA complexes are assembled in the ER (Rudolph 1987) and are thought to be transported to Golgi bodies from mobile ER export sites to Golgi bodies that move in close vicinity (DaSilva et al. 2004). Golgi bodies's main tasks are 1) the glycosylation of proteins, 2) the synthesis of large quantities of complex cell wall matrix polysaccharides, the hemicelluloses and pectins and 3) sorting. These tasks are reflected in the architecture of a Golgi body, a polarized stack of several flat compartments called cisternae, containing many compartmentalized glycosyltransferases. Golgi bodies are covered with myosin motor-molecules by which they travel over the actin cytoskeleton (Nebenführ 1999, Sparkes 2008, Avisar 2008).

The actin cytoskeleton is highly dynamic (Hussey 2006, Van der Honing et al. 2011). A pool of monomeric globular actin (G-actin) and filamentous actin (F-actin) is simultaneously present in the cytoplasm. G-actin can polymerize into F-actin, which in turn can depolymerize into G-actin. The formation and dynamics of the F-actin cytoskeleton are mediated by a variety of actin

binding proteins (Hussey et al., 2006). F-actin can occur in different configurations with different degrees of bundling: from single actin filaments and a fine filamentous form (fine F-actin) which consists of thin bundles of actin filaments and probably also single actin filaments (Miller et al. 1999, De Ruijter et al. 1999, Ketelaar et al. 2003, Collings et al. 2006, Akkerman et al. 2011) up to thick bundles of actin filaments. The balance between the different forms is regulated by actin binding proteins and depends on the type and developmental stage of a cell. The actin network serves in cooperation with myosins as an organelle transport system. Golgi bodies, mitochondria and peroxisomes have been shown to move over the actin cytoskeleton with myosin XI (Avisar et al. 2008, Sparkes et al. 2008).

Golgi bodies transport and deliver cargo throughout the cell. In most plant cells their main cargo is destined for cell wall deposition and packed into exocytosis vesicles that are delivered at exocytosis sites where cell growth takes place. The exocytosis vesicles contain cell wall matrix proteins and glycosides in their lumen and membrane proteins under which CESA complexes in their membranes. By means of tethering factors, in some cell types the exocyst complex (Hala et al. 2008), the vesicles are precisely positioned near an exocytosis site. The specificity of vesicle targeting is determined by tethering factors together with Rab GTPases (Hala et al. 2008). After tethering the v-SNARE (soluble N-ethylmaleimide-sensitive attachment protein receptor on the vesicle) pairs with a specific t-SNARE (on the target membrane) on the plasma membrane to mediate fusion (Uemura et al. 2004). By fusion with the plasma membrane the vesicle contents are secreted into the cell wall and the vesicle membrane, including the CESA complexes, fuses with the plasma membrane. In this way CESA complexes are inserted into the plasma membrane. Insertion sites have indeed been correlated with the presence of Golgi bodies in elongating hypocotyl cells (Gutierrez et al. 2009, Crowell et al. 2009). After insertion the complex starts to produce glucan chains that are spun out in the extracellular space and crystallize into a CMF (Somerville 2006).

Composition of cellulose synthase complexes

To date two components of the CESA complex are known; the catalytic subunit cellulose synthase (CESA) and the cellulose synthase-interactive protein 1 (CSI1) (Gu et al. 2010).

CESAs in *Arabidopsis* are represented by ten isoforms (Holland et al. 2000, Richmond 2000). The proteins consist of 985-1088 amino acids and have eight putative transmembrane domains. Two of these domains are near the amino terminus and the other six are clustered near the carboxy terminus. Between the two transmembrane regions lies a large central domain, which is thought to be cytoplasmic (Delmer 1999). This domain contains the catalytic center with the D,D,D,QxxRW motif, in which the D,D,D part is thought to bind UDP-glucose (Holland et al. 2000). The N-terminus contains two zinc finger domains thought to be involved in protein-protein interactions (Holland 2000, for review see Somerville 2006). The CESA complex in elongating cells, cells producing primary cell wall, is generally thought to consist of approximately 36 CESA subunits of 3 different kinds, CESA1, CESA3 and a member of the CESA6 family, CESA6, CESA2, CESA5 or CESA9, dependent on the developmental stage of the cell and the tissue type (Persson et al. 2007, Desprez et al. 2007). Secondary cell walls are produced by CESA complexes consisting of three different subunits: CESA4, CESA7 and CESA8 (Turner and Somerville 1997, Taylor et al 1999). The CESA subunits use UDP-glucose as a substrate and spin out polymer chains containing 500-14000 β -1,4-linked glucose molecules (Somerville 2006). Meanwhile the complex is thought to be pushed forward by the polymerization forces (for modeling see Diotallevi et al. 2007). In the extracellular space the probably 18-24 glucan chains (Kennedy et al. 2007, Fernandes et al. 2011) bind together via hydrogen bonds and Van der Waals forces to a partly crystalline CMF (Nishiyama et al. 2002, 2003).

The second component, CSI1, was only recently identified in a two-hybrid screen for proteins that interact with CESA1, CESA3 and CESA6 (Gu et al. 2010). Mutations in *CSI1* affect the distribution and movement of CESA complexes and cause defects in cell elongation. Li et al. (2011) and Bringmann

et al. (2012) conclude that CSI1 links a CESA complex to a CMT and is essential for the guidance of CESA complexes along CMTs during cellulose synthesis. Next to the CESA subunits and CSI1 a number of additional proteins are thought to be involved in CMF deposition (KORRIGAN, a putative membrane-bound endo-1,4- β -glucanase (Nicol et al. 1998, Lane et al. 2001, Sato et al. 2001, Paredez et al. 2008), COBRA, an extracellular Glycosyl-Phosphatidyl Inositol-Anchored Protein (Schindelman et al. 2001, Roudier et al. 2005), KOBITO, a plasma membrane protein (Pagant et al. 2002) and two chitinase-like (CTL) proteins (Sanchez-Rodriguez 2010).

Unraveling the mechanism by which cellulose synthase complexes are spatially organized

For more than 50 years scientists have tried to elucidate how the organized CMF textures are being generated and at the moment of writing this thesis it is still an intriguing subject of research and debate. Already in 1963 Ledbetter and Porter observed that the orientation of undefined structures that could be CMFs in cell walls of expanding cells is similar to that of cortical microtubules (CMTs), microtubules in the cytoplasm just underneath and linked to the plasma membrane. This led to the idea that CMFs are oriented by CMTs (Ledbetter and Porter 1963, Green 1962, Green 1963, Heath 1974). Microtubules, like actin filaments, are highly dynamic structures. They are formed by dimers that consist of α - and β -tubulin. They shrink by catastrophes, rapid depolymerisation events. The stability of microtubules is regulated by a large variety of microtubule associated proteins (MAPs). From the use of inhibitory agents it was concluded that next to CMFs also CMTs are important for controlling growth anisotropy and cell shape. Many observations of correlations between CMT and CMF orientation followed (reviewed by Baskin 2001). However, also inconsistencies between CMT organization and CMF organization were described (reviewed by Wasteneys 2004) and the question remained whether CMTs guide and orient CESA complexes during the deposition of CMFs.

In 2006 Paredez et al. caused a breakthrough in the CMT-CMF debate by live imaging of CESA complexes tagged with an YFP-CESA6 fusion protein in combination with CFP-TUA1 labeled CMTs in *Arabidopsis* hypocotyls. They showed that CESA complexes move bidirectionally along CMTs. In the following years the tools developed by Paredez et al. were used in a large number of additional publications (Debolt et al. 2007, Persson et al. 2007, Desprez et al. 2007, Crowell et al. 2009, 2011, Gutierrez et al. 2009, Chan et al., 2010, 2011, Gu et al. 2010, Fujita et al. 2011, Li et al. 2011, Bringmann et al. 2012). However, CMTs are not required for CMF production, not even for production of an ordered wall texture (Paredez et al. 2006, Emons et al. 2007). A geometrical model shows that, in principle, all CMF textures can be produced by modulating the density of active CESA complexes inside the plasma membrane (Emons and Mulder 1998, 2000, Mulder and Emons 2001, Mulder et al. 2004, Emons et al. 2007). Furthermore the mechanism by which CMTs guide CESA complexes is still unknown at this moment and many questions related to the CMF organization still are unanswered.

To analyze the positioning and patterning of CESA complexes we studied the following three aspects in this research: (1) the distribution and delivery (close) to the plasma membrane of CESA complexes via Golgi bodies on the actin cytoskeleton, (2) the distribution and movement of CESA complexes inside the plasma membrane while producing CMFs and finally (3) their product, the CMF texture of the cell wall. We choose epidermal root cells of *Arabidopsis thaliana* and compared cells of different growth stages. Epidermal root cells expand over their whole length mainly in axial direction, called axial, intercalary or diffuse growth. We chose the root epidermis because this proved to be a useful model to compare subsequent growth stages and root growth stages are well documented (Sugimoto 2000, Van der Weele 2003). After cell division in the apical meristem root cells enter the elongation zone. At the transition point around 0.3 mm. from the root tip (Sugimoto 2000, Van der Weele 2003), cell elongation accelerates abruptly. After rapid growth, cell elongation slows down and ceases when cells enter the root hair zone where trichoblasts form root hairs (Ma et al. 2003). Another advantage of studying epidermal root cells is that Golgi bodies in the cell cortex and cellulose synthase complexes near and inside the plasma

membrane could be tracked well due to the relative large surface area in focus in the microscope.

Outline of this thesis

This thesis contains three chapters reporting experimental research and a final chapter with a general discussion:

Chapter 2. In this chapter the movement and distribution of Golgi bodies in the cortex of cells of different growth stages, early elongation zone compared to late elongation zone, is studied in relation to the configuration of the actin cytoskeleton. In cells in the early elongation zone cell growth accelerates to rapid growth, while in cells in the late elongation zone cell growth declines to almost zero where root hairs emerge (Sugimoto 2000, Van der Weele 2003). In these cells we observed two kinds of actin configurations: the fine filamentous form (fine F-actin) and thick bundles of actin filaments. We analyzed the distribution and motility of Golgi bodies in relation to these configurations.

Chapter 3. In epidermal root cells, the distance between CMTs is larger than the distance between CMFs in the innermost wall layer. To understand how CESA complexes that run in lines along CMTs can produce a uniform layer of CMFs, instead of local thickenings, we studied the orientation, density, alignment and movement of CMTs and CESA complexes using immunocytochemistry and live cell imaging and we studied the orientation and density of CMFs in the innermost layer with Field Emission Scanning Electron Microscopy (FESEM). By recording timelapse movies of CMTs we tested our hypothesis that CMTs continuously reposition in order to achieve an even CMF texture.

Chapter 4 focuses on different electron microscopy techniques that we tested to visualize CMF wall texture; Transmission Electron Microscopy (TEM) of ultrathin sections after mild or complete matrix extraction, TEM of surface preparations and FESEM of surface preparations. We used root hairs of three

different species; *Arabidopsis thaliana*, *Medicago truncatula* and *Vicia sativa*. We compare and discuss the results of the techniques for the capacity to measure orientation, density, length and width of the CMFs.

Chapter 5 is a broad discussion of our work in comparison to the work in the field. We review what is known about the mechanism by which CMFs are deposited in organized textures in addition with own insights. We discuss the complete way that CESA complexes travel, from ER via Golgi bodies and exocytosis vesicles to active movement in the plasma membrane with attention to the role of the actin and CMT cytoskeleton.

References

- Akerman M, Overdijk O, Schel JHN, Emons AMC, Ketelaar T (2011) Golgi body motility in the plant cell cortex correlates with actin cytoskeleton organization. *Plant and Cell Physiology* 52: 1844 - 1855.
- Akerman M, Franssen-Verheijen T, Immerzeel P, Den Hollander L, Schel JHN, Emons AMC (2012) Texture of Cellulose Microfibrils of Root Hair Cell Walls of *Arabidopsis thaliana*, *Medicago truncatula*, and *Vicia sativa*. *Journal of Microscopy*. doi: 10.1111/j.1365-2818.2012.03611.x.
- Arioli T, Peng LC, Betzner AS, Burn J, Wittke W, Herth W, Camilleri C, Höfte H, Plazinski J, Birch R, Cork A, Glover J, Redmond J and Williamson RE (1998) Molecular analysis of cellulose biosynthesis in *Arabidopsis*. *Science* 279:717–20
- Avisar D, Prokhnovsky AI, Makarova KS, Koonin EV, Dolja VV (2008) Myosin XI-K is required for rapid trafficking of Golgi stacks, peroxisomes, and mitochondria in leaf cells of *Nicotiana benthamiana*. *Plant Physiol.* 146: 1098-1108.
- Avisar D, Abu-Abied M, Belausov E, Sadot E, Hawes C, Sparkes IA (2009) A comparative study of the involvement of 17 *Arabidopsis* myosin family members on the motility of Golgi and other organelles. *Plant Physiol.* 150: 700-709.
- Baskin TI (2001) On the alignment of cellulose microfibrils by cortical microtubules: a review and a model. *Protoplasma* 215: 150-171
- Baskin TI (2005) Anisotropic Expansion of the Plant Cell Wall. *Annu. Rev. Cell. Dev. Biol.* 21:203-222.
- Bringmann M, Li E, Sampathkumar A, Kocabek T, Hauser MT, Persson S (2012) POM2/CELLULOSE SYNTHASE INTERACTING1 Is Essential for the Functional Association of Cellulose Synthase and Microtubules in *Arabidopsis*. *Plant Cell* 24: 163–177
- Burn JE, Hocart CH, Birch RJ, Cork AC, Williamson RE (2002) Functional analysis of the cellulose synthase genes *CesA1*, *CesA2*, and *CesA3* in *Arabidopsis*. *Plant Physiol.* 129:797–807
- Carpita NC & Gibeau DM (1993) Structural models of primary cell walls in flowering plants: consistency of molecular structure with the physical properties of the walls during growth. *Plant Journal*, 3, 1-30.
- Chan J, Crowell E, Eder M, Calder G, Bunnewell S, Findlay K, Vernhettes S, Höfte H, Lloyd C (2010) The rotation of cellulose synthase trajectories is microtubule dependent and influences the texture of epidermal cell walls in *Arabidopsis* hypocotyls. *J Cell Sci.* 123: 3490-3495
- Chan J, Eder M, Crowell EF, Hampson J, Calder G, Lloyd C (2011) Microtubules and CESA tracks at the inner epidermal wall align independently of those on the outer wall of light-grown *Arabidopsis* hypocotyls. *J. Cell Sci.* 124: 1088-1094
- Collings DA, Lill AW, Himmelspach R and Wasteneys GO (2006) Hypersensitivity to cytoskeletal antagonists demonstrates microtubule–microfilament cross-talk in the control of root elongation in *Arabidopsis thaliana*. *New Phytologist* 170: 275-290
- Cosgrove DJ (2005) Growth of the plant cell wall. *Nat. Rev. Mol. Cell Biol.* 6: 850–61

- Crowell EF, Bischoff V, Desprez T, Rolland A, Stierhof YD, Schumacher K, Gonneau M, Höfte H, Vernhettes S (2009) Pausing of Golgi bodies on microtubules regulates secretion of cellulose synthase complexes in Arabidopsis. *Plant Cell* 21: 1141-1154
- Crowell EF, Timpano H, Desprez T, Franssen-Verheijen T, Emons AM, Höfte H, Vernhettes S (2011) Differential regulation of cellulose orientation at the inner and outer face of epidermal cells in the Arabidopsis hypocotyl. *Plant Cell*, in press.
- DaSilva LLP, Snapp EL, Denecke J, Lippincott-Schwartz J, Hawes C and Brandizzi F (2004) Endoplasmic Reticulum Export Sites and Golgi Bodies Behave as Single Mobile Secretory Units in Plant Cells. *Plant Cell* 16: 1753-1771
- DeBolt S, Gutierrez R, Ehrhardt DW, Melo CV, Ross L, Cutler SR, Somerville C, Bonetta D (2007) Morlin, an inhibitor of cortical microtubule dynamics and cellulose synthase movement. *Proc. Natl. Acad. Sci. USA* 104: 5854-5859
- Delmer DP (1999) Cellulose biosynthesis: exciting times for a difficult field of study. *Annu. Rev. Plant Physiol. Plant Mol. Biol.* 50:245-76
- De Ruijter NCA, Bisseling T, Emons AMC (1999) Rhizobium Nod factors induce an increase in sub-apical fine bundles of actin filaments in *Vicia sativa* root hairs within minutes. *Mol. Plant Micr. Interactions* 12: 829-832.
- Desprez T, Vernhettes S, Fagard M, Refregier G, Desnos T, Aletti E, Py N, Pelletier S, Höfte H (2002) Resistance against herbicide isoxaben and cellulose deficiency caused by distinct mutations in same cellulose synthase isoform CESA6. *Plant Physiology* 128: 482-490
- Desprez T, Juraniec M, Crowell EF, Jouy H, Pochylova Z, Parcy F, Höfte H, Gonneau M, Vernhettes S (2007) Organization of cellulose synthase complexes involved in primary cell wall synthesis in Arabidopsis thaliana. *Proc. Natl. Acad. Sci. USA* 104: 15572-15577
- Diotallevi F (2007) The physics of cellulose biosynthesis. Thesis. Amolf Amsterdam.
- Emons AMC & Wolters Arts AMC (1983) Cortical Microtubules and Microfibril Deposition in the Cell-Wall of Root Hairs of Equisetum-Hyemale. *Protoplasma* 117, 68-81.
- Emons AMC (1985) Plasma-membrane rosettes in root hairs of Equisetum hyemale. *Planta* 163: 350-359
- Emons AMC, Mulder BM (1998) The making of the architecture of the plant cell wall: how cells exploit geometry. *Proc. Natl. Acad. Sci. USA* 95:7215-19
- Emons AMC, Mulder BM (2000) How the deposition of cellulose microfibrils builds cell wall architecture. *Trends in Plant Science* 5: 35-40.
- Emons AMC, Derksen J, Sassen MMA (1992) Do microtubules orient plant cell wall microfibrils? *Physiol. Plant.* 84: 486-493.
- Emons AMC, Höfte H, Mulder B (2007) Microtubules and cellulose microfibrils: how intimate is their relationship? *Trends in Plant Science* 12: 279 - 281.
- Fagard M, Desnos T, Desprez T, Goubet F, Refregier G, Mouille G, McCann M, Rayon C, Vernhettes S, Höfte H (2000) PROCUSTE1 encodes a cellulose synthase required for normal cell elongation specifically in roots and dark-grown hypocotyls of Arabidopsis. *Plant Cell* 12: 2409-23
- Fernandes AN, Thomas LH, Altaner CM, Callow P, Forsyth VT, Apperley DC, Kennedy CJ, Jarvis MC (2011) Nanostructure of cellulose microfibrils in spruce wood. *PNAS* doi/10.1073/pnas.1108942108

- Fujita M, Himmelspach R, Hocart CH, Williamson RE, Mansfield SD, Wasteneys GO (2011) Cortical microtubules optimize cell-wall crystallinity to drive unidirectional growth in *Arabidopsis*. *Plant J.* 66: 915-928
- Gillmor CS, Poindexter P, Lorieau J, Palcic MM, Somerville C (2002) α -Glucosidase I is required for cellulose biosynthesis and morphogenesis in *Arabidopsis*. *J. Cell Biol.* 156: 1003-1013
- Green PB (1962). Mechanism for plant cellular morphogenesis. *Science* 138: 1404-1405
- Green PB (1963) On mechanisms of elongation In: Locke M (ed) *Cytodifferentiation and macromolecular synthesis*. Academic Press, New York: 203-234.
- Gu Y, Kaplinsky N, Bringmann M, Cobb A, Carroll A, Sampathkumar A, Baskin TI, Persson S, Somerville CR (2010) Identification of a cellulose synthase-associated protein required for cellulose biosynthesis. *PNAS* 107: 12866-12871
- Gutierrez R, Lindeboom JJ, Paredes AR, Emons AM, Ehrhardt DW (2009) *Arabidopsis* cortical microtubules position cellulose synthase delivery to the plasma membrane and interact with cellulose synthase trafficking compartments. *Nat. Cell Biol.* 11: 797-806
- Hala M, Cole R, Synek L, Drdova E, Pecenkova T, Nordheim A, Lamkemeyer T, Madlung J, Hochholdinger F, Fowler JE and Zarsky V (2008) An Exocyst Complex Functions in Plant Cell Growth in *Arabidopsis* and Tobacco. *The Plant Cell* 20: 1330-1345
- Haigler CH, Brown RM (1986) Transport of rosettes from the Golgi apparatus to the plasma membrane in isolated mesophyll cells of *Zinnia elegans* during differentiation to tracheary elements in suspension culture. *Protoplasma* 134: 111-20
- Heath IB (1974) A unified hypothesis for the role of membrane bound enzyme complexes and microtubules in plant cell wall synthesis. *J. Theor. Biol.* 48: 445-449.
- Holland N, Holland D, Helentjaris T, Dhugga KS, Xoconostle-Cazares B, Delmer DP (2000) A comparative analysis of the plant cellulose synthase (CesA) gene family. *Plant Physiol.* 123: 1313-23
- Hussey PJ, Ketelaar T and Deeks MJ (2006) Control of the Actin Cytoskeleton in Plant Cell Growth *Annu. Rev. Plant Biol.* 57: 109-25
- Jamet E, Canut H, Boudart G, Pont-Lezica RF (2006) Cell wall proteins: a new insight through proteomics. *TRENDS in Plant Science* 11: 1360-1385.
- Kennedy CJ, Cameron GJ, Sturcova A, Apperley DC, Altaner C, Wess TJ and Jarvis MC (2007) Microfibril diameter in celery collenchyma cellulose: X-ray scattering and NMR evidence. *Cellulose*, 14, 235-246.
- Ketelaar T, de Ruijter NC, Emons AM (2003) Unstable F-actin specifies the area and microtubule direction of cell expansion in *Arabidopsis* root hairs. *Plant Cell* 15: 285-292
- Kimura S, Laosinchai W, Itoh T, Cui X, Linder CR, Brown RM Jr. (1999) Immunogold labeling of rosette terminal cellulose-synthesizing complexes in the vascular plant *Vigna angularis*. *Plant Cell* 11: 2075-2085
- Lane DR, Wiedemeier A, Peng L, Höfte H, Hocart CH, Birch RJ, Baskin TI, Burn JE, Arioli T, Betzner AS, Williamson RE (2001) Temperature-sensitive alleles of radially swollen2 link the KORRIGAN endo-1,4- β -glucanase to cellulose synthesis and cytokinesis. *Plant Physiology* 126: 278 - 288.
- Ledbetter M, Porter K (1963) A microtubule in plant cell fine structure. *J. Cell Biol.* 19: 239

- Li S, Lei L, Somerville CR, Gu Y (2011) Cellulose synthase interactive protein 1 (CSI1) links microtubules and cellulose synthase complexes. *PNAS* 109: 185–190.
- Ma Z, Baskin TI, Brown KM, Lynch JP (2003) Regulation of root elongation under phosphorus stress involves changes in ethylene responsiveness. *Plant Physiology* 131: 1381–1390
- Miller DD, De Ruijter NCA, Bisseling T, Emons AMC (1999) The role of actin in root hair morphogenesis: studies with lipochito-oligosaccharide as a growth stimulator and cytochalasin as an actin perturbing drug. *Plant J.* 17: 141-154
- Mueller SC, Brown RM Jr. (1980) Evidence for an intramembrane component associated with a cellulose microfibril-synthesizing complex in higher plants. *J. Cell Biol.* 84: 315-326
- Mulder B, Emons AMC (2001) A dynamical model for plant cell wall architecture formation. *J. Math. Biol.* 42: 261-289.
- Mulder B; Schel JHN, Emons AMC (2004) How the geometrical model for plant cell wall formation enables the production of a random texture. *Cellulose* 11: 395 - 401.
- Nebenführ A., Gallagher LA, Dunahay TG, Frohlick JA, Mazurkiewicz AM, Meehl JB, Staehelin LA (1999) Stop-and-go movements of plant Golgi stacks are mediated by the acto-myosin system. *Plant Physiol.* 121: 1127-1141
- Nicol F, His I, Jauneau A, Vernhettes S, Canut H, Höfte H (1998) A plasma membrane-bound putative endo-1,4- β -D-glucanase is required for normal wall assembly and cell elongation in *Arabidopsis*. *EMBO J.* 17: 5563-5576.
- Nishiyama Y, Langan P, Chanzy H (2002) Crystal structure and hydrogen-bonding system in cellulose 1 β from synchrotron X-ray and neutron fiber diffraction. *J. Am. Chem. Soc.* 124: 9074–82
- Nishiyama Y, Sugiyama J, Chanzy H, Langan P (2003) Crystal structure and hydrogen bonding system in cellulose 1 α from synchrotron X-ray and neutron fiber diffraction. *J. Am. Chem. Soc.* 125:14300–6
- Pagant S, Bichet A, Sugimoto K, Lerouxel O, Desprez T, McCann M, Lerouge P, Vernhettes S, Höfte H (2002) KOBITO1 encodes a novel plasma membrane protein necessary for normal cellulose synthesis during cell expansion in *Arabidopsis*. *Plant Cell* 14: 13: 2001-2013
- Paradez AR, Somerville CR, Ehrhardt DW (2006) Visualization of cellulose synthase demonstrates functional association with microtubules. *Science* 312: 1491-1495
- Paradez AR, Persson S, Ehrhardt DW Somerville CR (2008) Genetic Evidence That Cellulose Synthase Activity Influences Microtubule Cortical Array Organization. *Plant Physiology* 147: 1723–1734
- Persson S, Paradez A, Carroll A, Palsdottir H, Doblin M, Poindexter P, Khitrov N, Auer M, Somerville CR (2007) Genetic evidence for three unique components in primary cell-wall cellulose synthase complexes in *Arabidopsis*. *Proc. Natl. Acad. Sci. USA* 104: 15566-15571
- Richmond T (2000) Higher plant cellulose synthases. *Genome Biol.* 4:30011–16
- Robert S, Mouille G, Hofte H (2004) The mechanism and regulation of cellulose synthesis in primary walls: lessons from cellulose-deficient *Arabidopsis* mutants. *Cellulose* 11:351–64
- Roudier F, Fernandez AG, Fujita M, Himmelspach R, Borner GHH, Schindelman G, Song S, Baskin TI, Dupree P, Wasteneys GO, Benfey PN (2005) COBRA, an *Arabidopsis* Extracellular Glycosyl-Phosphatidyl Inositol-Anchored Protein, Specifically Controls Highly Anisotropic

- Expansion through Its Involvement in Cellulose Microfibril Orientation. *Plant Cell* 17: 1749–1763.
- Rudolph U (1987) Occurrence of rosettes in the ER membrane of young *Funaria hygrometrica* protonemata. *Naturwissenschaften* 74: 439.
- Sanchez-Rodriguez C, Bauer S, Hematy K, Saxe F, Belen Ibanez A, Vodermaier V, Konlechner C, Sampathkumar A, Ruggeberg M, Aichinger E, Neumetzler L, Burgert I, Somerville C, Hauser MT, Persson S (2012) CHITINASE-LIKE1/POM-POM1 and Its Homolog CTL2 Are Glucan-Interacting Proteins Important for Cellulose Biosynthesis in *Arabidopsis*. *Plant Cell* 24: 589–607.
- Sato S, Kato T, Kakegawa K, Ishii T, Liu YG, Awano T, Takabe K, Nishiyama Y, Kuga S, Sato S, Nakamura Y, Tabata S, Shibata D (2001) Role of the putative membrane-bound endo-1,4-beta-glucanase KORRIGAN in cell elongation and cellulose synthesis in *Arabidopsis thaliana*. *Plant Cell Physiol.* 42:251-63
- Scheible WR, Eshed R, Richmond T, Delmer D, Somerville CR (2001) Modifications of cellulose synthase confer resistance to isoxaben and thiazolidinone herbicides in *Arabidopsis* *Ixr1* mutants. *Proc. Natl. Acad. Sci. USA* 98: 10079–84
- Schindelman G, Morikami A, Jung J, Baskin TI, Carpita NC, Derbyshire P, McCann M, Benfey PN (2001) COBRA encodes a putative GPI-anchored protein, which is polarly localized and necessary for oriented cell expansion in *Arabidopsis*. *Genes Dev.* 15:1115–27.
- Sparkes IA, Teanby NA, Hawes C (2008) Truncated myosin XI tail fusions inhibit peroxisome, Golgi, and mitochondrial movement in tobacco leaf epidermal cells: a genetic tool for the next generation. *J. Exp. Botany* 59: 2499-2512.
- Somerville C (2006) Cellulose synthesis in higher plants. *Annu Rev Cell Dev Biol*, 22, 53-78.
- Sugimoto K, Williamson RE, Wasteneys GO (2000) New techniques enable comparative analysis of microtubule orientation, wall texture, and growth rate in intact roots of *Arabidopsis*. *Plant Physiol.* 124: 1493-1506
- Taylor NG, Scheible WR, Cutler S, Somerville CR, Turner SR (1999) The irregular xylem3 locus of *Arabidopsis* encodes a cellulose synthase required for secondary cell wall synthesis. *Plant Cell* 11: 769–79
- Turner SR, Somerville CR (1997) Collapsed xylem phenotype of *Arabidopsis* identifies mutants deficient in cellulose deposition in the secondary cell wall. *Plant Cell* 9: 689–701
- Uemura T, Ueda T, Ohniwa RL, Nakano A, Takeyasu K, Sato MH (2004) Systematic analysis of SNARE molecules in *Arabidopsis*: Dissection of the post-Golgi network in plant cells. *Cell structure and function* 29: 49-65.
- Van der Honing H (2011) Actin-mediated cytoplasmic organisation of plant cells. Thesis Laboratory of Plant Cell Biology, Wageningen University.
- Van der Weele C, Jiang HS, Palaniappan KK, Ivanov VB, Palaniappan K, Baskin TI (2003) A New Algorithm for Computational Image Analysis of Deformable Motion at High Spatial and Temporal Resolution Applied to Root Growth. Roughly Uniform Elongation in the Meristem and Also, after an Abrupt Acceleration, in the Elongation Zone. *Plant Physiology* 132: 1138-1148
- Wasteneys GO (2004) Progress in understanding the role of microtubules in plant cells. *Curr. Opin. Plant Biol.* 7: 651–60

Williamson RE, Burn JE, Birch R, Baskin TI, Arioli T, et al. (2001) Morphology of *rsw1*, a cellulose-deficient mutant of *Arabidopsis thaliana*. *Protoplasma* 215:116–27.

Chapter2

Golgi body motility in the plant cell cortex correlates with actin cytoskeleton organization

**Miriam Akkerman, Elysa J. R. Overdijk, Jan H.N. Schel, Anne Mie C. Emons,
Tijs Ketelaar**

*Laboratory of Plant Cell Biology, Wageningen University, Droevendaalsesteeg 1,
6708 PB Wageningen, The Netherlands*

*This chapter has been published in Plant Cell Physiology 52(10):
1844–1855 (2011)*

Abstract

The actin cytoskeleton is involved in the transport and positioning of Golgi bodies, but the actin-based processes that determine the positioning and motility behavior of Golgi bodies are not well understood. In this work, we have studied the relationship between Golgi body motility behavior and actin organization in intercalary growing root epidermal cells during different developmental stages. We show that in these cells two distinct actin configurations are present, depending on the developmental stage. In small cells of the early root elongation zone, fine filamentous actin (F-actin) occupies the whole cell, including the cortex. In larger cells in the late elongation zone that have almost completed cell elongation, actin filament bundles are interspersed with areas containing this fine F-actin and areas without F-actin. Golgi bodies in areas with the fine F-actin exhibit a non-directional, wiggling type of motility. Golgi bodies in areas containing actin filament bundles move up to $7 \mu\text{ms}^{-1}$. Since the motility of Golgi bodies changes when they enter an area with a different actin configuration, we conclude that the type of movement depends on the actin organization and not on the individual organelle. Our results show that the positioning of Golgi bodies depends on the local actin organization.

Introduction

Cell growth is the irreversible increase in cell volume (Ketelaar and Emons 2001). The basis of cell growth is the secretion of cell wall matrix material containing vesicles in a cell with a flexible wall under turgor pressure. Whilst the contents of vesicles are deposited against the existing cell wall, the membrane of these vesicles fuses with the plasma membrane, which increases the plasma membrane surface and inserts transmembrane proteins into the plasma membrane.

One of the transmembrane protein complexes that is inserted into the plasma membrane is the cellulose microfibril-producing cellulose synthase (CESA) complex. The insertion of fluorescently tagged CESA complexes into the plasma membrane can be followed in living cells using fluorescence

microscopy (Paredes et al. 2006) and serves as an excellent marker for (part of the) secretory events. Secretory vesicles are derived from Golgi bodies. Recently, it has been found that, while cortical microtubules position CESA complex delivery to the plasma membrane and interact with small cellulose synthase-containing compartments, SmaCCs (Gutierrez et al. 2009), the acto-myosin system traffics CESA-containing Golgi bodies (Crowell et al. 2009, Gutierrez et al. 2009, Kato et al. 2010). This finding implicates a role for the actin cytoskeleton in the secretion during cell wall formation.

Experimental depolymerization of the actin cytoskeleton causes aggregation of Golgi bodies in specific areas of the cell cortex, whereas in other regions Golgi bodies are absent. The insertion of CESA complexes into the plasma membrane occurs predominantly at the locations where Golgi bodies aggregate during actin depolymerization, but also, in situations where the actin cytoskeleton is intact, more CESA complex insertion into the plasma membrane occurs at locations where Golgi bodies coincidentally aggregate (Crowell et al. 2009, Gutierrez et al. 2009). Thus, the actin-dependent positioning and motility of Golgi bodies determines where secretion of CESA complex-containing vesicles occurs. Since CESA complex insertion occurs predominantly close to Golgi bodies, it appears plausible that there could be an actin-based mechanism that positions Golgi bodies at locations where secretion is required.

In tip-growing root hairs, the role of the actin cytoskeleton in polarized secretion has been well studied. The actin cytoskeleton in growing root hairs consists of thick actin filament bundles (Miller et al. 1999, Ketelaar et al. 2003) which branch into finer bundles of actin filaments (fine F-actin) in the subapex (Arabidopsis: Ketelaar et al. 2003). The fine F-actin configuration is only present in growing cells, and experimental depolymerization of specifically the fine F-actin inhibits cell growth (Miller et al. 1999, Ketelaar et al. 2003), strongly suggesting that in the tips of growing root hairs the presence of fine F-actin is a prerequisite for cell growth. The correlation between fine F-actin and cell growth becomes even more evident from the response of the legume root hair actin cytoskeleton to Rhizobium nodulation factor during the early stages of symbiosis. This host-specific lipochito-oligosaccharide induces root hair curling and initiates the production of nitrogen-fixing root nodules. Its

application affects the actin cytoskeleton (Ca'rdenas et al. 1999) such that fine F-actin and cell elongation are reinitiated in growth-terminating root hairs (De Ruijter et al. 1999). In tip-growing pollen tubes a configuration of fine F-actin that correlates with cell growth, similar to that in root hairs, has been reported (Gibbon et al. 1999, Geitmann et al. 2000, Lovy-Wheeler et al. 2005, Vidali et al. 2009). It has been suggested that, amongst others, the fine F-actin configuration plays a role in maintaining Golgi vesicles close to the growing root hair tip by locally inhibiting the cytoplasmic streaming (Miller et al. 1999).

Unlike tip-growing root hairs and pollen tubes, most plant cells grow by intercalary, also called diffuse, growth. This is a type of polar growth in which cells expand over their whole length in one direction. These cells have a highly dynamic cortical array of F-actin (Staiger et al. 2009, Smertenko et al. 2010). In the present work, we have studied the relationship between Golgi body motility and the configuration of the actin cytoskeleton in intercalary expanding cells. We compared the organization of the cortical actin cytoskeleton and the behavior of Golgi bodies in the cortex root epidermal cells of different developmental stages: the early elongation zone and the late elongation zone. While in the cortex of root epidermal cells in the early elongation zone Golgi bodies only showed slow undirected movement, hereafter called wiggling, in the cortex of cells in the late elongation zone, there are, next to areas where Golgi bodies wiggle, also areas where Golgi bodies move with a velocity up to $7 \mu\text{ms}^{-1}$. This velocity is similar to that observed in cytoplasmic strands. We show that the areas where Golgi body movement is slow and undirected co-localize with fine F-actin, and areas where Golgi body movement is fast and directional co-localize with thick actin filament bundles. When Golgi bodies enter an area with a different actin cytoskeleton configuration they change their type of motility concomitantly. These observations show that Golgi dynamics correlate with the actin cytoskeleton organization.

Results

In the cortex of intercalary growing root atrichoblasts two actin configurations are present, fine F-actin in small cells of the early elongation zone and thick actin filament bundles interspersed with fine F-actin and areas devoid of filamentous actin in larger cells during later stages of cell elongation.

For the study of the actin cytoskeleton we used 35S::GFP: FABD2 (green fluorescent protein:fimbrin actin binding domain 2)-expressing Arabidopsis seedlings (Ketelaar et al. 2004) combined with spinning disk microscopy. We compared two developmental stages of atrichoblasts: young, small cells located just above the root meristem, which we defined as the early elongation zone, and large, still growing cells just below the area where root hairs emerge, which we defined as the late elongation zone (Fig. 1A; see Sugimoto et al. 2000). We used non-root hair-forming epidermal cells, atrichoblasts, to exclude possible changes in actin configuration due to root hair initiation and growth. Young atrichoblasts were identified by tracking a non-root hair-forming cell file from the root hair zone towards the root tip.

In cells in the early elongation zone the configuration of the cortical F-actin was comprised of a diffuse network of (bundles of) actin filaments (fine F-actin; Fig. 1A, C; Ketelaar et al. 2003). Collings et al. (2006) describe a similar F-actin configuration, which they call 'weakly bundled F-actin'. In these cells no thick bundles of actin filaments, hereafter called actin filament bundles, were present in the cell cortex. In cells of the late elongation zone, i.e. cells at the end of their rapid elongation (Baskin 2001), actin filament bundles, often interconnected and branching, were present in the cell cortex. The space between these bundles was occupied by fine F-actin or did not contain detectable actin filaments (Fig. 1B).

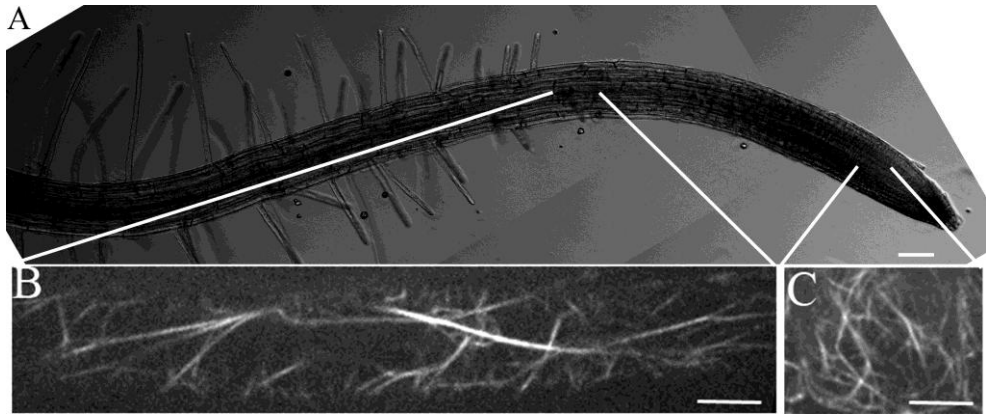


Figure 1. The actin organization (GFP:FABD2) in the cortex of atrichoblasts in the early elongation zone and the late elongation zone. A. overview of a root in which the locations where 1B and 1C have been taken are indicated. B. the cortex of a atrichoblast in the late elongation zone shows dispersed actin filament bundles. The areas without actin filament bundles either contain fine F-actin or are devoid of detectable actin filaments. C. the cortex of atrichoblasts in the early elongation zone is occupied by fine F-actin and no actin filament bundles are visible. Bar in A = 100 μm . Bars in B and C = 10 μm .

Golgi bodies wiggle in areas occupied by fine F-actin and move with velocities up to 7 $\mu\text{m}\cdot\text{s}^{-1}$ along actin filament bundles

We studied the influence of the different actin configurations on organelle motility. For this, we used a line with fluorescently tagged Golgi bodies [expressing 35S::STtmd:GFP (sialyltransferase transmembrane domain:GFP)]. Fig. 2 shows a comparison of the motility of Golgi bodies in the cortical cytoplasm of a typical atrichoblast in the early elongation zone (Fig. 2A) with that of a typical atrichoblast in the late elongation zone (Fig. 2B). To analyze the routes and velocities of Golgi bodies in the cortical cytoplasm, we manually tracked six Golgi bodies in time projections (cell from the early elongation zone, Fig. 2C; cell from the late elongation zone, Fig. 2D) for a total duration of 2 min. The Golgi bodies showed two types of motion: wiggling (Fig. 2E) and directed motion (Fig. 2F). Fig. 2I and J shows velocity graphs of the individual tracked Golgi bodies (colors correspond to the colors in Fig. 2E and F). The motility of Golgi bodies throughout the whole cortex of cells in the early elongation zone can best be described as ‘wiggling’: non-directional

displacement of $<2 \mu\text{ms}^{-1}$. In the cortical cytoplasm of cells in the late elongation zone, two types of Golgi body motility were observed: fast directed motion with velocities ranging from 2 to $7 \mu\text{ms}^{-1}$ (yellow and blue Golgi bodies) and wiggling (green and purple Golgi bodies). This wiggling motility was similar to the Golgi body behavior in cells of the early elongation zone (Fig. 2E, F). Golgi bodies switched between the two types of dynamic behavior when they moved from an area where directed, high velocity motility occurred to an area where wiggling occurred, and vice versa. The blue colored Golgi body in Fig. 2F illustrates this. In the first 60 s it traveled by fast, directed motion. Then, when it entered a different cortical area, its velocity dropped and it showed a typical wiggling behavior. Besides this organelle, many others behaved similarly. Thus, the kind of motility is not a property of the organelles, but of the area in which they reside. The positions of areas where fast, directed motion and wiggling occurred were flexible. During the 10 min time frame, a repositioning of these areas was clearly visible (data not shown).

A novel algorithm was developed to quantify the motility of large populations (approximately 10–80 per cell) of Golgi bodies simultaneously over time (see Supplementary data). The algorithm discriminates between fast, directed ($>2 \mu\text{ms}^{-1}$) and wiggling ($<2 \mu\text{ms}^{-1}$) motion by removing the fluorescence from Golgi bodies that move at velocities $\geq 2 \mu\text{ms}^{-1}$ from the images. The output of this algorithm only shows Golgi bodies with a velocity $<2 \mu\text{ms}^{-1}$ (Fig. 3). In Fig. 4A, images of a cell in the early elongation zone over time are shown. Image processing with the algorithm revealed that Golgi bodies move with a velocity $<2 \mu\text{ms}^{-1}$ throughout the cortical cytoplasm of the cells in the early elongation zone (Fig. 4B). Figs. 4C and D show time projections of the time series from which output data of the algorithm (Fig. 4A, B) have been taken, before (Fig. 4C) and after (Fig. 4D) processing with the algorithm. Fig. 4E–H shows similar images of a cell in the late elongation zone. In this cell, more distal from the root tip, areas where Golgi bodies wiggle are interlaced with areas where Golgi bodies show fast, directed motion (Fig. 4F, H). To compare the Golgi body behavior in atrichoblasts of the early elongation zone and atrichoblasts of the late elongation zone, we determined the fraction of the total fluorescent signal that was still present after processing with the algorithm. In cells of the early elongation zone, the fraction of the total fluorescence produced by Golgi

bodies was 0.90 ± 0.03 ($n = 9$ cells), while in cells in the late elongation zone it was 0.76 ± 0.08 ($n = 9$ cells). The difference is highly significant (Kolmogorov–Smirnov test, $\alpha < 0.01$).

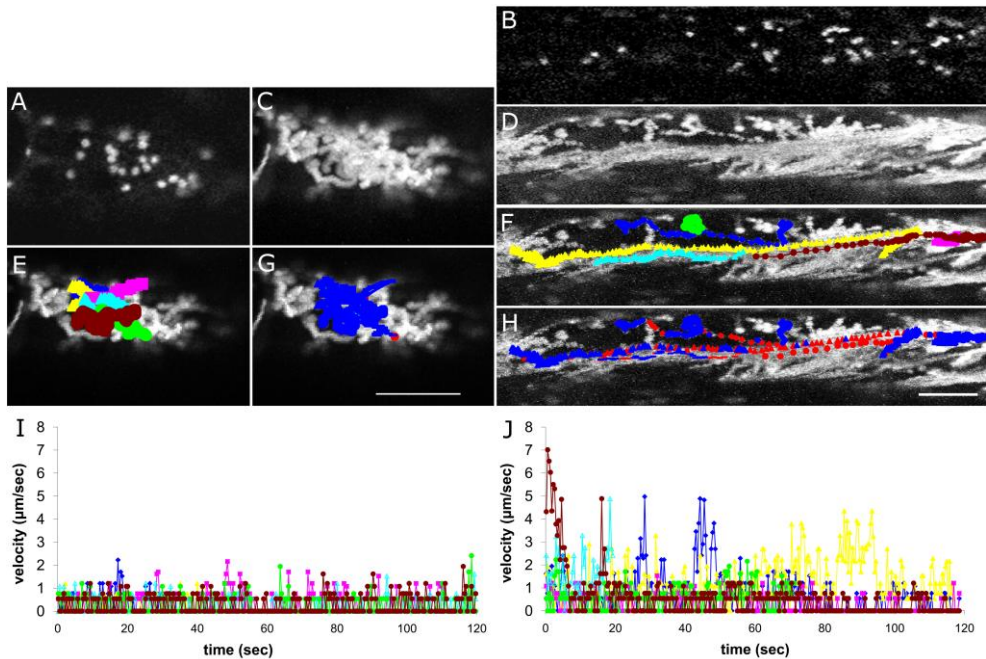


Figure 2. Distribution and movement of Golgi bodies in the cortical cytoplasm of atrichoblasts in the early elongation zone (left) and late elongation zone (right). A and B depict confocal images of the outer layer of the cortical cytoplasm. C and D are time projections of Golgi bodies in the outer layer of the cortical cytoplasm over a period of 120 seconds; maximum projections of 301 images acquired at 0.4 second intervals. E and F show the same time projections as C and D overlaid with colored routes of 6 manually tracked Golgi bodies. In G and H the same time projections are used as in C and D, however slow ($< 2 \mu\text{m s}^{-1}$) moving Golgi bodies are colored blue, and rapidly moving ($\geq 2 \mu\text{m s}^{-1}$) Golgi bodies are colored red. I and J are graphs of the velocity of tracked Golgi bodies plotted over time, I of the atrichoblast in the early elongation zone and J of the atrichoblast in the late elongation zone. Colors correspond with the colors used in E and F. Bar = $10 \mu\text{m}$.

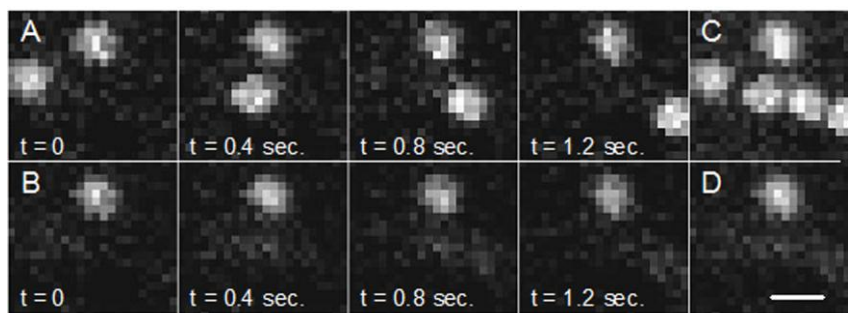


Figure 3. Example of the image processing with our algorithm on an atrichoblast in the late elongation zone. A shows the original time series in which one Golgi body does not move while another is passing. B shows the same time series after processing with the algorithm. Each pixel contains the minimum intensity value that was present at each pixel during 2 subsequent images. Hence, only the immobile Golgi body is visible. C and D are maximum projections of the four images of the time series on the left. Bar = 1 μ m.

Motility behavior of Golgi bodies in the cell cortex depends on the actin configuration

To investigate whether the different types of velocity behavior of Golgi bodies correlate with the local actin organization, we studied Golgi body motility in the cortex of atrichoblasts of dual labeled plants expressing the 35S::STmd:mRFP (monomeric red fluorescent protein) Golgi marker and the 35S::GFP:FABD2 actin markers. Fig. 5 shows frames taken from a cell in the late elongation zone in which Golgi bodies move rapidly over a defined path where an actin filament bundle was present, whereas they do not show any directional motion in an area with fine F-actin or an area without detectable F-actin (Supplementary movie S1).

In an atrichoblast in the early elongation phase, the whole cortex is covered with fine F-actin (Fig. 1C), and no directional motion of Golgi bodies was observed (Fig. 6A, Supplementary movie S2). In an atrichoblast in the late elongation zone, the cortical cytoplasm contained both actin filament bundles and the fine F-actin (Figs. 1B, 6B, Supplementary movie S3). We quantified the dynamic behavior of Golgi bodies and correlated it to the different actin configurations in cells in the early and late elongation zone. To discriminate between fine F-actin and actin filament bundles we measured the fluorescence intensities of both configurations. Supplementary Fig. 1 shows that the

fluorescence intensity in the majority of the cortical areas with fine F-actin is maximally 60 gray levels above the background intensity. The fluorescence intensity of the majority of the cortical areas with actin filament bundles is minimally 80 gray levels above the background intensity. We used this to define fine F-actin and actin filament bundles; every fluorescence peak of >80 gray levels above the background level we considered as an actin filament bundle, whereas any peak <80 gray levels above the background level was considered to be fine F-actin. The cut-off is indicated as a green line in Supplementary Fig. 1C.

We then measured the displacement of individual Golgi bodies over five subsequent 2 s intervals, with a total duration of 10s. Only Golgi bodies maximally 4 pixels (0.45 μm) away from actin filaments during the 10 s time interval were considered. Average velocities were calculated by measuring the displacements over 2 s intervals (Table 1). The directionality of the movement was calculated by dividing the sum of the displacements during five 2 s intervals (average summed displacement; Table 1) by the absolute displacement over a 10s interval (average net displacement; Table 1). These measurements show that in cortical areas with fine F-actin (in both the early and late elongation zone), Golgi bodies move significantly more slowly than in cortical areas with actin filament bundles (Table 1, Fig. 7). In areas with actin filament bundles, the directionality of Golgi body motion is significantly larger than that in areas with fine F-actin. Thus, the configuration of the actin cytoskeleton correlates with the type of Golgi body motion in the cortex of *Arabidopsis* root epidermal cells. Since the Golgi bodies switch from one type of motion to the other (Fig. 4), this result shows that the actin configuration determines the motility type of Golgi bodies.

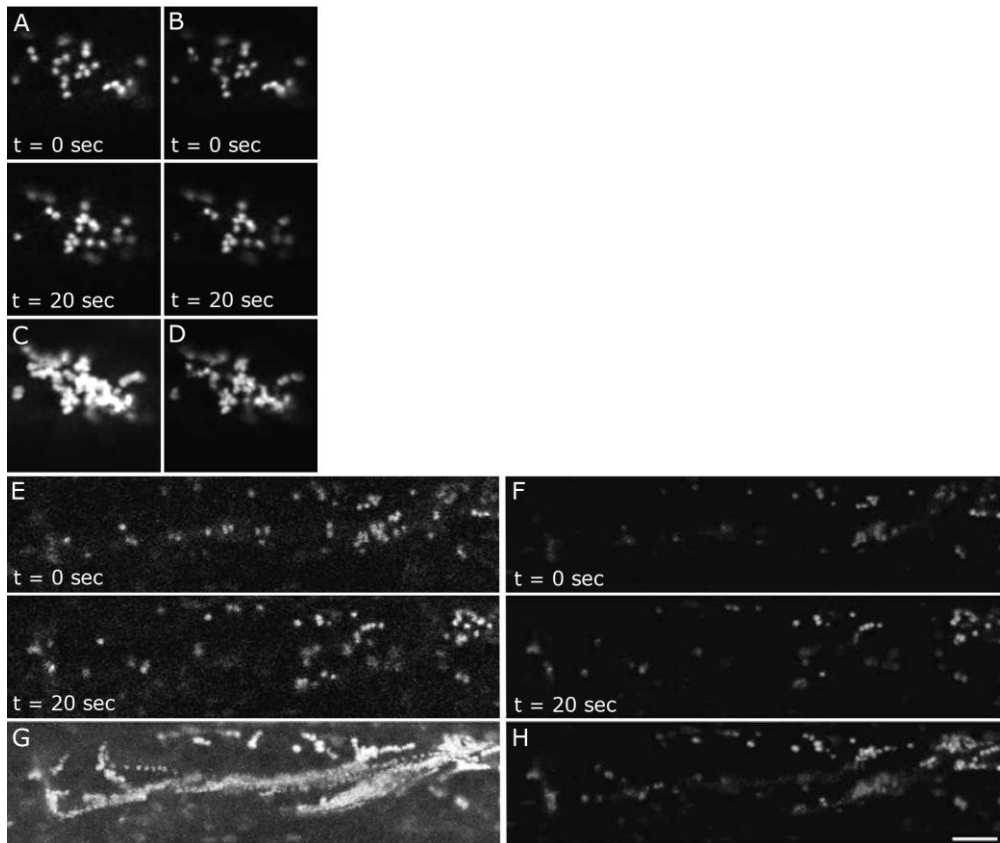


Figure 4. A higher percentage of Golgi bodies in the outer layer of the cortical cytoplasm of an atrichoblast in the early elongation zone exhibits slow, undirected movement than in the late elongation zone. A-D show an atrichoblast in the early elongation zone. E-H show an atrichoblast in the late elongation zone. A and E show the first and the last single images of a 20 seconds time series in an atrichoblast of the early elongation zone (A) and the late elongation zone (E). B and F show the same images after processing of the time series (0.4 seconds intervals) with the algorithm. Only Golgi bodies with a velocity $< 2 \mu\text{m s}^{-1}$, are visible. Slowly moving Golgi bodies are partially visible depending on their velocity. Golgi bodies with a velocity of $0 \mu\text{m s}^{-1}$ are completely visible. C and G are maximum projections of all the images from the 20 sec. time series. D and H show the same projections after processing with the algorithm. Bars = $10 \mu\text{m}$.

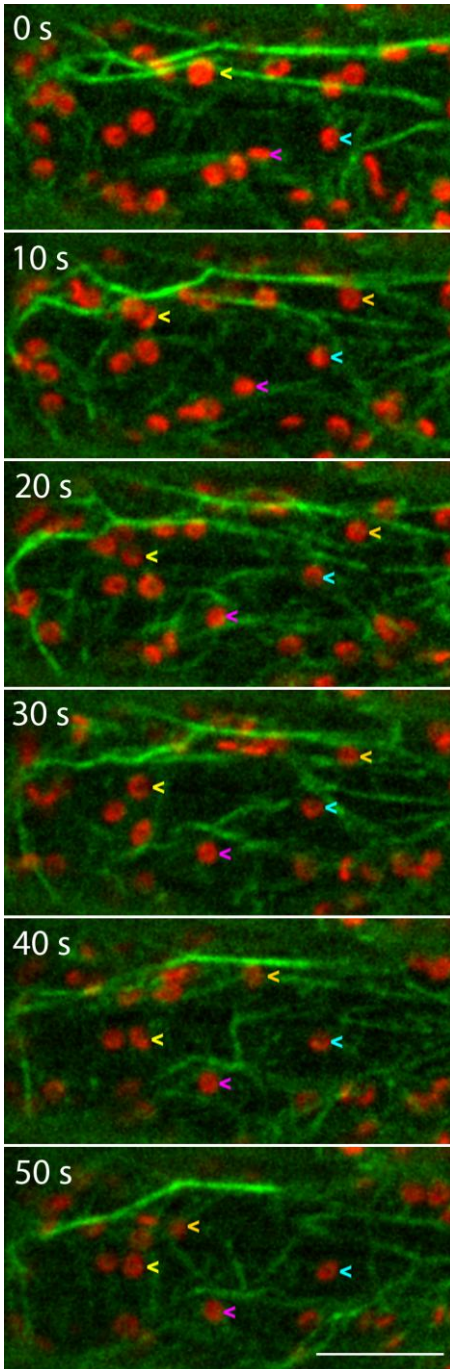


Figure 5. Golgi movement depends on the local actin configuration. Frames with 10 sec. intervals are shown in which 4 Golgi bodies that exhibit different types of motion are indicated with arrowheads. The Golgi bodies labeled with the orange and yellow arrowhead show a burst of rapid, directed movement when located close to an actin filament bundle. When they dissociate from the bundle, their movement changes to the wiggling type. The other two labeled Golgi bodies do not associate with actin bundles and only show wiggling motion. The complete time series is shown in supplemental movie S1. Bar = 10 μ m.

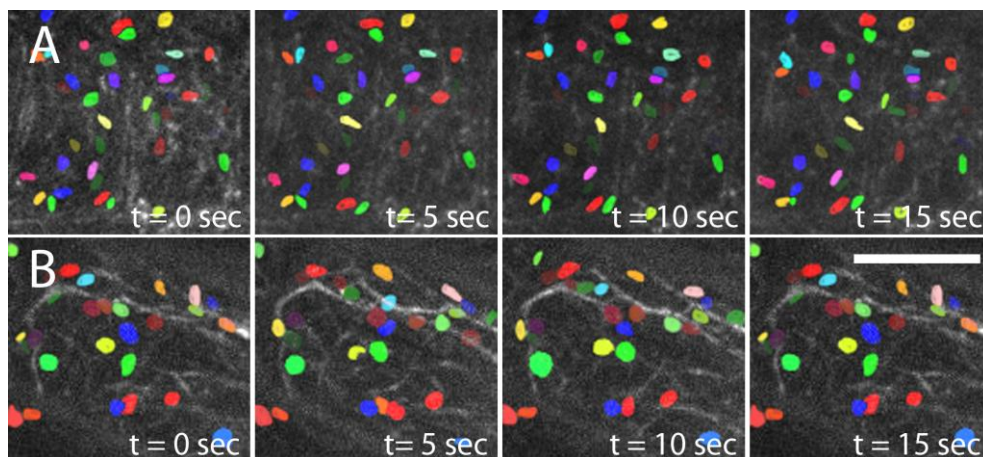


Figure 6. In young atrichoblasts, wiggling motion of Golgi bodies correlates with the presence of fine F-actin throughout the cell cortex (A), whereas in atrichoblasts in the late elongation zone, Golgi bodies display directional movement over an actin filament bundle, and wiggle in a cortical area where only fine F-actin is present (B). Golgi bodies have been pseudo-colored to simplify identification of individual Golgi bodies. An image of the actin organization (black and white) has been merged with the image displaying the Golgi bodies. The full time series, both elapsing 20 seconds real time, are shown in supplemental movies S2 (early elongation phase) and S3 (late elongation phase). Bar = 10 μm .

Table I: Measured velocities and displacements of Golgi bodies and mitochondria

	Golgi bodies		Mitochondria	
	actin filament bundles	fine F-actin	actin filament bundles	fine F-actin
Average velocity ($\mu\text{m s}^{-1}$)	$0,60 \pm 0,51^{***}$	$0,14 \pm 0,12$	$0,25 \pm 0,28$	$0,11 \pm 0,14$
n velocity*	595	535	295	380
Average net displacement (μm)	$4,65 \pm 3,55$	$0,75 \pm 0,67$	$1,86 \pm 2,11$	$0,46 \pm 0,60$
Average summed displacement (μm)	$5,97 \pm 3,96$	$1,40 \pm 0,86$	$2,47 \pm 2,28$	$1,04 \pm 0,54$
Directionality	78%	54%	75%	44%
n displacement**	122	106	59	76

* the number of measured velocities within 1 interval (2 sec)

** the number of measured displacements in 10 seconds

*** standard deviations are used

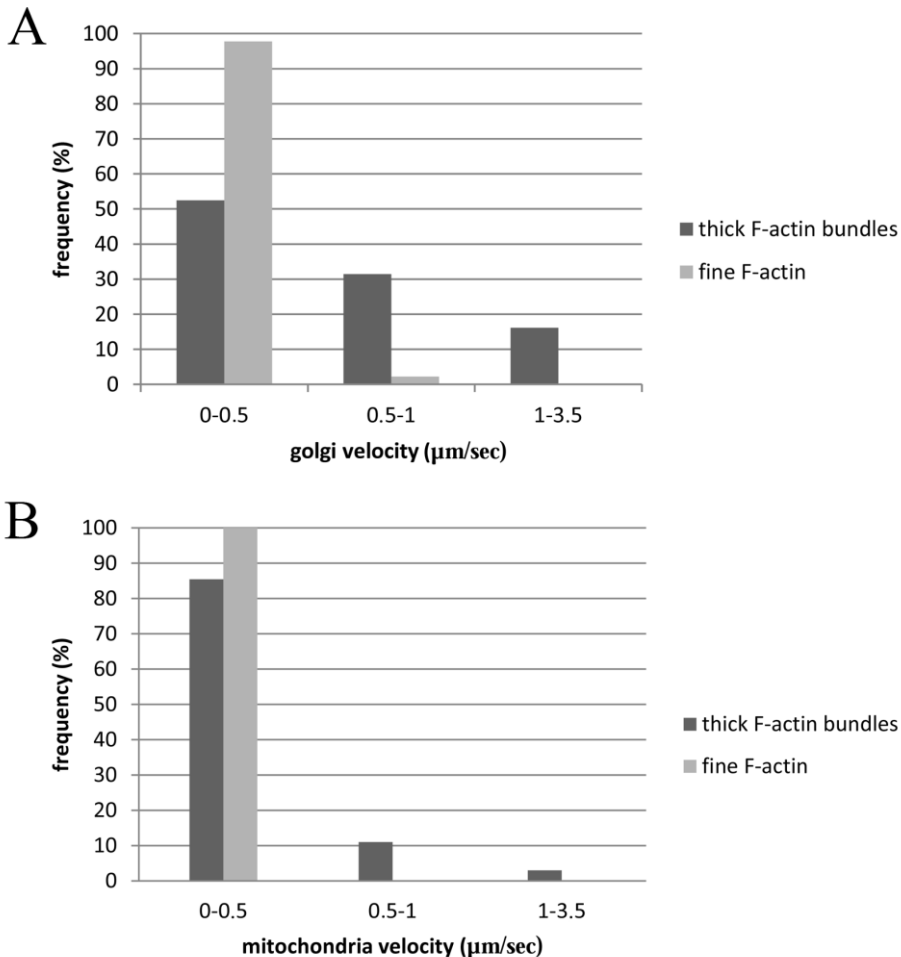


Figure 7. The movement velocities of Golgi bodies (A) and mitochondria (B) in cortical areas with fine F-actin and actin filament bundles.

Differences in motility in cortical areas with fine F-actin and actin filament bundles are not specific for Golgi bodies: mitochondria behave similarly

Besides actin organization, other properties of the Golgi bodies that are independent of actin organization could be involved in their motility. We measured the motility of mitochondria in areas with fine F-actin and actin filament bundles in the cortex of atrichoblasts to test whether the behavior

that we observed is specific for Golgi bodies or generic for all organelles. Like Golgi bodies, mitochondria moved by fast, directed movement along cortical areas with actin filament bundles and exhibited wiggling in cortical areas with fine F-actin configuration. Although the motility behavior of mitochondria and Golgi bodies was similar, the absolute velocity of mitochondria was lower, mainly because fewer mitochondria in the vicinity of actin filaments were moving than Golgi bodies. Even so, the same trend is clearly visible: the local actin organization, and not the organelle properties, determines the organelle motility (Table 1, Fig. 7).

Discussion

Golgi body motility correlates with actin filament organization in the cortex of root epidermal cells

Here we show that the movement of Golgi bodies and mitochondria in the cell cortex depends on the local actin configuration in the cortical cytoplasm, namely on the level of bundling of actin filaments. In the cortical cytoplasm of all atrichoblasts in the early elongation zone, the actin cytoskeleton is organized as fine F-actin. Collings et al. (2006) describe fine F-actin in the cortex of elongating plant cells. Staiger et al. (2009) show that the randomly oriented highly dynamic, short-lived, structures most probably represent single actin filaments. Golgi bodies in these small young cells exhibit slow ($<2 \mu\text{ms}^{-1}$) undirected motion, wiggling, which was previously described by Nebenführ et al. (1999) to occur in the cortical cytoplasm of tobacco BY-2 suspension cultured cells (Nebenführ et al. 1999).

In all cells in the late elongation zone, we found two types of spatially separated areas with distinct actin filament configurations and motility behavior of Golgi bodies. In cell areas with an actin cytoskeleton similar to that in the cortex of cells in the early elongation zone of the root, Golgi bodies wiggled. In cell areas with actin filament bundles Golgi bodies moved as fast as those in cytoplasmic strands. The highest velocity that we measured in the cell's cortex was $7 \mu\text{ms}^{-1}$. There is large variation in the velocities of Golgi bodies reported for higher plant cells, and those that have been measured

previously in similar cells are considerably lower: 0.8–4.2 μms^{-1} (Boevink et al. 1998, Nebenführ et al. 1999, Peremyslov et al. 2008). These differences may be explained by the different time intervals that have been used for analysis. The time interval that we used, 0.4 s, was much shorter than those used in other works. Indeed, when we used longer time intervals, velocities dropped sharply (Fig. 7, Table 1). In vitro, the maximum measured velocity of the higher plant myosin XI is 7 μms^{-1} (Tominaga et al. 2000), which we measured in the fastest moving organelles, and has been found for organelle movement in various plant cell types.

Why do myosins move their organelle cargo more slowly along fine F-actin than over actin filament bundles? There could be several reasons for this: the dynamicity of fine F-actin could negatively affect prolonged binding of Golgi bodies for directed transport. Myosin XI binding sites on fine F-actin could be occupied by other actin-binding proteins, a minimal number of actin filaments in a bundle could be required for prolonged directional transport or myosin XI attached at different surface areas of Golgi bodies could bind to different actin filaments in fine F-actin networks such that counteracting forces are produced. In vitro studies could provide insight into these matters.

If the local actin organization determines Golgi body motility, it is possible that other organelles, which are at least partially equipped with the same myosins (Prokhnovsky et al. 2008, Avisar et al. 2009), behave similarly. Zheng et al. (2009) indeed have shown that mitochondria in root hairs show very similar motility behavior to Golgi bodies. Our observation that mitochondria show the same overall motility behavior, albeit slower on average, as the Golgi bodies in root epidermal cells agrees with a hypothesis that the actin configuration is the source of the signal causing the specific conduct of the organelles.

In animal cells, the role of myosins in long-distance transport remains controversial since long actin cables with uniform polarity are lacking (Pollard and Cooper 2009, Woolner and Bement 2009) and long-distance transport is mainly governed by microtubules (reviewed in Kapitein and Hoogenraad 2011). In budding yeast cells, myosin V is involved in directional transport of vesicles over actin cables, but does not localize to actin patches that are

involved in endocytosis (reviewed in Pruyne et al. 2004). This shows that the budding yeast myosin V somehow discriminates between actin cables and patches and that also in budding yeast the type of actin network determines the mode of transport, albeit by a mechanism that probably differs from that in plant cells. Besides transporting organelles, myosins themselves are capable of reorganizing the actin cytoskeleton in vitro (Soares e Silva et al. 2011) and in plant cells (Hoffmann and Nebenführ 2004, Van der Honing et al. 2010), although there are no indications that the myosins that are involved in actin reorganization are the same as those that decorate and transport organelles.

The actin cytoskeleton organization and Golgi membrane trafficking

In the *Arabidopsis* arichoblasts that we studied, Golgi bodies move along actin filament bundles and wiggle in areas with fine F-actin. Collings et al. (2006) discriminated between fine F-actin, present in the cell cortex and involved in anisotropic cell expansion, and cytoplasmic actin filament bundles responsible for organelle motility. Disruption of the actin filaments reduces *Arabidopsis* root cell elongation and induces radial swelling in a dose-dependent manner (Baskin and Bivens 1995, Collings et al. 2006), in onion (Thomas et al. 1973) and maize roots (Blancaflor 2000, Baluska et al. 2001). In accordance with these results, mutations in actin-binding proteins that disrupt actin organization affect cell elongation (Ramachandran et al. 2000, Dong et al. 2001, Barrero et al. 2002, Nishimura et al. 2003, Ketelaar et al. 2004).

With the reported exception of etiolated *Arabidopsis* hypocotyl cells (Refregier et al. 2004, Derbyshire et al. 2007), plant cell elongation and cell wall formation are coupled processes in which the cell wall keeps more or less its original width as a result of simultaneous stretching and deposition of new material (Roberts 1989). The wall matrix precursors are being made in the Golgi system and deposited against the existing cell wall by exocytosis (Vaughan and Vaughn 1987, Boevink et al. 1998, Nebenführ et al. 1999, Wasteneys and Galway 2003), whereas cellulose microfibrils are produced by CESA complexes moving in the plane of the plasma membrane, which are also thought to be inserted into the plasma membrane via the membrane of Golgi vesicles, i.e. the exocytosis process (reviewed in Emons and Ketelaar 2009). Gutierrez et al. (2009) treated *Arabidopsis* plants expressing yellow

fluorescent protein (YFP)::CESA6 with 1 mM latrunculin B for 4 h to severely depolymerize the actin cytoskeleton. As a result, cortical cytoplasmic streaming was reduced, including Golgi body motility. In addition, Golgi body distribution in the cell cortex was disrupted during this treatment, indicating that a functional actin cytoskeleton is essential for this process. The disrupted Golgi body positioning caused a patchy and co-incident CESA complex distribution in the plasma membrane. Actin depolymerization did not, however, prevent the delivery of the CESA complexes to the plasma membrane. The authors concluded that actin filament function is necessary for appropriate global dispersion of Golgi bodies and uniform delivery of CESA complexes. This supports the hypothesis that there is a role for the actin cytoskeleton in regulating Golgi body positioning and dynamics in the cell cortex.

What happens to Golgi bodies between their movement along actin filament bundles and insertion of their vesicle membranes into the plasma membrane, i.e. the event of exocytosis? Since the only individual exocytotic events that can currently be visualized light microscopically are CESA complex insertions into the plasma membrane, let us use the route of a CESA complex from the Golgi body to its movement in the plasma membrane while producing a cellulose microfibril as an example. In etiolated *Arabidopsis* hypocotyl cells, Golgi bodies containing CESA complexes move on actin filament bundles through the cytosol. This transport of Golgi bodies has been shown to be acto-myosin based (Boevink et al. 1998, Nebenführ et al. 1999, Avisar et al. 2008, Sparkes et al. 2008, Avisar et al. 2009). Once Golgi bodies have reached the cell cortex, CESA complexes are inserted into the plasma membrane, possibly via a SmaCC (Gutierrez et al. 2009). SmaCCs occur especially under stress conditions. The structural identity of SmaCCs is not known; they may be groups of CESA complexes contained in the membrane of one or a small group of Golgi-derived compartments/vesicles. SmaCCs have been observed to associate with Golgi bodies (Gutierrez et al. 2009). Since one SmaCC can deliver at least two CESA complexes to the plasma membrane (Gutierrez et al. 2009), it could possibly represent the secretory vesicle cluster (SVC; Toyooka et al. 2009). Insertion of CESA complexes occurs preferentially in the proximity of cortical microtubules.

The above-described research (Crowell et al. 2009, Gutierrez et al. 2009) makes clear that somehow at the end of the anterograde trafficking of CESA complexes in the Golgi membranes microtubules take over from the actin cytoskeleton. Making use of the temperature-sensitive Arabidopsis mutant microtubule organization 1 (*mor1-1*; Whittington et al. 2001), Collings et al. (2006) have already shown an interdependency of actin filaments and cortical microtubules in the process of plant cell elongation. Moreover, actin and microtubule organization in the cell cortex depend on each other (Sampathkumar et al. 2011).

In spite of this example of an exocytotic pathway of CESA complexes from Golgi bodies to the plasma membrane, the Golgi bodies themselves are not the active agents in the exocytosis process. Moreover, during polarized secretion of pectin in the seed coat, for instance, the position of the Golgi bodies themselves is irrelevant (Young et al. 2008). The determination of the plasma membrane region that accepts Golgi body-derived Golgi vesicle clusters/vesicles for exocytosis is likely to be a crucial factor. What determines their docking to and tethering at the plasma membrane, to deliver the cell wall material, cell wall polymer-producing enzymes and other secreted products and transmembrane proteins, is of prime importance for plant cell growth and therefore plant development.

Materials and Methods

Plant growth

Arabidopsis transgenic plants expressing 35S::GFP:FABD2 (Ketelaar et al., 2004), 35S::STmd:GFP or 35S::STmd:mRFP (kindly provided by C.Hawes, Oxford Brookes University, U.K.) were germinated on a glass micro-chamber containing ½ strength MS medium with vitamins, pH 5.7 (Duchefa, Haarlem, The Netherlands) as described previously (Ketelaar et al., 2002), plated out on petridishes with the same medium, complemented with 1% phyto agar (Duchefa, Haarlem, The Netherlands), or grown in 'biofoil sandwiches' as described by Ketelaar et al. (2004). Selection of the two types of cells that

were compared was on the basis of their position in the root: small young cells just above the meristem, large mature cells above the root hair growth cone.

Image acquisition

Root epidermal cells were imaged on a Zeiss LSM510 META confocal microscope, with a 40x oil immersion objective (PlanApo, NA 1.3) using standard filter combinations. The pinhole of the confocal microscope was adjusted such that thickness of optical sections was approximately 2 μm . This thickness allowed imaging of only the Golgi bodies in the outer cortical layer of cytoplasm and covered a large surface area. For quantitative analysis of the stop behavior all images of atrichoblasts were acquired with the same pinhole settings and the same scan rate. Time series were generated by collecting images with 0.4 second intervals. Cell lengths were measured by counterstaining cell walls with 1 $\mu\text{g ml}^{-1}$ propidium iodide (VWR International, Amsterdam, The Netherlands).

Actin imaging and combined actin and organelle imaging was performed on a Roper Spinning Disk confocal microscope (Roper Scientific, SAS France) using standard filter settings.

Data analysis

Velocity of Golgi bodies in the cortical cytoplasm

Measurements and tracking of Golgi bodies was performed using ImageJ (rsb.info.nih.gov/ij/). The velocity of individual Golgi bodies was calculated by dividing the measured displacement by the elapsed time.

Fraction of wiggling Golgi bodies

The number of Golgi bodies that showed random movement $< 2 \mu\text{m s}^{-1}$ was counted and divided by the total number of Golgi bodies present in the focal plane. This was done at an arbitrary time-point in the movie, for 9 atrichoblasts from the early elongation zone and 9 atrichoblasts from the end elongation zone.

Fraction of fluorescence of arresting and slow moving Golgi bodies

A novel algorithm was developed to analyse Golgi body motility. Processing a time series by the algorithm renders a movie that only shows fluorescence

from Golgi bodies that move slower than $2 \mu\text{m s}^{-1}$. The algorithm is based on the principle of “overlapping”: The average diameter of the detected image of a Golgi body was $0.8 \mu\text{m}$. for both developmental stages (data not shown). When a Golgi body moves with $2 \mu\text{m s}^{-1}$, it moves $0.8 \mu\text{m}$. in 0.4 s . Thus when a Golgi body, in a time series in which the images are taken every 0.4 second , is overlapping itself in a time projection, it moves with a velocity of $< 2 \mu\text{m s}^{-1}$. A resulting time series after algorithm processing only shows these “overlaps”, by selecting for each pixel the lowest intensity level during 2 subsequent images. An example is shown in figure 3. Processing of the time series by the algorithm was performed in Matlab.

Quantification of the slow movement was achieved as follows:

Fraction of fluorescence of arresting and slow moving Golgi bodies = $(\text{total intensity after processing} - \text{background intensity}) \times (\text{total original intensity} - \text{background intensity})^{-1}$.

Financial support

This work (AMCE) was supported by European Union New and Emerging Science and Technology (NEST) [project number: 028974 CASPIC (Cellulose Architecture Systems biology for Plant Innovation Creation)].

Acknowledgements

We would like to thank Chris Hawes, Oxford Brookes University, UK, for the STtmd:YFP plasmids and expressing plants; MA thanks Norbert de Ruijter for help with microscopes, and Bela Mulder for help with Matlab programming. This work (AMCE) was supported by European Union New and Emerging Science and Technology (NEST) [project number: 028974 CASPIC (Cellulose Architecture Systems biology for Plant Innovation Creation)].

References

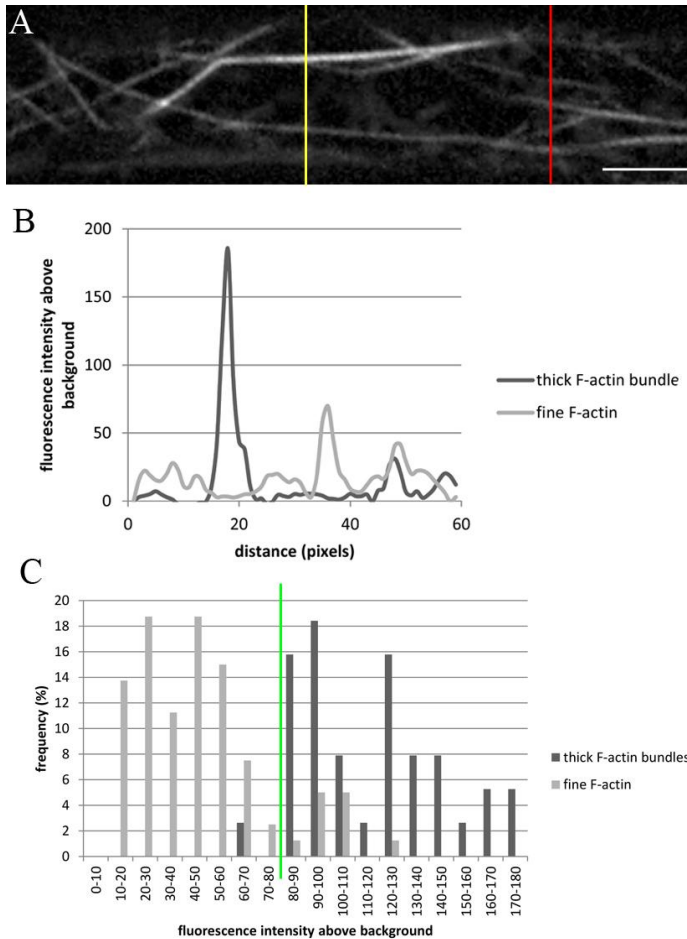
- Avisar, D., Prokhnevsky, A.I., Makarova, K.S., Koonin, E.V., Dolja, V.V. (2008) Myosin XI-K is required for rapid trafficking of Golgi stacks, peroxisomes, and mitochondria in leaf cells of *Nicotiana benthamiana*. *Plant Physiol.* 146: 1098-1108.
- Avisar, D., Abu-Abied, M., Belausov, E., Sadot, E., Hawes, C., Sparkes, I.A. (2009) A comparative study of the involvement of 17 Arabidopsis myosin family members on the motility of Golgi and other organelles. *Plant Physiol.* 150: 700-709.
- Baluska, F., Jasik, J., Edelmann, H.G., Salajová, T., Volkmann, D. (2001) Latrunculin B-induced plant dwarfism: Plant cell elongation is F-actin-dependent. *Dev. Biol.* 231: 113-124.
- Barrero, R.A., Umeda, M., Yamamura, S., Uchimiya, H. (2002) Arabidopsis CAP regulates the actin cytoskeleton necessary for plant cell elongation and division. *Plant Cell* 14: 149-163.
- Baskin, T.I. and Bivens, N.J. (1995) Stimulation of radial expansion in Arabidopsis roots by inhibitors of actomyosin and vesicle secretion but not by various inhibitors of metabolism. *Planta* 197: 514-521.
- Baskin, T.I. (2001) On the alignment of cellulose microfibrils by cortical microtubules: A review and a model. *Protoplasma* 215: 150-171
- Blancaflor, E.B. (2000) Cortical actin filaments potentially interact with cortical microtubules in regulating polarity of cell expansion in primary roots of maize (*Zea mays* L.) *J. Plant Growth Regulation* 19: 406-414.
- Boevink, P., Oparka, K., Santa Cruz, S., Martin, B., Betteridge, A. and Hawes, C.R. (1998) Stacks on tracks: the plant Golgi apparatus traffics on an actin/ER network. *Plant J.* 15: 441-447.
- Cárdenas, L., Feijo, J.A., Kunkel, J.G., Sanchez, F., Holdaway-Clarke, T., Hepler, P.K., Quinto, C. (1999) Rhizobium nod factors induce increases in intracellular free calcium and extracellular calcium influxes in bean root hairs. *Plant J.* 19: 347-352.
- Collings, D.A., Lill, A.W., Himmelsbach, R. and Wasteneys, G.O. (2006) Hypersensitivity to cytoskeletal antagonists demonstrates microtubule-microfilament cross-talk in the control of root elongation in *Arabidopsis thaliana*. *New Phytologist* 170: 275-290.
- Crowell, E.F., Bischoff, V., Desprez, T., Rolland, A., Stierhof, Y.D., Schumacher, K., Gonneau, M., Höfte, H., Vernhettes, S. (2009) Pausing of Golgi bodies on microtubules regulates secretion of cellulose synthase complexes in Arabidopsis. *Plant Cell* 21: 1141-1154.
- Derbyshire, P., Findlay, K., McCann, M.C., Roberts, K. (2007) Cell elongation in Arabidopsis hypocotyls involves dynamic changes in cell wall thickness. *J. Exp. Botany* 58: 2079-2089.
- De Ruijter, N.C.A., Bisseling, T., Emons, A.M.C. (1999) *Rhizobium* Nod factors induce an increase in sub-apical fine bundles of actin filaments in *Vicia sativa* root hairs within minutes. *Mol. Plant Micr. Interactions* 12: 829-832.
- Dong, C.H., Xia, G.X., Hong, Y., Ramachandran, S., Kost, B., Chua, N.H. (2001) ADF proteins are involved in the control of flowering and regulate F-actin organization, cell expansion, and organ growth in Arabidopsis. *Plant Cell* 13: 1333-1346.
- Emons, A.M.C., Ketelaar, T. (2009) Intracellular organization: A prerequisite for root hair elongation and cell wall deposition. In: Emons AMC and Ketelaar T, eds. *Roots Hairs*. Plant Cell Monographs. Springer, Berlin, Heidelberg, 27-44.

- Geitmann, A., Snowman, B.N., Emons, A.M., Franklin-Tong, V.E. (2000) Alterations in the actin cytoskeleton of pollen tubes are induced by the self-incompatibility reaction in *Papaver rhoeas*. *Plant Cell* 12: 1239-1251.
- Gibbon, B.C., Kovar, D.R., Staiger, C.J. (1999) Latrunculin B has different effects on pollen germination and tube growth. *Plant Cell* 11: 2349-2363.
- Gutierrez, R., Lindeboom, J.J., Paredes, A.R., Emons, A.M.C., Ehrhardt, D.W. (2009) Arabidopsis cortical microtubules position cellulose synthase delivery to the plasma membrane and interact with cellulose synthase trafficking compartments. *Nature Cell Biol.* 11: 797 - 806.
- Hoffmann, A., Nebenführ, A. (2004) Dynamic rearrangements of transvacuolar strands in BY-2 cells imply a role of myosin in remodeling the plant actin cytoskeleton. *Protoplasma* 224: 201-210.
- Kapitein, L.C., Hoogenraad, C.C. (2011) Which way to go? Cytoskeletal organization and polarized transport in neurons. *Mol Cell Neurosci* 46: 9-20.
- Kato, T., Morita, M.T., Tasaka, M. (2010) Defects in dynamics and functions of actin filament in Arabidopsis caused by the dominant-negative actin fiz1-induced fragmentation of actin filament. *Plant Cell Physiol.* 51: 333-338.
- Ketelaar, T., Emons, A.M.C. (2001) The cytoskeleton in plant cell growth: lessons from root hairs. *New Phytologist* 152: 409-418.
- Ketelaar, T., De Ruijter, N.C.A., Emons, A.M.C. (2003) Unstable F-actin specifies area and microtubules direction of cell expansion in Arabidopsis root hairs. *Plant Cell* 15: 285-292.
- Ketelaar, T., Allwood, E.G., Anthony, R., Voigt, B., Menzel, D., Hussey, P.J. (2004) The actin-interacting protein AIP1 is essential for actin organization and plant development. *Curr. Biol.* 14: 145-149
- Lovy-Wheeler, A., Wilsen, K.L., Baskin, T.I., Hepler, P.K. (2005) Enhanced fixation reveals the apical cortical fringe of actin filaments as a consistent feature of the pollen tube. *Planta* 221: 95-104.
- Miller, D.D., de Ruijter, N.C.A., Bisseling, T., Emons, A.M.C. (1999) The role of actin in root hair morphogenesis: studies with lipochito-oligosaccharide as a growth stimulator and cytochalasin as an actin perturbing drug. *Plant J.* 17: 141-154.
- Nebenführ, A., Gallagher, L.A., Dunahay, T.G., Frohlick, J.A., Mazurkiewicz, A.M., Meehl, J.B., Staehelin, L.A. (1999) Stop-and-go movements of plant Golgi stacks are mediated by the acto-myosin system. *Plant Physiol.* 121: 1127-1141.
- Nishimura, T., Yokota, E., Wada, T., Shimmen, T., Okada, K. (2003) An Arabidopsis ACT2 dominant-negative mutation, which disturbs F-actin polymerization, reveals its distinctive function in root development. *Plant Cell Physiol.* 44: 1131-1140.
- Paredes, A.R., Somerville, C.R., Ehrhardt, D.W. (2006) Visualization of cellulose synthase demonstrates functional association with microtubules. *Science* 312: 1491-1495.
- Peremyslov, V.V., Prokhnevsky, A.I., Avisar, D., Dolja, V.V. (2008) Two class XI myosins function in organelle trafficking and root hair development in Arabidopsis. *Plant Physiol.* 146: 1109-1116.
- Pollard, T.D., Cooper, J.A. (2009) Actin, a central player in cell shape and movement. *Science* 326: 1208-1212.

- Prokhnevsky, A.I., Peremyslov, V.V. and Dolja, V.V. (2008) Overlapping functions of the four class XI myosins in Arabidopsis growth, root hair elongation, and organelle motility. *PNAS* 105: 19744-19749.
- Pruyne, D., Legesse-Miller, A., Gao, L., Dong, Y., Bretscher, A. (2004) Mechanisms of polarized growth and organelle segregation in yeast. *Annu Rev Cell Dev Biol* 20: 559-591.
- Ramachandran, S., Christensen, H.E.M., Ishimaru, Y., Dong, C., Chao-Ming, W., Cleary, A.L., Chua, N. (2000) Profilin plays a role in cell elongation, cell shape maintenance, and flowering in Arabidopsis. *Plant Physiol.* 124: 1637-1647.
- Refrégier, G., Pelletier, S., Jaillard, D., and Höfte, H. (2004) Interaction between wall deposition and cell elongation in dark-grown hypocotyl cells in Arabidopsis. *Plant Physiol.* 135: 959-968.
- Roberts, K. (1989) The plant extracellular matrix. *Curr. Opin. Cell Biol.* 1: 1020-1027.
- Sampathkumar, A., Lindeboom, J.J., Debolt, S., Gutierrez, R., Ehrhardt, D.W., Ketelaar, T., Persson, S. (2011) Live Cell Imaging Reveals Structural Associations between the Actin and Microtubule Cytoskeleton in Arabidopsis. *Plant Cell* in press.
- Smertenko, A.P., Deeks, M.J., Hussey, P.J. (2010) Strategies of actin reorganisation in plant cells. *J. Cell Sci.* 123: 3019-3028.
- Sparkes, I.A., Teanby, N.A., Hawes, C. (2008) Truncated myosin XI tail fusions inhibit peroxisome, Golgi, and mitochondrial movement in tobacco leaf epidermal cells: a genetic tool for the next generation. *J. Exp. Botany* 59: 2499-2512.
- Soares e Silva, M., Depken, M., Stuhmann, B., Korsten, M., MacKintosh, F.C., Koenderink, G.H. (2011) Active multistage coarsening of actin networks driven by myosin motors. *Proc Natl Acad Sci USA.* 108: 9408-9413.
- Staiger, C.J., Sheahan, M., Khurana, P., Wang, X., McCurdy, D.W., Blanchoin, L. (2009) Actin filament dynamics are dominated by rapid growth and prolific severing activity in the Arabidopsis cortical array. *J. Cell Biol.* 184: 269-280.
- Sugimoto, K., Williamson, R.E., Wasteneys, G.O. (2000) New techniques enable comparative analysis of microtubule orientation, wall texture, and growth rate in intact roots of Arabidopsis. *Plant Physiol.* 124: 1493-1506.
- Thomas, D.D.S., Lager, N.M., Manavathu, E.K. (1973) Cytochalasin B: effects on root morphogenesis in *Allium cepa*. *Can. J. Botany* 51: 2269-2273.
- Tominaga, M., Yokota, E., Sonobe, S., Shimmen, T. (2000) Mechanism of inhibition of cytoplasmic streaming by a myosin inhibitor, 2,3-butanedione monoxime. *Protoplasma* 213: 46-54.
- Toyooka, K., Goto, Y., Asatsuma, S., Koizumi, M., Mitsui, T., Matsuoka, K. (2009) A mobile secretory vesicle cluster involved in mass transport from the Golgi to the plant cell exterior. *Plant Cell* 21: 1212-1229.
- Van der Honing, H.S., de Ruijter, N.C., Emons, A.M., Ketelaar, T. (2010) Actin and myosin regulate cytoplasm stiffness in plant cells: a study using optical tweezers. *New Phytol* 185: 90-102.
- Vaughan, M.A. and Vaughn, K.C. (1987) Effects of microfilament disrupters on microfilament distribution and morphology in maize root cells. *Histochemistry* 87: 129-137.
- Vidali, L., Rounds, C.M., Hepler, P.K., Bezanilla, M. (2009) Lifeact-mEGFP reveals a dynamic apical F-actin network in tip growing plant cells. *PLoS One* 4: e5744.

- Wasteneys, G.O., Galway, M.E. (2003) Remodelling the cytoskeleton for growth and form: An overview with some new views. *Ann. Rev. Plant Biol.* 54: 691-722
- Whittington, A.T., Vugrek, O., Wei, K.J., Hasenbein, N.G., Sugimoto, K., Rashbrooke, M.C., Wasteneys, G.O. (2001) MOR1 is essential for organizing cortical microtubules in plants. *Nature* 411: 610-613.
- Woolner, S., Bement, W.M. (2009) Unconventional myosins acting unconventionally. *Trends Cell Biol* 19: 245-252.
- Young, R.E., McFarlane, H.E., Hahn, M.G., Western, T.L., Haughn, G.W., Samuels, A.L. (2008) Analysis of the Golgi apparatus in Arabidopsis seed coat cells during polarized secretion of pectin-rich mucilage. *Plant Cell* 20: 1623-1638
- Zheng, M., Beck, M., Müller, J., Chen, T., Wang, X., Wang, F., Wang, Q., Wang, Y., Baluška, F., Logan, D.C., Šamaj, J., Lin, J. (2009) Actin turnover is required for myosin-dependent mitochondrial movements in Arabidopsis root hairs. *PLoS One* 4: e5961.

Supporting information



Supplemental figure 1. Actin filament bundles generally have an intensity of at least 80 greyscales above the background intensity, whereas the intensity of fine F-actin generally is at most 60 greyscales above the background intensity. A shows an image of the actin configuration in the cortex of a GFP:FABD2 expressing epidermal cell in the late root elongation zone. The intensity profiles of the yellow and red lines are plotted in B. The dark line in B represents the yellow line in A and the light line in B represents the red line in A. In C, we plotted fluorescence intensities (number of greyscales above the background level) of cortical area containing fine F-actin or actin filament bundles (defined arbitrarily, based on actin organization). The green line in C shows the cut-off that we used during image processing.

Chapter 3

Cellulose synthase complex, cortical microtubule and cellulose microfibril alignment in *Arabidopsis* root epidermal cells

**Ying Zhang¹, Miriam Akkerman¹, Tiny Franssen-Verheijen, Anne Mie C.
Emons, Tijs Ketelaar**

¹These authors contributed equally to this work

*Laboratory of Cell Biology, Department of Plant Sciences, Wageningen
University, Droevendaalsesteeg 1, 6708 PB Wageningen, The Netherlands*

Abstract

Cellulose microfibrils (CMFs) are the main load bearing structures of plant cell walls. They are produced by cellulose synthase (CESA) complexes that move through the plasma membrane. In axially growing hypocotyl cells CMF alignment is determined by microtubules guiding the CESA complexes (Paredez et al. 2006). In these cells, spacing of cortical microtubules (CMTs) is wider than that of the CMFs, which are deposited as a uniform layer (Crowell et al. 2011). To understand how CESA complexes that are guided by CMTs can produce a uniform layer of CMFs, we studied the orientation, density, alignment and movement of CMTs and CESA complexes using immunocytochemistry and live cell imaging of root epidermal cells. Furthermore we studied the orientation and density of CMFs in the innermost cell wall layer of these cells with Field Emission Scanning Electron Microscopy (FESEM). The CMTs, the rows of CESA complexes and the innermost CMFs lay in the same orientation, approximately transverse to the elongation axis in both the inner and outer periclinal cell face in the elongation zone and root hair zone. CESA complexes predominantly move in rows along CMTs in both directions. While the density of CMTs and CESA rows corresponds, the density of CMFs in the innermost cell wall layer is much higher and CMFs form an even layer. After analysis of timelapse movies of CMTs we conclude that CMTs reposition over time, so that CESA complexes produce an even cell wall layer.

Introduction

Plant cells are surrounded by cell walls, which expand during cell elongation. The load bearing polymers in these cell walls are crystalline cellulose microfibrils (CMFs). It is generally thought that in axially (also called diffuse or intercalary) growing cells, the orientation of these CMFs determines the cell elongation direction, which is perpendicular to the orientation of the CMFs (Green 1962; Baskin 2005).

CMFs are produced by cellulose synthase (CESA) complexes in the plasma membrane, which at electron microscopy resolution can be seen as

hexameric rosettes (Kimura et al., 1999; Mueller and Brown; 1980 Emons, 1985). Live cell imaging of these CESA complexes tagged with fluorescent proteins has shown their movement within the plane of the plasma membrane in *Arabidopsis* hypocotyl cells (Paredez et al. 2006; Debolt et al. 2007; Persson et al. 2007; Desprez et al. 2007; Gu et al. 2010, Crowell et al. 2009, 2011; Gutierrez et al. 2009; Chan et al. 2010, 2011), guided by the cortical microtubules (CMTs) (Paredez et al. 2006, Fujita et al. 2011, Bringmann et al. 2012), which in addition function in localizing the insertion of CESA complexes into the plasma membrane. However, in the absence of the CMTs CESA complexes still move in an ordered, though different, pattern through the plasma membrane (Paredez et al. 2006; see also Emons et al. 2007).

In axially growing root cells studied by means of immuno-cytochemistry and transmission electron microscopy, respectively, alignment of CMTs and CMFs is in the same overall direction, transverse to the elongation axis of the cell (reviewed in Baskin, 2001). Later studies, using live cell imaging of both CMTs and CESA complexes, have increased our understanding of the process of CMF alignment (Paredez et al., 2006; Debolt et al., 2007; Persson et al., 2007; Crowell et al., 2009, 2011; Gutierrez et al., 2009; Chan et al., 2010, 2011). In elongating etiolated *Arabidopsis* hypocotyl cells different orientations of both CMTs and CMFs are found in the outer epidermal cell surface (Chan et al., 2010), but at the wall of the inner epidermal cell surface both polymers remain transverse (Crowell et al., 2011, Chan et al 2011) during the whole cell elongation phase, implicating that a transverse CMF orientation in the inner periclinal wall could be sufficient and required for cell elongation in these cells (Crowell et al. 2011).

Since we were not able to study CESA movement in the inner cell face of root epidermal cells using live cell probes, CESA complex localization was in addition studied using immuno-cytochemistry on sections, which also allowed studying CESA localization in deeper cell layers. Moreover, an antibody raised against a conserved domain of CESA proteins labels all CESA complexes, which is not necessarily the case for the live cell imaging probes. We used an anti-CESA antibody, raised against the conserved cytoplasmic loop of the CESA catalytic subunit for visualization of the CESA complexes (Gillmor et al., 2002;

Cai et al., 2011). Analysis of samples that were labelled with this antibody revealed lines of dots in the cell cortex, presumably the plasma membrane. In epidermal cells of the root elongation zone and root hair zone the orientation of the lines was transverse to the long axis of the cell at both the inner and outer periclinal cell face. This CESA complex patterning, and density, appeared to be similar to that in GFP:CESA3 expressing root epidermal cells, in which CESA complexes move in rows along CMTs. Using Field Emission Scanning Electron Microscopy (FESEM), we found that spacing between CMFs in the lastly deposited layer of the cell wall is uniform over the cell surface, as already shown earlier (Sugimoto et al 2000; Baskin et al. 2004) and the distance between neighbouring CMFs is much smaller than that between CMTs at the other side of the plasma membrane. How can such a uniform distribution of CMFs in the cell wall be obtained? We analyzed two hypotheses: CESA complexes in between the CMTs contribute considerably to CMF layer formation and/or CMTs reposition continuously. Our data favour the second alternative.

Results

Immunolabeling with an antibody against CESAs reveals that CESA complexes are present in rows of dots at the plasma membrane of Arabidopsis root epidermal and cortical cells

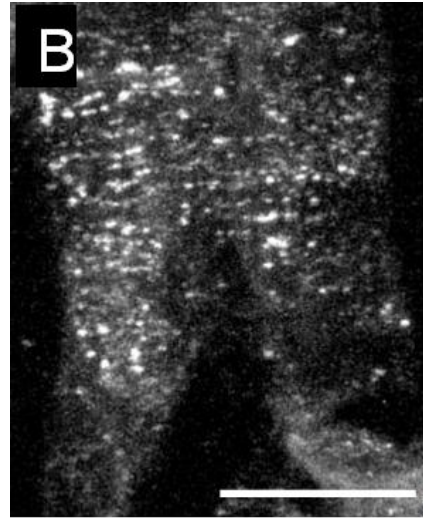
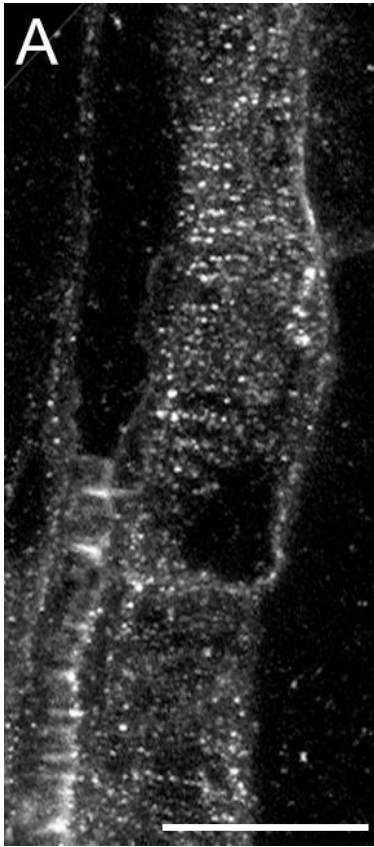
We used the CESA antibody characterized by Gillmor et al. (2002) and Cai et al. (2011) to label 4-5 μm thick sections of butylmethacrylate (BMM; Baskin et al., 1992) embedded, cryo-fixed Arabidopsis roots. The antibody was raised against the conserved cytoplasmic loop of the CESA catalytic subunit and cross-reacts specifically with an intrinsic Arabidopsis plasma membrane protein of 120 kD (Gillmor et al., 2002; Cai et al., 2011).

To test the specificity of the CESA labelling, we checked whether CESA complexes could be detected in the plasma membrane underlying developing secondary cell wall thickenings in differentiating xylem cells. Many rosettes, which represent the CESA complexes (Kimura et al. 1999) are present at these locations (Herth, 1985; Gardiner et al., 2003). Supplemental Figure 1 shows

that our immunolabeling procedure recognizes these accumulations of CESA complexes in developing tracheary elements of the xylem. After confirmation of the antibody specificity in our samples, we proceeded to study the CESA complex localization at the outer and inner faces of root epidermal cells and root cortical cells. Figure 1 shows typical examples of sections containing large stretches of the plasma membrane underlying the outer and inner periclinal cell faces of root epidermal cells. The antibody against CESA localizes to dots patterned in more or less transversely oriented rows in the cell cortex of the inner and outer periclinal cell faces of epidermal cells in the root elongation zone and the root hair zone (Figure 1A: cells in the root elongation zone and Figure 1B: cells in the root hair zone). We have two reasons to presume that these dots are in the plasma membrane: biochemistry shows an accumulation of the antigen that is being recognized by the antibody in the plasma membrane fraction (Cai et al. 2011), and GFP-tagged CESA complexes localize to the plasma membrane with a similar pattern, where they move with the velocity of approx. 300 nm min⁻¹ known from CESA complexes producing CMFs (Paredes et al. 2006), see below.

The CESA rows were oriented transversely to the elongation axis of the root and helically in older cells located further away from the root tip. We measured the density of CESA dots in the rows and the density of rows in both the inner and outer periclinal cell face of cells in the elongation zone and cells in the root hair zone, where cell elongation ceases (Beemster and Baskin 1998). The density of rows was measured along a line perpendicular to the rows. Table 1 gives an overview of the measurements. The density of rows of CESA complexes in cells in the elongation zone is slightly higher than this density in the root hair zone. For the inner and outer periclinal cell faces we found similar values. The density of dots in a row in cells in the elongation zone and cells in the root hair zone is similar both in inner and outer periclinal cell face.

The immunocytochemistry data were compared with live cell imaging data of CESA complexes in GFP:CESA3 (Gutierrez et al., 2009) expressing root epidermal cells. Figure 2 shows micrographs taken from time series (Supplemental Movies 1 and 2) of *Arabidopsis* root epidermal cells from the



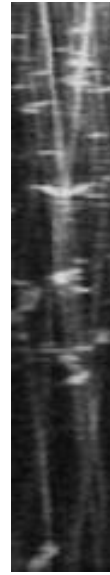
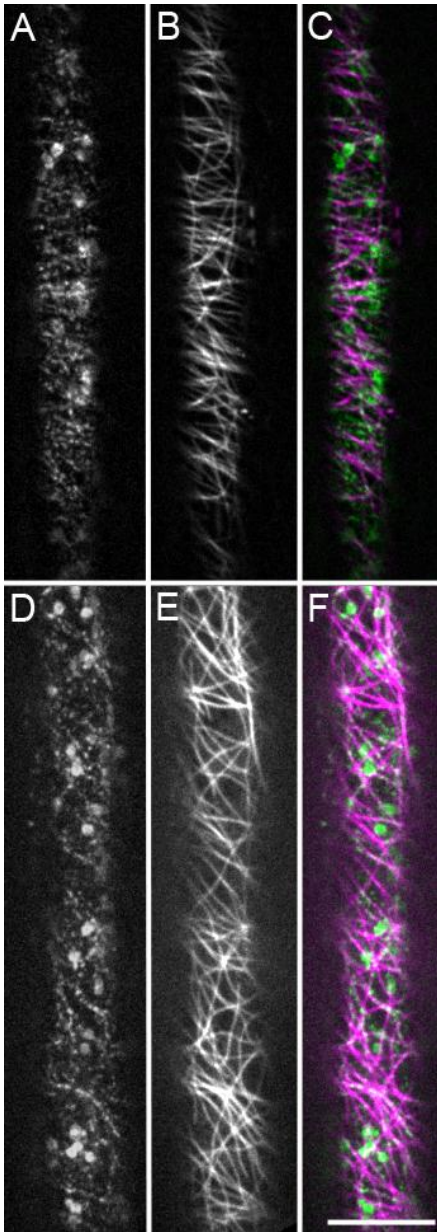
Figures 1A and 1B. Immunolabeling with a CESA antibody on BMM sections of cryo-fixed Arabidopsis roots reveals rows of dots that are oriented transversely to the long cell axis in epidermal cells of A the root elongation zone and B of the root hair zone. Bars: 10 μm .

root elongation zone (figure 2A-C) and root hair zone (figure 2D-F). Although the overall image is the same as for the immunolabeled cells, particles are less distinct and, therefore, numbers of particles were more difficult to count. In addition, only the outer periclinal cell face could be studied. Over time, CESA complexes in a row move, one after the other, with velocities of $283 \pm 56 \text{ nm min}^{-1}$ in cells of the root elongation zone and $301 \pm 60 \text{ nm min}^{-1}$ in the root hair zone (supplemental movies 1 and 2), Kymographs show that the movement is bidirectional (Figure 3). Similar to the immunolabeled samples, we measured the angles of the CESA rows to the long axis of the root, and the density of the rows. These data are given in table I. Although the rows of CESA complexes are oriented transversely to the long axis of the cells in both immunolabeled and GFP:CESA3 expressing samples of elongating cells, there

there is more variation in the angles of rows in the cells expressing GFP:CESA3 (table I). For all measurements, at least 5 cells were measured.

CESA complexes follow CMTs in growing and fully-grown root epidermal cells

To relate the orientation and density of the rows of CESA complexes to the orientation and density of the CMTs, we immuno-labelled the CMTs using the same fixation and labelling procedures as used for CESA detection. In addition CMTs were visualized by live cell imaging using 35S::mCherry:MAP4-MBD (Figure 2C), which we used previously (Gutierrez et al., 2009); Both methods gave similar results, but in immunolabeled samples it was possible to observe the CMTs of the inner cell faces of epidermal cells and sub-epidermal tissues as well (see supplement). Of the total amount of CESA complexes in the plasma membrane of GFP:CESA3 expressing cells, 93.7 ± 1.5 % of them tracked the CMTs in root epidermal cells in the elongation zone (n= 442 CESA complexes in 4 cells) and 95.8 ± 2.0 % in root epidermal cells in the root hair zone (n= 1050 CESA complexes in 8 cells). In the root elongation zone (bundles of) CMTs and rows of CESA complexes were all transversely orientated to the root axis, both in the inner and outer cell face (sections). The density of the CMT (bundles) was similar to that of the CESA complex rows ($1.41 \pm 0.17 \mu\text{m}^{-1}$) measured in the sections of cells of the root elongation zone (n=102 CMTs in 6 cells) and $1.08 \pm 0.23 \mu\text{m}^{-1}$ in cells of the root hair zone (n=98 CMTs in 5 cells).



On the left figure 2. Micrographs of cells expressing the CESA complex marker GFP:CESA3 (A and D) and the microtubule marker mCherry:MBD (B and E). A-C show images from an epidermal cell in the root elongation zone. Most CMTs and rows of CESA complexes are oriented transversely to the growth axis of the cell. D-F show images from an epidermal cell in the root hair zone. In this cell the net orientation of CMTs and rows of CESA complexes is also transverse to the growth axis, but more variation in angle can be observed. C and F show overlays of GFP:CESA3 (green) and mCherry:MBD (red). The large lumps in the GFP:CESA3 images are Golgi bodies containing GFP:CESA3. Image sequences over time

of these cells can be seen in supplemental movie 1 (cell from the elongation zone) and 2 (cell from the root hair zone). Bars: 10 μ m.

On the right figure 3. Kymograph of CESA complexes in fully grown cells showing bidirectional motility of CESA complexes over a single CMT.

FESEM-imaged microfibril orientation and density in root epidermal cells

CESA complexes produce CMFs. We visualized CMFs using Field Emission Scanning Electron Microscopy (FESEM) of cell walls from which the cell wall matrix material had been removed. Figure 4 shows overviews of roots (Figure 4A-B) with details of the most recently deposited CMFs of the inner and outer periclinal walls of an epidermal cell in the root elongation zone (Figure 4C-D). The CMF orientation in different wall facets of these cells was uniform. In epidermal cells of the root hair zone (Figure 5) we also found transversely oriented CMFs in the most recently deposited layers of inner (Figure 5C) and outer walls (Figure 5D). FESEM images of CMFs of plant cell wall show fibrillar structures of up to 10 nm in diameter. This is including the Platinum/Carbon deposit. In preparations of KMnO₄ stained thin sections of material in which the cell wall matrix is removed almost completely (van der Wel et al., 1996) the diameter of single CMFs is approx. 3 nm (Emons, 1988), comparable to what is found by X-ray analysis (Kennedy et al., 2007). Comparison of thin sections and surface preparations indicate that the CMFs in such FESEM preparations do not coalesce, and are single CMFs (see for instance Akkerman et al., 2012 and references therein for *Arabidopsis* root hairs).

Measurements of CMF densities and angles reveal an evenly spread layer of CMFs with densities of CMFs varying between 42.0 and 48.9 CMF μm^{-1} (table I; $n > 200$ CMFs in at least 5 independent cells per given value) and CMF angles to the long axis of the root were similar to those of CMTs and rows of CESA complexes (table I). Although the distances between FESEM-imaged microfibrils may not be very accurate, and it cannot be observed which CMFs are produced at a particular moment in time, it is clear that an even layer is produced.

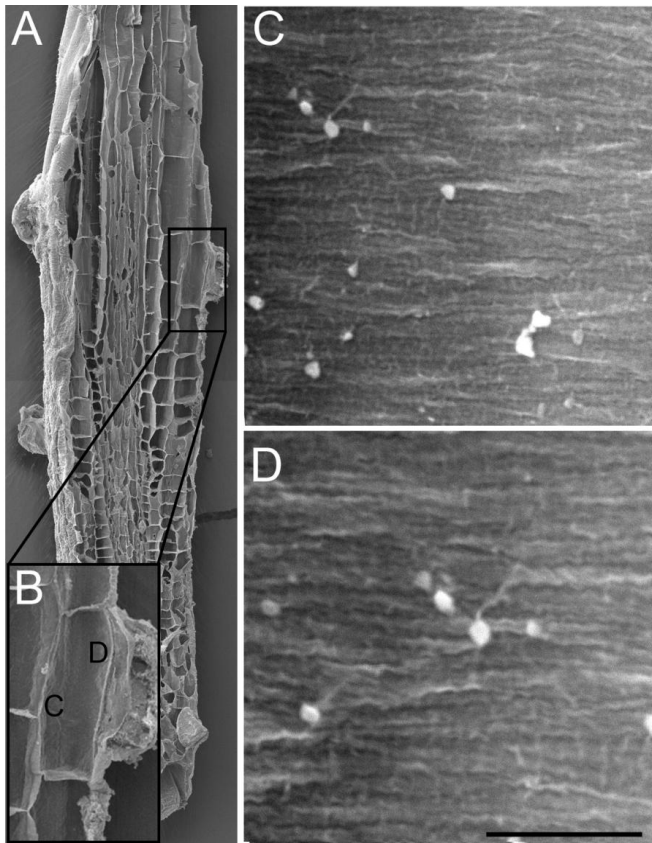


Figure 4. The orientation of the most recently deposited CMFs in the inner (C) and outer (D) periclinal wall of an epidermal cell in the root elongation zone. A and B show the exact locations of C and D. Bar: 500 nm.

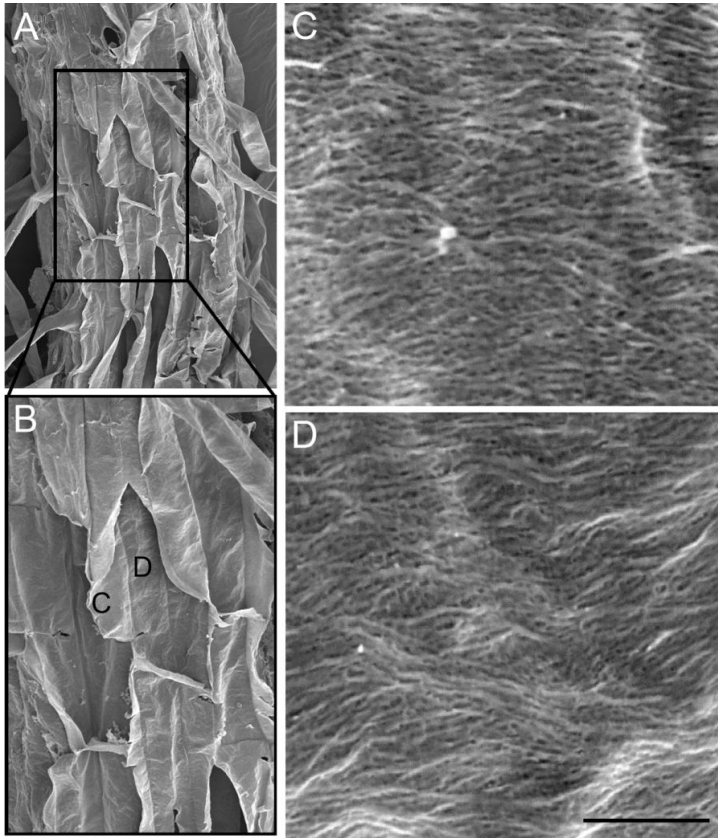


Figure 5. The orientation of the most recently deposited CMFs in the inner (C) and outer (D) periclinal wall of an epidermal cell in the root hair zone. A and B give the exact locations of C and D. Bar: 500 nm.

Table I. Values measured in root epidermal cells using different techniques

Outer periclinal cell face Elongation zone	Immuno	Live imaging GFP:CESA3	FESEM
Density of rows CESA complexes*	1.79 ± 1.15	0.93 ± 0.03	n/a
Orientation of rows CESA complexes**	0.3 ± 5.6°	3.1 ± 19.9°	n/a
Dots per micrometer in a row	1.80 ± 0.56	1.94 ± 0.30	n/a
Angles of cellulose microfibrils**	n/a	n/a	1.4 ± 3.0°
Density cellulose microfibrils (CMF µm ⁻¹)	n/a	n/a	44.8 ± 5.7
Density of CMT (bundles) (CMT µm ⁻¹)	1.41 ± 0.17		
Outer periclinal cell face Root hair zone	Immuno	Live imaging GFP:CESA3	FESEM
Density of rows CESA complexes*	1.08 ± 0.23	0.75 ± 0.11	n/a
Orientation of rows CESA complexes**	10.7 ± 6.9°	10.6 ± 32.0°	n/a
Dots per micrometer in a row	1.54 ± 0.45	1.60 ± 0.21	n/a
Angles of cellulose microfibrils**	n/a	n/a	10.1 ± 10.1°
Density cellulose microfibrils (CMF µm ⁻¹)	n/a	n/a	48.2 ± 7.7
Density of CMT (bundles) (CMT µm ⁻¹)	1.08 ± 0.23		
Inner periclinal cell face Elongation zone	Immuno	Live imaging GFP:CESA3	FESEM
Density of rows CESA complexes*	1.59 ± 0.93	n/a	n/a
Orientation of rows CESA complexes**	2.1 ± 3.0°	n/a	n/a
Dots per micrometer in a row	1.85 ± 0.24	n/a	n/a
Angles of cellulose microfibrils**	n/a	n/a	0.3 ± 7.2°
Density cellulose microfibrils (CMF µm ⁻¹)	n/a	n/a	48.9 ± 8.2
Inner periclinal cell face Root hair zone	Immuno	Live imaging GFP:CESA3	FESEM
Density of rows CESA complexes*	0.97 ± 0.36	n/a	n/a
Orientation of rows CESA complexes**	7.2 ± 5.1°	n/a	n/a
Dots per micrometer in a row	1.44 ± 0.50	n/a	n/a
Angles of cellulose microfibrils**	n/a	n/a	7.2 ± 10.0°
Density cellulose microfibrils (CMF µm ⁻¹)	n/a	n/a	42.0 ± 9.4

* Densities in µm⁻¹.

** Deviation from transverse to the elongation axis (transverse is 0°).

CMTs reposition continuously

There is a discrepancy between the more or less uniform distribution of CMFs in the most recently deposited layer of the cell wall and the rows of CESA complexes in the plasma membrane that produce CMFs. To solve the paradox that CESA complexes move in rows along CMTs while producing an evenly spread layer of CMFs, we tested whether CMT positions change over time by recording long-term movies of the CMTs. Since cell elongation would interfere with determination of CMT positions over time, for these experiments we used cells in the zone where root hair growth had just terminated and collected an image every 10 minutes (Figure 6). CMTs in these cells are still transversely oriented. When a time projection is made of 3 subsequent images, the percentage of the cell cortex that is covered by the CMTs was much higher than in individual images, showing that the CMTs indeed reposition continuously.

Discussion

We studied the relation between CMTs, CESA complexes and CMFs in root epidermal cells of *Arabidopsis* using live imaging of CESA complexes and CMTs with spinning disc microscopy, immunofluorescence labeling of CESA complexes and CMTs, and FESEM of CMFs.

In the plasma membrane of *Arabidopsis* root epidermal cells, CESA complexes are present as dots positioned in rows, where they move with an average velocity of approximately 300 nm min^{-1} . This is in accordance with the results on CESA complex movement as observed in hypocotyl cells of *Arabidopsis* (Paredes et al. 2006; Debolt et al. 2007; Persson et al. 2007; Desprez et al. 2007; Crowell et al. 2009; Gutierrez et al. 2009; Chan et al. 2010). This velocity was observed throughout the elongation and root hair zone of the root, from early stages of cell elongation, just after cell division, up to the root hair zone with fully-grown cells and also those higher up in the root having obliquely oriented CMFs (data not shown). Lower or higher velocities of CESA complexes might be measured depending on the temperature (Fujita et al. 2011).

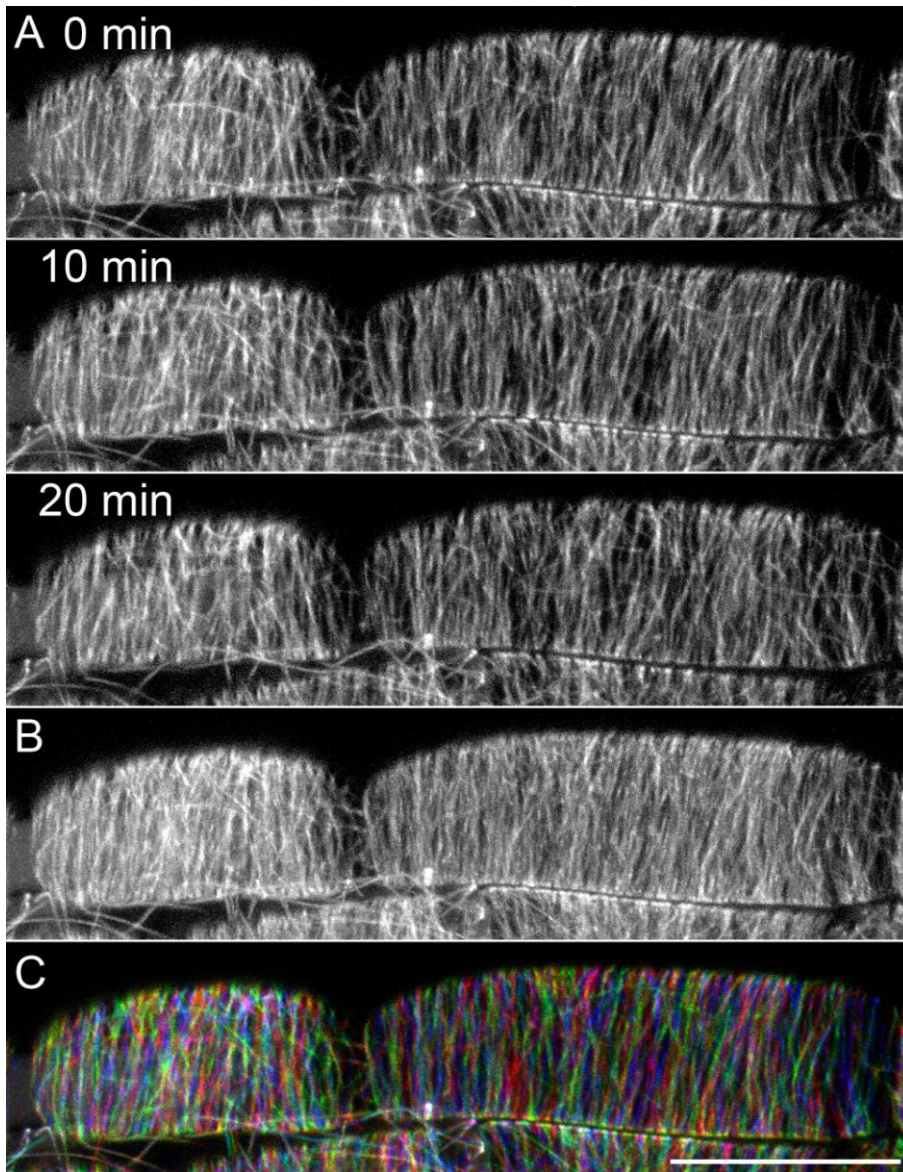


Figure 6. CMT organization changes over time to cover a larger part of the cell cortex. A shows three frames of a time series with 10 minutes intervals. B shows a black and white overlay of the three images shown in A and C shows a pseudocoloured overlay of the images shown in A, with CMTs at 0 min in red, at 10 min in green and at 20 min in blue. Bar: 10 μ m.

The orientation of CMTs, CESA complex movement, and CMFs in elongating root epidermal cells up to the root hair zone is transverse to the elongation axis of the root. In older cells located further away from the root tip the orientation is helical. Orientations are similar in the inner and outer face of the root epidermal cell. This is different from the situation in elongating hypocotyl cells in which only in the inner cell face the orientation remains transverse during the whole elongation period (Chan et al., 2011; Crowell et al., 2011; Fujita et al., 2011). A difference in cell morphology is, however, that hypocotyl cells are more rounded at the outside than root epidermal cells.

Differences in the density of CESA rows and the variation in CESA row angles are observed using different visualization methods.

Most results that were obtained using the different techniques are in accordance with each other. However some results are different when we compare the outcomes of the analyses of images obtained with different techniques.

The density of clear rows of CESA complexes in epidermal cells of the root elongation zone is almost twice as low in GFP:CESA3 lines compared to the immunocytochemistry results ($0.93 \pm 0.03 \mu\text{m}$ compared to $1.79 \pm 1.15 \mu\text{m}$). Since CESA complexes move along CMTs, this could be caused by the constant reorganization of CMTs and stabilization during fixation. We can also not exclude that the antibody labels more CESA complexes than the live probe so that more CESA complexes are detected. However the density of dots in a row does not differ between the different methods so this explanation is not very likely.

Although the average orientation of the rows of CESA complexes is similar in immunolabeled and live samples, the standard deviation is much higher in live samples. The variation in angle of CESA rows in the immunolabeled cells is similar to that of CMFs but much smaller than that of CESA rows in GFP:CESA3 expressing cells. One should realize that the CMFs that we see at the inside of the cell wall represent the tracks of CESA complexes during a certain period of time. An explanation for the difference in angle variation of CESA rows between the two different techniques could be that due to the laser light some

CMTs might react by reorientation during live imaging. Also during fixation changes may occur in the CMT array and probably in the CESA complex rows that follow these CMTs.

CESA complexes run in rows but produce an even layer of CMFs because the CMTs that they follow reposition continuously

Analysis of the densities of CMTs, CMFs and CESA complex rows shows a similarity between the densities of CMTs and rows of CESA complexes that follow the CMTs, but a discrepancy between these two densities and that of the CMFs. Whereas the density of CMFs varies from 42.0 to 48.9 per μm , the maximal average density of CESA rows that we found was 1.79 per μm . This is understood when we realize that these CMFs have been made in a certain time period. How can CESA complexes that move in rows produce a layer of uniformly distributed and oriented CMFs as seen in the CMF preparations obtained with FESEM, and do not produce local wall thickenings of several CMFs on top of each other?

Firstly, the limited resolution of the light microscope requires attention: a CMT is 25 nm across, a dimension like that of a CESA complex. In the light microscope these objects are imaged at a size consistent with the relevant airy disc, typically about 10 times larger. This indicates that the precise location of a CMF that is deposited by a CESA complex that co-localizes with a CMT cannot be resolved. If CESA complexes do not move over CMTs, but move up to several hundred nanometers away from CMTs, this could explain part, but not all of the even distribution of CMFs, since the distance between CMTs is much larger than the resolution limit.

Secondly, the majority of CESA complexes moves along CMTs, just like in etiolated hypocotyl cells (Paredes et al. 2006). We show that in the root epidermal cells over 90% of CESA complexes move, bidirectionally, along CMTs. Since less than 10% of the CESA complexes produces a CMF between the CMTs, these cannot produce all the CMFs located between the CMTs. We hypothesized that the CMTs shift their orientation constantly. We were not able to measure this in elongating cells, since the constant elongation of these cells under the microscope is a complicating factor. Therefore we used cells

from the root hair zone in which elongation just ceased but CMFs are still transverse to the elongation direction. We show that the CMTs constantly reorganise (Figure 6). Thus, CMT reorganization over time produces a uniform layer of CMFs, instead of producing a cell wall with local accumulations of CMFs on top of each other. The mechanism for the reorganization is probably the dynamic instability of the CMT ends in combination with the action of several known microtubule binding proteins (MAPs) as shown in a theoretical model that explains alignment of CMTs (see Tindemans et al, 2010). Among many regulatory MAPs the microtubule severing protein katanin plays an important role in microtubule dynamics (Uyttewaal et al 2012, Bichet et al., 2001; Burk et al., 2001; Burk and Ye, 2002; Nakamura et al., 2010; Stoppin-Mellet et al., 2006; Wasteneys and Ambrose, 2009). Furthermore the dynamic instability might also be regulated by a kinesin. Kinesins of the KinI/Kinesin-13 family are thought to have a regulatory role in the depolymerization at both ends of microtubules in *Drosophila* (Wu et al. 2006) and kinesin 13A has been localized to Golgi associated vesicles in *Arabidopsis* root cap peripheral cells using immunogold labeling for transmission electron microscopy (Wei et al. 2009).

Given the circumference of root epidermal cells, the movement velocity of CESA complexes, the density of CESA complexes in a row and the CMT reorganization velocity, our results on shifting CMTs explain how a uniform layer of CMFs can be formed.

Materials and methods

Plant growth

Surface sterilized *Arabidopsis* Col-0 seeds were germinated on vertically positioned agar plates containing half strength MS medium and 1.2% phyto-agar (Duchefa, Haarlem, The Netherlands) at 25°C with a 16/8 hr photoperiod at 150 $\mu\text{mol m}^{-2} \text{s}^{-1}$.

Rapid freeze fixation, sectioning and immunolabeling

3-day old seedlings were plunged into liquid propane, followed by freeze-substitution in methanol + 0.5% - 1% water free glutaraldehyde (GA) over a

period of 4 days during which the temperature was gradually raised from -90°C to 0°C. The freeze substitution medium was gradually exchanged to 100% ethanol on ice, followed by a graded series of ethanol: butyl-methyl-metacrylate (BMM) (Baskin et al. 1992) followed by a 1 day wash in 100% BMM. BMM containing samples were polymerized at -20°C by exposure to UV light. 4-5 µm thick sections were produced using a Reichert Ultracut microtome. Sections were placed on a droplet of water on an object slide, stretched by exposure to chloroform vapour and baked onto the slides at a heating plate of 56°C for 30 minutes. Samples were labeled as described previously (Ketelaar et al., 2003) with an antibody against CESA, a polyclonal antibody against 15 amino acids (NH₂-NELPRLVYVSREKRPGC-COOH) present in all 10 isoforms of CesaA in Arabidopsis (Gillmor et al., 2002). The peptide sequence is located in the large central cytoplasmic domain of CesaA (Pear et al., 1996). The antibody was kindly provided by Prof. Chris Somerville.

Imaging and analysis of immunolabeled samples

Z-series were acquired of the immunolabeled sections using the standard FITC settings of a Zeiss LSM510 Pascal confocal laser scanning microscope. Image processing using Image J was performed as follows. Background signal was removed using the Subtract Background command (100 pixels ball size) and maximum intensity z-projections were made of the z-series. Figures were made in Adobe Photoshop CS2.

Live cell imaging

Roots were grown in Biofoil sandwiches as described by Ketelaar et al., 2004. 4-5 days old seedlings were used. Imaging was performed on a spinning disk confocal microscope (Roper) using the settings as described by Gutierrez et al. (2009). Collected time series were processed by applying the Walking Average plugin and Image J rolling average algorithm and the Subtract Background command (ball size 100 pixels).

FESEM analysis of cellulose microfibril texture

Plants were fixed with 3% glutaraldehyde in 0.1 M phosphate buffer (pH 7.2) for 3 hours at room temperature, followed by 3 washes in demi water of 10 minutes each. Plants were infiltrated with 20% sucrose for 1 hour, where after

roots were dissected, placed on a rivet stud with Tissue Tek (Sakura Finetek Europe B.V., Alphen aan de Rijn, The Netherlands) and frozen in liquid nitrogen. To allow observation of the cell walls, the outer part of the roots was removed by longitudinal sectioning using cryo ultramicrotomy. The remaining parts of the roots were thawed and washed in demi water 3 times for 10 minutes, where after cell contents were extracted during a 20 minutes treatment with 0.1% sodium hypochlorite. After extraction, samples were washed in demi water (3 times 10 minutes) and dehydrated through a graded ethanol series. Ethanol infiltrated samples were critical point dried with carbon dioxide, attached to a SEM sample holder using carbon adhesive tabs (EMS, Washington, USA) and sputter coated with 5 nm platinum in a dedicated preparation chamber (CT 1500 HF, Oxford Instruments, Oxford, UK). The roots were analyzed with a field emission scanning electron microscope (JEOL 6300 F, Tokyo, Japan) at ambient temperature at a working distance of 8 mm with SE detection at 3,5 – 5 kV. Images were digitally recorded using an Orion 6 camera (ELI, Charleroi, Belgium) and were resized and contrast stretched using Adobe Photoshop CS2.

Financial support

YZ and AMCE were supported by a grant from the EU Commission (FP6-2004-NEST-C1-028974). Funding for the Spinning Disc confocal microscope was obtained from the Division for Earth and Life Sciences (ALW) with financial aid from the Netherlands Organization for Scientific Research (NWO).

Acknowledgements

We thank Chris Somerville for the kind gift of the anti-CESA antibody, and Jelmer Lindeboom for *Arabidopsis* plants carrying fluorescent CESA and microtubule markers and helpful discussions.

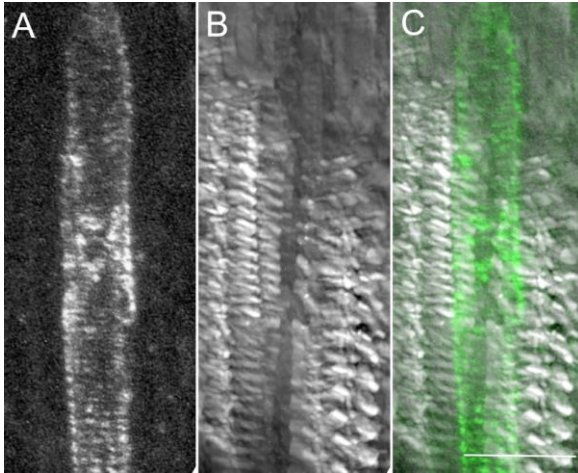
References

- Baskin TI, Busby CH, Fowke LC, Sammut M, Gubler F (1992) Improvements in immunostaining samples embedded in methacrylate: localization of microtubules and other antigens throughout developing organisms in plants of diverse taxa. *Planta* 187: 405-413
- Baskin TI (2001) On the alignment of cellulose microfibrils by cortical microtubules: a review and a model. *Protoplasma* 215: 150-171
- Baskin TI (2005) Anisotropic Expansion of the Plant Cell Wall. *Annu. Rev. Cell. Dev. Biol.* 21:203-222.
- Baskin TI, Beemster GT, Judy-March JE, Marga F (2004) Disorganization of cortical microtubules stimulates tangential expansion and reduces the uniformity of cellulose microfibril alignment among cells in the root of *Arabidopsis*. *Plant Physiol.* 135: 2279-2290
- Beemster GT, Baskin TI (1998) Analysis of cell division and elongation underlying the developmental acceleration of root growth in *Arabidopsis thaliana*. *Plant Physiol.* 116: 1515-1526
- Cai G, Falero C, Del Casino C, Emons AM, Cresti M (2011) Distribution of callose synthase, cellulose synthase, and sucrose synthase in tobacco pollen tube is controlled in dissimilar ways by actin filaments and microtubules. *Plant Physiol.* 155: 1169-1190
- Chan J, Calder G, Fox S, Lloyd C (2007) Cortical microtubule arrays undergo rotary movements in *Arabidopsis* hypocotyl epidermal cells. *Nat. Cell Biol.* 9: 171-175
- Chan J, Crowell E, Eder M, Calder G, Bunnewell S, Findlay K, Vernhettes S, Höfte H, Lloyd C (2010) The rotation of cellulose synthase trajectories is microtubule dependent and influences the texture of epidermal cell walls in *Arabidopsis* hypocotyls. *J Cell Sci.* 123: 3490-3495
- Chan J, Eder M, Crowell EF, Hampson J, Calder G, Lloyd C (2011) Microtubules and CESA tracks at the inner epidermal wall align independently of those on the outer wall of light-grown *Arabidopsis* hypocotyls. *J. Cell Sci.* 124: 1088-1094
- Crowell EF, Bischoff V, Desprez T, Rolland A, Stierhof YD, Schumacher K, Gonneau M, Höfte H, Vernhettes S (2009). Pausing of Golgi bodies on microtubules regulates secretion of cellulose synthase complexes in *Arabidopsis*. *Plant Cell* 21: 1141-1154
- Crowell EF, Timpano H, Desprez T, Franssen-Verheijen T, Emons AM, Höfte H, Vernhettes S (2011) Differential regulation of cellulose orientation at the inner and outer face of epidermal cells in the *Arabidopsis* hypocotyl. *Plant Cell*, in press.
- DeBolt S, Gutierrez R, Ehrhardt DW, Melo CV, Ross L, Cutler SR, Somerville C, Bonetta D (2007). Morlin, an inhibitor of cortical microtubule dynamics and cellulose synthase movement. *Proc. Natl. Acad. Sci. USA* 104: 5854-5859
- Desprez T, Juraniec M, Crowell EF, Jouy H, Pochylova Z, Parcy F, Höfte H, Gonneau M, Vernhettes S (2007) Organization of cellulose synthase complexes involved in primary cell wall synthesis in *Arabidopsis thaliana*. *Proc. Natl. Acad. Sci. USA* 104: 15572-15577
- Emons AMC (1985). Plasma-membrane rosettes in root hairs of *Equisetum hyemale*. *Planta* 163: 350-359

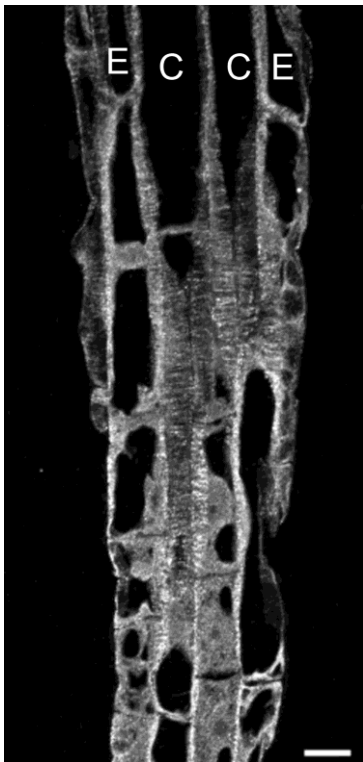
- Emons AMC, Höfte H, Mulder BM (2007) Microtubules and cellulose microfibrils: how intimate is their relationship? *Trends Plant Sci.* 12: 279-281
- Fujita M, Himmelspach R, Hocart CH, Williamson RE, Mansfield SD, Wasteneys GO (2011) Cortical microtubules optimize cell-wall crystallinity to drive unidirectional growth in *Arabidopsis*. *Plant J.* 66: 915-928
- Gardiner JC, Taylor NG, Turner SR (2003) Control of cellulose synthase complex localization in developing xylem. *Plant Cell* 15: 1740-1748
- Gillmor CS, Poindexter P, Lorieau J, Palcic MM, Somerville C (2002) α -Glucosidase I is required for cellulose biosynthesis and morphogenesis in *Arabidopsis*. *J. Cell Biol.* 156: 1003-1013
- Green PB (1962). Mechanism for plant cellular morphogenesis. *Science* 138: 1404-1405
- Gutierrez R, Lindeboom JJ, Paredez AR, Emons AM, Ehrhardt DW (2009) *Arabidopsis* cortical microtubules position cellulose synthase delivery to the plasma membrane and interact with cellulose synthase trafficking compartments. *Nat. Cell Biol.* 11: 797-806
- Hamant O, Traas J, Boudaoud A (2010) Regulation of shape and patterning in plant development. *Curr. Opin. Genet. Dev.* 20: 454-459
- Hamant O, Heisler MG, Jönsson H, Krupinski P, Uyttewaal M, Bokov P, Corson F, Sahlin P, Boudaoud A, Meyerowitz EM, Couder Y, Traas J (2008) Developmental patterning by mechanical signals in *Arabidopsis*. *Science* 322: 1650-1655
- Herth W (1985) Plasma-membrane rosettes involved in localized wall thickening during xylem vessel formation of *Lepidium sativum* L. *Planta* 164:12-21
- Ketelaar T, de Ruijter NC, Emons AM (2003) Unstable F-actin specifies the area and microtubule direction of cell expansion in *Arabidopsis* root hairs. *Plant Cell* 15: 285-292
- Kimura S, Laosinchai W, Itoh T, Cui X, Linder CR, Brown RM Jr. (1999) Immunogold labeling of rosette terminal cellulose-synthesizing complexes in the vascular plant *Vigna angularis*. *Plant Cell* 11: 2075-2085
- Mueller SC, Brown RM Jr. (1980) Evidence for an intramembrane component associated with a cellulose microfibril-synthesizing complex in higher plants. *J. Cell Biol.* 84: 315-326
- Nicol F, His I, Jauneau A, Vernhettes S, Canut H, Höfte H (1998) A plasma membrane-bound putative endo-1,4- β -D-glucanase is required for normal wall assembly and cell elongation in *Arabidopsis*. *EMBO J* 17: 5563-5576
- Paredez AR, Somerville CR, Ehrhardt DW (2006) Visualization of cellulose synthase demonstrates functional association with microtubules. *Science* 312: 1491-1495
- Persson S, Paredez A, Carroll A, Palsdottir H, Doblin M, Poindexter P, Khitrov N, Auer M, Somerville CR (2007) Genetic evidence for three unique components in primary cell-wall cellulose synthase complexes in *Arabidopsis*. *Proc. Natl. Acad. Sci. USA* 104: 15566-15571
- Schindelman G, Morikami A, Jung J, Baskin TI, Carpita NC, Derbyshire P, McCann MC, Benfey PN (2001) COBRA encodes a putative GPI-anchored protein, which is polarly localized and necessary for oriented cell expansion in *Arabidopsis*. *Genes Dev.* 15: 1115-1127
- Sugimoto K, Williamson RE, Wasteneys GO (2000) New techniques enable comparative analysis of microtubule orientation, wall texture, and growth rate in intact roots of *Arabidopsis*. *Plant Physiol.* 124: 1493-1506
- Tindemans SH, Hawkins RJ, Mulder BM (2010) Survival of the aligned: ordering of the plant cortical microtubule array. *Phys. Rev. Lett.* 104: 058103

Zhong R, Kays SJ, Schroeder BP, Ye ZH (2002) Mutation of a chitinase-like gene causes ectopic deposition of lignin, aberrant cell shapes, and overproduction of ethylene. *Plant Cell* 14: 165-179

Supporting information



Supplemental figure 1. The CESA antibody labels bands in the plasma membrane of developing root xylem cells. A = anti-CESA, B = DIC, C = overlay with A in green.



Supplemental figure 2. Microtubule organization in an immunolabeled section through the root elongation zone. Microtubules in different root cell types all are transversely oriented to the long axis of the root. This image shows both cortical (indicated with a C) and epidermal (indicated with an E) cell files. Bar: 10 μ m.

Chapter 4

Texture of cellulose microfibrils of root hair cell walls of *Arabidopsis thaliana*, *Medicago truncatula* and *Vicia sativa*

**Miriam Akkerman¹, Tiny Franssen Verheijen^{1,2}, Peter Immerzeel^{1,3},
Lianne Den Hollander^{1,4}, Jan H.N. Schel¹, Anne Mie C. Emons^{1*}**

¹ *Laboratory of Cell Biology, Wageningen University*

Droevendaalsesteeg 1, 6708 PB Wageningen, the Netherlands

² *Present address: Wageningen Electron Microscopy Center, Laboratory of Virology, Wageningen University*

³ *Present address: Umeå Plant Science Centre, Department of Forest Genetics and Plant Physiology, SLU, 90183, Umeå, Sweden*

⁴ *Present address: Department of Cell and Molecular Biology (CMB), Karolinska Institute, Box 285, S-171 77 Stockholm, Sweden*

*This chapter has been published in the Journal of Microscopy. doi:
10.1111/j.1365-2818.2012.03611.x (2012)*

Abstract

Cellulose is the most abundant biopolymer on earth, and has qualities that make it suitable for biofuel. There are new tools for the visualization of the cellulose synthase complexes in living cells, but those do not show their product, the cellulose microfibrils (CMFs). In this study we report the characteristics of cell wall textures, i.e. the architectures of the CMFs in the wall, of root hairs of *Arabidopsis thaliana*, *Medicago truncatula* and *Vicia sativa* and compare the different techniques we used to study them. Root hairs of these species have a random primary cell wall deposited at the root hair tip, which covers the outside of the growing and fully-grown hair. The secondary wall starts between 10 (*Arabidopsis*) and 40 (*Vicia*) μm from the hair tip and the CMFs make a small angle, Z as well as S direction, with the long axis of the root hair. CMFs are 3-4 nm wide in thin sections, indicating that single cellulose synthase complexes make them. Thin sections after extraction of cell wall matrix, leaving only the CMFs, reveal the type of wall texture and the orientation and width of CMFs, but CMF density within a lamella cannot be quantified, and CMF length is always underestimated by this technique. Field emission scanning electron microscopy and surface preparations for transmission electron microscopy reveal the type of wall texture and the orientation of individual CMFs. Only when the orientation of CMFs in subsequent deposited lamellae is different, their density per lamella can be determined. It is impossible to measure CMF length with any of the EM techniques.

Introduction

Cellulose is an unbranched β -1,4-D- glucan polymer. The cellulose microfibril (CMF) consists of about 18 cellulose chains (Kennedy *et al.*, 2007), it is the most abundant biopolymer on earth and an important asset for biofuel (Somerville, 2006). New tools to study the cellulose production in plants have become available, the fluorescent CESA constructs make direct visualization of CMF production in living cells under experimental condition possible (Paredes

et al., 2006, Gutierrez *et al.*, 2009, Persson *et al.*, 2005, Paredez *et al.*, 2008, Crowell *et al.*, 2009, Chan *et al.*, 2010.). Cellulose synthases (CESAs) are the glucosyltransferases inside the cellulose synthase complex that produce the CMFs (Persson *et al.*, 2007). Together, these two aspects, new tools as well as industrial importance, make cellulose biosynthesis an active area of research (Somerville, 2006) and are giving new interest in cell wall texture visualization.

Cell walls are classified as primary and secondary. Primary walls are deposited by growing cells. They are dynamic structures as the linkages between the different polymers bind and unbind to give flexibility and the possibility for the wall to stretch during cell elongation (Carpita & Gibeaut, 1993). In primary walls CMFs reorient during cell elongation (Wolters-Arts & Sassen, 1991). Secondary walls are produced by fully-grown cells and are mechanically more static structures that maintain size and shape of mature cells. The secondary cell wall is mostly deposited as an even layer with a higher fraction of cellulose than the primary wall (Fry, 1988), and it may be deposited in bands, as is the case in xylem cells (Turner *et al.*, 2007). With respect to this primary and secondary cell wall nomenclature defined by the participants of the first international Cell Wall Meeting held in Nijmegen the Netherlands in 1978, root hairs are a special case. They grow at the cell tip where the primary cell wall is deposited, which shifts over the cell's hemisphere and covers the whole outside of the tube. At the same time, a secondary wall is deposited inside the tube (Emons & Wolters Arts, 1983). Because this inner wall does not expand, it is secondary by definition. Since all CMFs in the secondary cell wall stay in place, they show the history of wall deposition in sections through the cell wall. Moreover, along the plasma membrane in elongating hairs, CMF deposition can be observed from the youngest CMF texture at the tip to a more and more mature texture in the direction of the root hair base (Emons, 1989).

Cellulose microfibril texture is considered as the architecture of all the CMFs in a cell wall. The main function of the CMF texture is to provide mechanical strength for every plant cell and for the plant as a whole. In growing cells it determines the orientation of cell elongation (Baskin, 2001, Sugimoto *et al.*,

2000). Cell wall textures have been studied in more depth in root hairs than in other cell types. Being tubular extensions of epidermal cells, root hairs anchor plants in the soil and facilitate the intake of water and minerals from it. They develop from specialized epidermal cells, trichoblasts, which occur in files as in *Arabidopsis thaliana* (Dolan *et al.*, 1994), or else, all epidermal cells are trichoblastic and form root hairs as in the studied legumes (Lhuissier *et al.*, 2001, Miller *et al.*, 1997). In legumes they are important for the formation of symbiosis between these plants and *Rhizobium* bacteria (Esseling *et al.*, 2004, Heidstra *et al.*, 1997). The extending outer root surface makes root hairs easily accessible to fixation, drug treatment, signal application, and microscopical visualization.

Cell wall textures are species-, cell- and developmental cell stage specific. They have been studied in root hairs of several species and are classified as axial, helical, helicoidal, crossed and random (Emons & Mulder, 2000, Emons *et al.*, 2002). All primary walls of root hairs studied have random wall texture (Mulder *et al.*, 2004); all other texture types have been found in the wall of the tube of root hairs in a species- and developmental stage specific fashion, except the transverse wall texture. In general, root hairs of aquatic plants have helicoidal, including crossed textures, and those of terrestrial plants have axial/helical textures (Emons & van Maaren, 1987) but exceptions do occur.

Questions that should be answered using methods to reveal the wall texture relate to length, width, shape, density, and orientation of individual CMFs within one cell wall lamella, as well as those same parameters for CMFs of neighbouring lamellae, all together making the cell wall texture. Here we discuss a number of methods available for the study of wall texture at the ultrastructural scale by reporting new data about the cell wall textures of root hairs of *Arabidopsis thaliana*, *Medicago truncatula*, and *Vicia sativa*. These species were chosen because of their importance in research of root hair development (*Arabidopsis thaliana*) and their response to *Rhizobium* bacteria (*Medicago truncatula* and *Vicia sativa*).

Materials and Methods

TEM analysis of ultrathin sections after extraction of cell wall matrix and KMnO₄ staining: *Arabidopsis thaliana* and *Medicago truncatula*

4 Days old seedlings of *Arabidopsis thaliana* (Columbia) were boiled in 30% hydrogen peroxide and 100% acetic acid (1:1) (H₂O₂/HAc) for 50 minutes to remove all cell components and cell wall matrix (Van der Wel *et al.*, 1996). Hereafter they were rinsed in water, dehydrated in a graded ethanol series and ultra-flat embedded in Spurr's resin between two Teflon coated microscope slides. After re-embedding, 90 nm longitudinal sections were made with a Reichert ultracut S of the root part with growing root hairs. Sections were collected on formvar coated grids, post-stained with 3% KMnO₄ for 30 minutes and analyzed with TEM (JEOL 1200 EXII, Tokyo, Japan).

TEM analysis of ultrathin sections after mild extraction of cell wall matrix and PATAg staining: *Medicago truncatula*

3 Days old seedlings of *Medicago truncatula* (line A17) were fixed in 3% glutaraldehyde in 0.1M phosphate buffer pH 7.2. After 15 minutes the roots were cut in pieces. The different root hair zones: growing, growth terminating and fully-grown (Heidstra *et al.*, 1994, de Ruijter *et al.*, 1998) were collected separately, after which fixation was continued during 1 hour and 45 minutes. After fixation the root pieces were washed 3 times for 10 minutes in 0.1M phosphate buffer. The material was postfixated in 4% osmium tetroxide for 1 hour and rinsed 3 times for 10 minutes in water. To reveal the cell wall texture, the cell wall matrix was partially and aspecifically extracted for 24 hours at 37°C in 40% methylamine under continuous mild stirring. Hereafter the material was dehydrated in a graded ethanol series, and ultra-flat embedded in Spurr's resin between two microscope slides coated with liquid releasing agent (EMS).

After re-embedding, ultrathin sections of 90 nm were made with a Reichert ultracut S and were collected on golden 200 mesh grids. For PATAg staining (Thiéry, 1967) the sections were treated with 1% periodic acid for 30 minutes and rinsed with water, 3 x 10 minutes. The grids were transferred to 0.2% thiocarbohydrazide in 20% acetic acid. After 20 h the grids were rinsed in

15% acetic acid 3 x 10 minutes, in 5% acetic acid 2 x 10 minutes, in 2% acetic acid 2 x 10 minutes and in water 1 x 10 minutes. In a dark room the grids were treated with 1% silver proteinate for 30 minutes followed by thoroughly rinsing with water. Imaging has been done with TEM (JEOL1200EX II).

TEM analysis of critical point dried surface preparations after extraction of cell wall matrix: *Vicia sativa*

Roots of two days old seedlings of *Vicia sativa* subspecies *nigra* were fixed in glutaraldehyde (6%) in PBS. The cell wall matrix was extracted with H₂O₂ (30%)/HAc (100%) 1:1 for 1h. at 90-100°C. Roots were washed in water (5x) and attached to poly-L-lysine coated grids for critical point drying (Emons, 1989). The roots on the grids were dehydrated in an ethanol series and critical point dried with CO₂ in a Balzers CPD 020 critical point dryer. Finally the root hairs were cleaved by gently sweeping them over filter paper. The cell wall material remaining on the grids was shadowed at an angle of 45° with approx. 2 nm Platinum and coated with Carbon in a Balzers BAF 400D freeze-etching system. Preparations were examined with TEM, (JEOL 1200 EXII, Tokyo, Japan).

FESEM analysis of root hair walls after extraction of cell wall matrix: *Arabidopsis thaliana*

Roots were boiled for 90 minutes in H₂O₂ (30%)/HAc (100%) 1:1. After washing, the roots were placed on formvar coated TEM grids. The grids were placed on a FESEM sample holder by carbon adhesive tabs (EMS Washington USA) and sputter coated with 5 nm Platinum in a dedicated preparation chamber (CT 1500 HF, Oxford Instruments, Oxford UK). The roots were analyzed with a FESEM (JEOL 6300 F, Tokyo, Japan) at ambient temperature at a working distance of 8 mm with SE detection at 3,5 – 5 kV.

Alternatively, seedlings were fixed in 3% glutaraldehyde in 0.1M phosphatebuffer pH7.2 . After rinsing they were infiltrated with 20% sucrose (cryo-protectant). Root tips were excised with a razor blade, placed on a nail head and frozen in liquid nitrogen. Root surfaces were sliced off with a glass knife on a cryo-ultra-microtome and the remaining portions of the roots were thawed in 20% sucrose. After rinsing the cell wall matrix was extracted with 0.1% sodiumhypochlorite for 10 minutes. Specimens were rinsed and treated

with 1% Osmiumtetroxide in water for 15 minutes. After rinsing they were dehydrated through a graded ethanol series till 100% and transferred to 100% acetone. Specimens were critical point dried using CO₂. They were placed on a FESEM sample holder by carbon adhesive tabs (EMS Washington USA) and sputter coated with 10 nm Platinum. The samples were analyzed at room temperature at 3.5 KV with a JEOL 6300 F FESEM (Tokyo, Japan).

Results

Arabidopsis thaliana has root epidermal cell files with root hairs (trichoblasts) and without root hairs (atrachoblasts) (Dolan et al., 1994). In the legumes (*Vicia sativa* (Miller et al., 1997), *Medicago truncatula* (Sieberer et al., 2000)) all root epidermal cells are trichoblasts.

Cellulose microfibril texture of the cell wall of *Arabidopsis thaliana* root hairs, TEM analysis of ultrathin sections

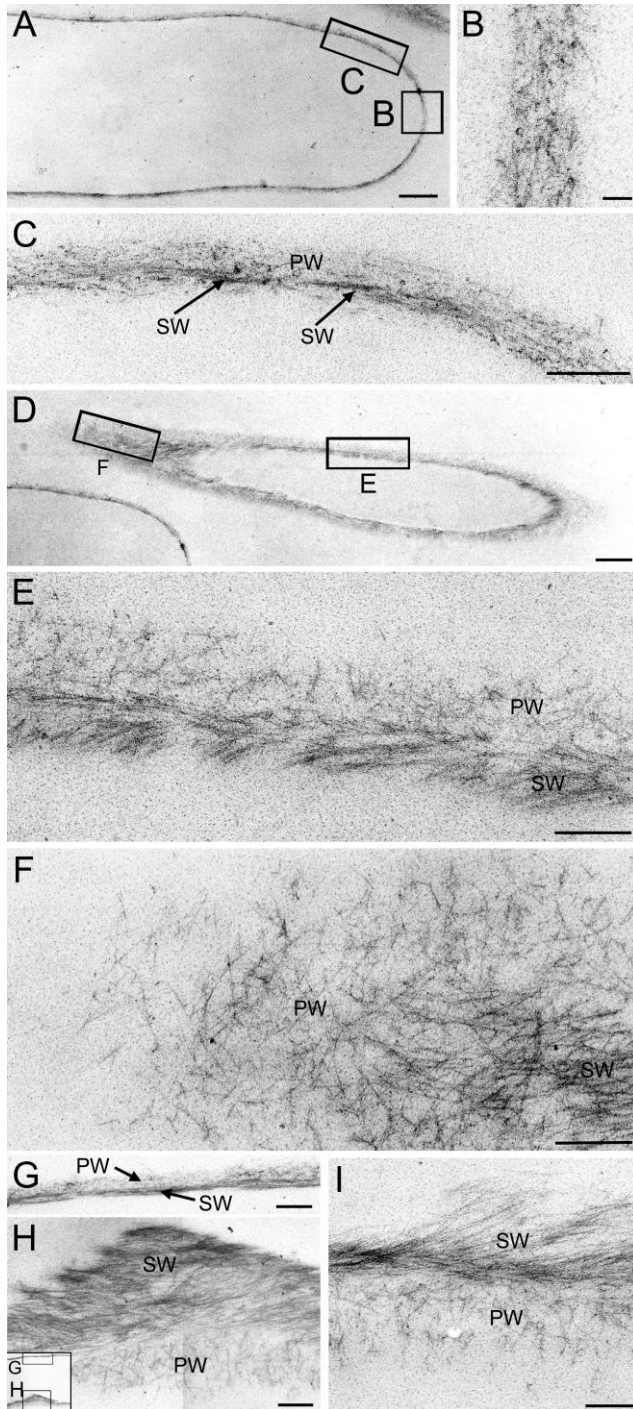
From *Arabidopsis thaliana* roots the cell content and the cell wall matrix were extracted by boiling for 50 minutes in a H₂O₂/acetic acid mixture (see methods), a procedure that leaves almost only crystalline cellulose, as was determined using pyrolysis mass spectrometry analysis (Van der Wel *et al.*, 1996). This remaining material was embedded in Spurr's resin, sectioned, and the sections were stained with KMnO₄, which a-specifically stains the CMFs, virtually the only material left.

In the dome of a growing root hair (Fig. 1A) only the primary wall (PW) is present, a loosely structured assemblage of randomly oriented CMFs (Fig. 1B). During root hair elongation this primary wall is continuously pushed aside by the advancing root hair tip and covers the outside of the whole hair (Figs. 1: PW). Close to the tip of a growing root hair, at a distance of approx. 10 µm from the apex, the formation of the secondary cell wall with more densely packed and longitudinally aligned CMFs starts (Fig. 1C). Fig. 1D represents a tangential section through a hair of approx. 200 µm length, 20 µm from the hair's apex, of which figure 1E is a detail, showing that this inner wall layer, the secondary cell wall, consists of CMFs in two overall orientations, both

making a small angle with the long axis of the hair. Figure 1F is a detail of an obliquely sectioned wall part, partially grazing the primary wall (left side of image). Figure 1G shows a longitudinal section through the basal part of a hair (inset shows overview). At one side the wall has become dented caused by preparation. Here the wall has been sectioned tangentially. The opposite wall was sectioned radially. Figure 1H represents a longitudinal section through the basal part of a growing hair clearly showing the ordered almost axially oriented CMFs facing the cell surrounded by the randomly textured primary wall.

With this extraction and staining method the orientation of CMFs relative to the cell's axis and to each other can be measured. CMF density cannot be determined reliably. The lengths of individual CMFs cannot be determined, since one never knows if the full fibril is in the 90 nm thick section. The width of CMFs is approximately 3 nm, in the primary, as well as in the secondary cell wall, indicating production of CMFs by single cellulose synthase complexes as is normal for higher plants (Somerville, 2006). All freeze fracture studies performed on higher plants show single rosettes and approx. 3 nm thick CMFs, while the thicker CMFs of green algae, like *Valonia* are made by more rosettes together (for review see Emons 1991).

Figure 1 on the next page: TEM micrographs of ultrathin sections of the CMF texture of the cell wall of growing Arabidopsis thaliana root hairs. A. Radial section through the apical part. B. Detail of the primary wall at the very tip. C. Detail of the primary and secondary wall close to the very tip. D. Tangential section through a hair of approx. 200 μm length at about 20 μm from its tip. E. Detail of fig. D, showing the random primary wall texture and the axially/helicallly aligned secondary wall texture. F. Detail of obliquely sectioned wall part, partially grazing the primary wall (left side of image). G,H. Longitudinal section through the basal part of a hair; inset is overview. At one side (G) the wall has been sectioned radially, at the other side (H) the wall has been sectioned tangentially. I. Longitudinal section through basal part of a growing hair showing the ordered helically/axially oriented CMFs, at the side of the cytoplasm (upper side) bordered at the outside by the randomly textured primary wall. (pw; primary wall, sw: secondary wall). Bars: A and D: 1 μm , B: 50 nm, C E F G H I: 200 nm.



Cellulose microfibril texture of the cell wall of *Arabidopsis thaliana* root hairs, FESEM analysis of surface preparations

In surface preparations of the root hair walls CMFs can be visualized after extraction of the cell wall matrix and sputtering with Platinum for observation with Field Emission Scanning Electron Microscopy (FESEM). FESEM of growing *Arabidopsis thaliana* root hairs shows a smooth surface but after wall matrix extraction the random cell wall texture at the outside of the hairs is visible (Fig. 2A). Figure 2B shows a FESEM micrograph taken at the inside of the base of a long hair, showing the axial/helical texture of the secondary cell wall.

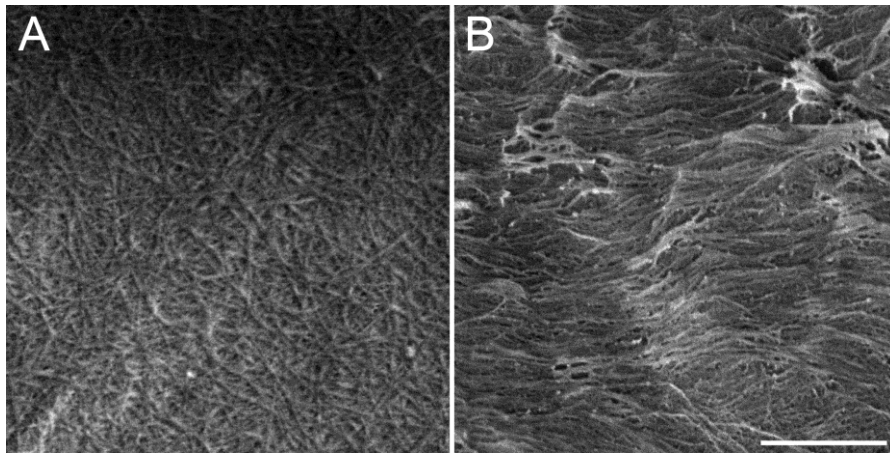


Figure 2: FESEM micrographs of surface preparations of an Arabidopsis thaliana root hair. A: outside of a hair, primary wall texture. B: taken at the base of a fully-grown hair, showing the axial/helical texture of the secondary cell wall. Bar for both images: 250 nm.

It is possible to measure CMF orientation from samples prepared with this technique. The lengths of individual CMFs can only be determined if preparations are as long as individual CMFs but it is difficult to see where CMFs start and end. The width of CMFs including shadow is up to 10 nm., as has been seen in cell walls of higher plants for decennia in such preparations, however the measurement is very imprecise. It does agree with the TEM sections, since the thickness of the deposited shadowing metal has to be subtracted.

Cellulose microfibril texture of the cell wall of *Medicago truncatula* root hairs, TEM analysis of ultrathin sections

In order to visualize the cell wall texture of *Medicago truncatula* root hairs the same method was used as for *Arabidopsis thaliana*, but in addition a more subtle extraction treatment with 40% methylamine, followed by embedding, sectioning and staining of sections with Periodic acid Schiff (PAS) according to the PATAg method developed by Thiéry to keep cell content and especially the cortical microtubules intact (Thiéry, 1967) and for instance used for hypocotyl cells (Refrégier *et al.*, Chan *et al.*, 2010) was carried out instead of the H₂O₂/HAc treatment. Comparison of the two methods shows that the more harsh treatment with H₂O₂/HAc gives a crisper image (Fig. 3B) than the milder extraction procedure (Fig.3A), but both methods show the same features of the overall textures. At the outside of the root hair a random texture is present, and at the inside an additional layer of longitudinally oriented CMFs is observed. CMF length measurement is impossible and density of CMFs are difficult to measure. The measured CMF width is 5-8 nm, however not all the matrix material is extracted with this method.

Cellulose microfibril texture of the cell wall of *Vicia sativa* root hairs, TEM analysis of surface preparations

The visualization of the CMF texture by dry cleaving of *Vicia sativa* root hair cell walls can be seen in Fig. 4. We studied three developmental stages of *Vicia sativa* root hairs, in root zones as typified in earlier studies (Heidstra *et al.*, 1994, de Ruijter *et al.*, 1998). Root zone I contains growing root hairs, root zone II has root hairs that are in the process of growth arrest, the hairs of root zone III are fully-grown.

For the visualization of the CMFs the cell wall matrix of root hairs was extracted with H₂O₂/HAc at 100 °C for 1 h. The outside texture, the primary cell wall, was random in all developmental stages (Fig. 4A, fully-grown cell), as has been observed for all root hairs studied (Emons & van Maaren, 1987). Figure 4B shows the inner part of the cell wall of a growing *Vicia sativa* root hair, approx. 40 µm from the hair tip. Here longitudinal CMF deposition has just started. More to the base of growing root hairs and in growth arresting and fully-grown hairs, the secondary cell wall CMFs are longitudinally/helically aligned (Fig. 4C).

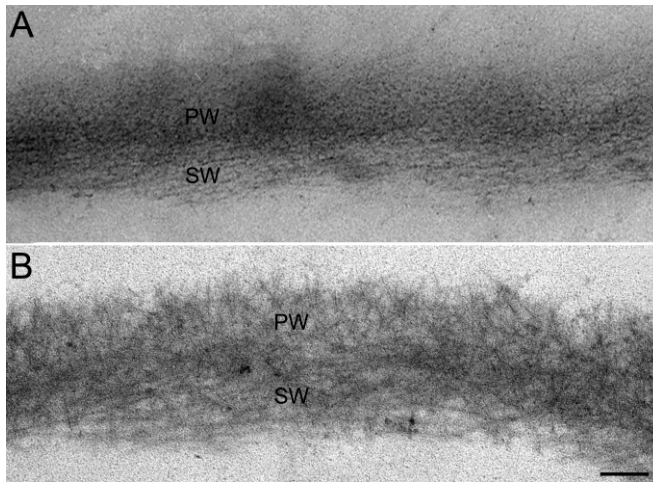


Figure 3: TEM micrographs of ultrathin sections of the CMF texture of a *Medicago truncatula* root hair in the growth-terminating stage. A: Longitudinal section of a root hair extracted for 24 h with 40% methylamine and stained with PATAg. B: Longitudinal section of a root hair extracted for 1.5 hours with H_2O_2/HAc , and stained with $KMnO_4$. With both methods primary wall has random texture and secondary wall axial/steep helical texture, but H_2O_2/HAc extraction gives a more clear image. (PW: primary cell wall. SW: secondary cell wall). Bar: 200 nm.

To our surprise the CMFs were well visible with extraction in water only (Fig. 4C), which has not been reported for other species. The CMF orientation in root hairs was the same in extracted and non-extracted cells.

The angle that secondary cell wall CMFs make with the cell's long axis in *Vicia sativa* root hairs is steeply helical and can be in the S as well as Z direction. In zone I root hairs this angle in the tube was between 0 and 52 degrees (N=11 root hairs) from the cell's long axis; in the tube of zone II hairs this was between 0 and 28 degrees (N=11 root hairs) and in zone III hairs between 0 and 32 degrees (N=9 root hairs) (Figure 5). In conclusion, growing hairs differ from fully-grown hairs in having a wider range of CMF angles to the cell's long axis but the average angle does not differ much (growing hairs -1.7, sd 28.3, hairs at growth arrest -0.5, sd 14.5 and fully-grown hairs 0.5, sd 17.6.)

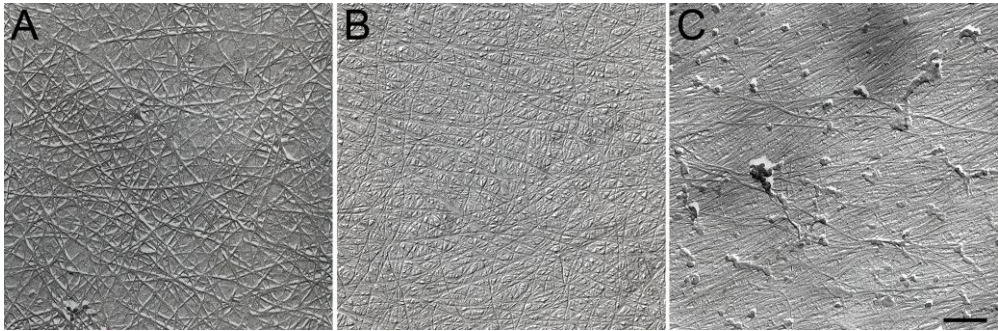


Figure 4: TEM micrographs of surface preparations of the CMF texture of root hairs of *Vicia sativa*. Longitudinal axis from right to left. A: The random outside texture of a fully grown hair. The outside texture is random in all developmental stages. B: The inner part of the cell wall of a growing root hair, approx. 40 μm from the hair tip, where longitudinal CMF deposition has just started. C: Further to the base and in growth terminating and fully grown hairs CMFs are more axially/helicallly aligned (Fig. 4C fully grown hair only extracted with water). Bar for three images: 200 nm.

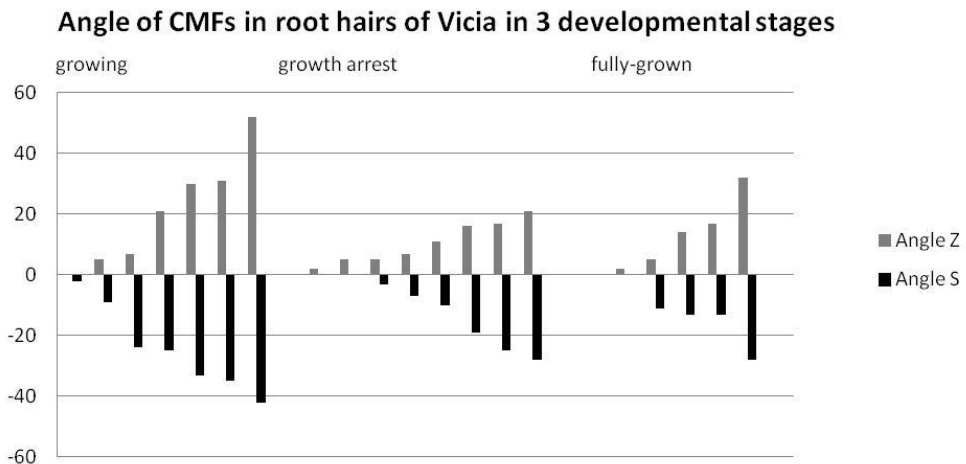


Figure 5: The angle of CMFs measured from surface preparations of *Vicia sativa* in three developmental stages of root hairs: growing, at growth arrest and fully-grown.

As shown, it is well possible to measure CMF orientation from samples prepared with this cleaving technique for surface preparations. CMF width

including Platinum/Carbon deposit is around 8 nm and up to 10 nm, but dependent on the shadowing angle, like in the surface preparations of *Arabidopsis thaliana*. When the thickness of deposited shadowing metal is taken into account, this is the same as found for other higher plants. Density of CMFs can be measured if in every subsequent wall lamella the angle of deposition changes, but it is not possible to determine which CMFs have been deposited at the same time and which ones were deposited later between the existing ones. Maximal CMF length observed is 1855 nm. but because it ran out of the picture it is almost sure that CMFs are longer. Table 1 summarizes which parameters can be measured with the different techniques available for CMF visualization.

Overview of different EM techniques for CMF visualization (+: possible, -: impossible)

	orientation	density	length	width
TEM sections after complete matrix extraction	+	-	-	+
TEM sections after mild matrix extraction	+	-	-	-
TEM surface preparations after matrix extraction	+	+	-	-
FESEM after matrix extraction	+	-	-	-

Table 1: Overview of the parameters that can be measured with the different techniques available for high resolution imaging of CMFs.

Discussion

Different methods were used to visualize the CMFs in root hairs of *Arabidopsis thaliana*, *Medicago truncatula* and *Vicia sativa*. We studied the cell wall textures of these three species because there is ample research performed on them in relation to general root hair development (*Arabidopsis thaliana*) and reaction of root hairs to encounters with rhizobia (*Medicago truncatula* and *Vicia sativa*).

To reveal the cell wall texture clearly with TEM, it is necessary to extract the cell wall matrix. Extraction by boiling in 30% H₂O₂ 100% HAc (1:1) gave better results than extraction with 40% methylamine and PATAg staining; it removes virtually all non-cellulose material (van der Wel *et al.*, 1996) while it

does not disturb the cell wall texture. In general, the matrix:fibril ratio of a primary cell wall is very high. The primary wall contains 20-30% CMFs, whereas the relative content of CMFs in the secondary wall is much higher, 40-90% (Fry, 1988). The optimal extraction procedure/time depends on the amount and nature of the wall matrix in between the CMFs, which differs per species, cell type and developmental stage. Recently, for *Arabidopsis thaliana* hypocotyl epidermal cells the PATAg method, which we used for *Medicago truncatula*, worked sufficiently to reveal the change in wall texture after application of microtubule inhibitors (Chan *et al.*, 2010).

Staining of ultrathin sections after cell wall matrix extraction provides overall CMF texture, orientation of individual CMFs in lamellae, width of CMFs, and minimal length of CMFs. Actual CMF length cannot be determined with this method. CMF width in *Arabidopsis* is approx. 3 nm which is the same as has been reported before from TEM images for other species of higher plants (Emons, 1988), and X-ray analysis (Kennedy *et al.*, 2007).

Surface preparations of cleaved extracted cell walls that have been shadow casted with metal, gold or Platinum and Carbon for FESEM or TEM, can provide information about the wall texture if multiple images from different surface areas are combined. To determine whether a certain cell wall texture is helicoidal, i.e. a cell wall texture in which the CMFs of a lamella make a constant angle with those of the previously deposited lamella, images of ultrathin sections or freeze fracturing preparations are needed as proof. That a cell wall texture is not helicoidal however, can only be inferred if many surface preparations are observed. In a helicoidal wall a lamella with a transverse orientation has to be present. When a transverse orientation is not seen in many preparations it is not likely that a wall has a helicoidal CMF texture.

CMF width cannot be determined accurately and is often reported too wide, up till 10 nm. With surface preparations it is important to keep in mind that a Platinum/Carbon, or Platinum coat covers every single CMF, showing the structure broader than its actual size. Therefore with this method it is more difficult to determine whether one CMF is made by one or two CMF synthase

complexes; however, the method is sufficient to determine whether a few or a field of cellulose synthase complexes produce a single CMF, as is the case in some algae (Giddings *et al.*, 1980).

In large preparations of the inner side of the cell wall, the side against the plasma membrane, the largest measured CMF length that can be measured is larger than the length measured in sections. Although in a surface preparation the whole CMF may be in the plane of observation, it appears to be difficult to determine the CMF ends, and therefore CMF length.

The three species studied here, *Arabidopsis thaliana*, *Medicago truncatula* and *Vicia sativa*, all have an axial/helical root hair cell wall texture, like most root hairs of terrestrial plants studied (Emons & van Maaren, 1987), while aquatic plants have helicoidal textures (Emons and Van Maaren 1987). The latter texture is thought to be strong in a variety of bend directions, a useful adaptation to the environment.

In the three species studied here, the CMF texture of the primary wall, deposited at the hair tip, is random, as has been seen in root hairs of all species studied before (Emons and van Maaren, 1987). From CMF width it can be inferred that single cellulose synthase complexes produce CMFs; this is thought to be the case for all higher plant cells but has not been proven yet.

With the technique in which GFP, green fluorescent protein, is coupled to the cellulose synthase protein, we can see in the spinning disc microscope the movement of cellulose synthase complexes inside the plasma membrane while depositing the CMFs (Gutierrez *et al.*, 2009, Paredez *et al.*, 2006, Paredez *et al.*, 2008, Crowell *et al.*, 2009, Chan *et al.*, 2010). With this method CMF velocity of production and orientation of production, as well as the number of CMFs being produced per surface area at the same time can be determined, and possibly in the future CMF length and lifetime, but not CMF texture. Therefore, to uncover the organizing principle of CMF texture formation, data about trafficking of the cellulose synthase complex have to be combined with analysis of the product these complexes make, the CMFs.

Acknowledgement

AMCE acknowledges funding by EU NEST project 028974 CASPIC (Cellulose Architecture Systems biology for Plant Innovation Creation). We thank Adriaan van Aelst, Wageningen Electron Microscopy Center for help with microscopy.

References

- Baskin, T. I. (2001) On the alignment of cellulose microfibrils by cortical microtubules: a review and a model. *Protoplasma*, **215**, 150-171.
- Carpita, N. C. & Gibeaut, D. M. (1993) Structural models of primary cell walls in flowering plants: consistency of molecular structure with the physical properties of the walls during growth. *Plant Journal*, **3**, 1-30.
- Chan, J., Calder, G., Fox, S. & Lloyd, C. (2007) Cortical microtubule arrays undergo rotary movements in Arabidopsis hypocotyl epidermal cells. *Nat Cell Biol*, **9**, 171-175.
- Chan, J., Crowell, E., Eder, M., Calder, G., Bunnell, S., Findlay, K., Vernhettes, S., Hofte, H. & Lloyd, C. (2010) The rotation of cellulose synthase trajectories is microtubule dependent and influences the texture of epidermal cell walls in Arabidopsis hypocotyls. *J Cell Sci*, **123**, 3490-3495.
- Crowell, E. F., Bischoff, V., Desprez, T., Rolland, A., Stierhof, Y. D., Schumacher, K., Gonneau, M., Hofte, H. & Vernhettes, S. (2009) Pausing of Golgi bodies on microtubules regulates secretion of cellulose synthase complexes in Arabidopsis. *Plant Cell*, **21**, 1141-1154.
- De Ruijter, N. C. A., Rook, M. B., Bisseling, T. & Emons, A. M. C. (1998) Lipochito-oligosaccharides re-initiate root hair tip growth in *Vicia sativa* with high calcium and spectrin-like antigen at the tip. *Plant Journal*, **13**, 341-350.
- Dolan, L., Duckett, C. M., Grierson, C., Linstead, P., Schneider, K., Lawson, E., Dean, C., Poethig, S. & Roberts, K. (1994) Clonal Relationships and Cell Patterning in the Root Epidermis of Arabidopsis. *Development*, **120**, 2465-2474.
- Emons, A. M. C. (1988) Methods for Visualizing Cell-Wall Texture. *Acta Botanica Neerlandica*, **37**, 31-38.
- Emons, A. M. C. (1989) Helicoidal Microfibril Deposition in a Tip-Growing Cell and Microtubule Alignment During Tip Morphogenesis - a Dry-Cleaving and Freeze-Substitution Study. *Canadian Journal of Botany-Revue Canadienne De Botanique*, **67**, 2401-2408.
- Emons, A. M. C. & Mulder, B. M. (2000) How the deposition of cellulose microfibrils builds cell wall architecture. *Trends in Plant Science*, **5**, 35-40.
- Emons, A. M. C., Schel, J. H. N. & Mulder, B. M. (2002) The geometrical model for microfibril deposition and the influence of the cell wall matrix. *Plant Biology*, **4**, 22-26.
- Emons, A. M. C. and Van Maaren, N. (1987) Helicoidal Cell-Wall Texture in Root Hairs. *Planta*, **170**, 145-151.
- Emons, A. M. C. & Wolters Arts, A. M. C. (1983) Cortical Microtubules and Microfibril Deposition in the Cell-Wall of Root Hairs of *Equisetum-Hyemale*. *Protoplasma*, **117**, 68-81.
- Emons, A.M.C. (1991) Role of particle rosettes and terminal globules in cellulose synthesis. In: Biosynthesis and biodegradation of cellulose and cellulosic materials. Haigler CH & RJ. Weimer (eds). Marcel Dekker, New York, 71-98.
- Esseling, J. J., Lhuissier, F. G. P. & Emons, A. M. C. (2004) A nonsymbiotic root hair tip growth phenotype in dulation NORK-mutated legumes: Implications for nodulation factor-induced signaling and formation of a multifaceted root hair pocket for bacteria. *Plant Cell*, **16**, 933-944.

- Fry, S. C. (1988) *The growing plant cell wall: chemical and metabolic analysis*, The Blackbourn Press.
- Giddings, T. H., Brower, D. L. & Staehelin, L. A. (1980) Visualization of particle complexes in the plasma membrane of *Micrasterias denticulata* associated with the formation of cellulose microfibrils in primary and secondary cell walls. *Journal of Cell Biology*, **84**, 328-339.
- Gutierrez, R., Lindeboom, J. J., Paredez, A. R., Emons, A. M. & Ehrhardt, D. W. (2009) Arabidopsis cortical microtubules position cellulose synthase delivery to the plasma membrane and interact with cellulose synthase trafficking compartments. *Nat Cell Biol*, **11**, 797-806.
- Heidstra, R., Geurts, R., Franssen, H., Spaink, H. P., Van Kammen, A. & Bisseling, T. (1994) Root Hair Deformation Activity of Nodulation Factors and Their Fate on *Vicia sativa*. *Plant Physiol*, **105**, 787-797.
- Heidstra, R., Yang, W. C., Yalcin, Y., Peck, S., Emons, A. M., vanKammen, A. & Bisseling, T. (1997) Ethylene provides positional information on cortical cell division but is not involved in Nod factor-induced root hair tip growth in Rhizobium-legume interaction. *Development*, **124**, 1781-1787.
- Kennedy, C. J., Cameron, G. J., S' turcova', A., Apperley, D. C., Altaner, C., Wess, T. J. & Jarvis, M. C. (2007) Microfibril diameter in celery collenchyma cellulose: X-ray scattering and NMR evidence. *Cellulose*, **14**, 235-246.
- Lhuissier, F. G. P., De Ruijter, N. C. A., Sieberer, B. J., Esseling, J. J. & Emons, A. M. C. (2001) Time course of cell biological events evoked in legume root hairs by Rhizobium Nod factors: State of the art. *Annals of Botany*, **87**, 289-302.
- Miller, D. D., deRuijter, N. C. A. & Emons, A. M. C. (1997) From signal to form: aspects of the cytoskeleton plasma membrane cell wall continuum in root hair tips. *Journal of Experimental Botany*, **48**, 1881-1896.
- Mulder, B. M., Schel, J.H.N., Emons, A.M.C. (2004) How the geometrical model for plant cell wall formation enables the production of a random texture. *Cellulose*, **11**, 395-401.
- Paredez, A. R., Persson, S., Ehrhardt, D. W. & Somerville, C. R. (2008) Genetic evidence that cellulose synthase activity influences microtubule cortical array organization. *Plant Physiol*, **147**, 1723-1734.
- Paredez, A. R., Somerville, C. R. & Ehrhardt, D. W. (2006) Visualization of cellulose synthase demonstrates functional association with microtubules. *Science*, **312**, 1491-1495.
- Persson, S., Paredez, A., Carroll, A., Palsdottir, H., Doblin, M., Poindexter, P., Khitrov, N., Auer, M. & Somerville, C. R. (2007) Genetic evidence for three unique components in primary cell-wall cellulose synthase complexes in Arabidopsis. *Proc Natl Acad Sci U S A*, **104**, 15566-15571.
- Persson, S., Wei, H., Milne, J., Page, G. P. & Somerville, C. R. (2005) Identification of genes required for cellulose synthesis by regression analysis of public microarray data sets. *Proc Natl Acad Sci U S A*, **102**, 8633-8638.
- Refrégier, G., Pelletier, S., Jaillard, D., and Höfte, H. (2004) Interaction between wall deposition and cell elongation in dark-grown hypocotyl cells in Arabidopsis. *Plant Physiol*, **136**, 959-968.

- Sieberer, B. & Emons, A. M. C. (2000) Cytoarchitecture and pattern of cytoplasmic streaming in root hairs of *Medicago truncatula* during development and deformation by nodulation factors. *Protoplasma*, **214**, 118-127.
- Somerville, C. (2006) Cellulose synthesis in higher plants. *Annu Rev Cell Dev Biol*, **22**, 53-78.
- Sugimoto, K., Williamson, R. E. & Wasteneys, G. O. (2000) New techniques enable comparative analysis of microtubule orientation, wall texture, and growth rate in intact roots of *Arabidopsis*. *Plant Physiology*, **124**, 1493-1506.
- Thiéry, J. P. (1967) Mise en évidence de polysaccharides sur coupes fines en microscopie électronique. *Journal of Microscopy*, **6**, 987-1017.
- Turner, S., Gallois, P. & Brown, D. (2007) Tracheary element differentiation. *Annu Rev Plant Biol*, **58**, 407-433.
- Van der Wel, N. N., Putman, C. A. J., Noort, S. J. T., Grooth, B. G. d. & Emons, A. M. C. (1996) Atomic force microscopy of pollen grains, cellulose microfibrils, and protoplasts. *Protoplasma*, **194**, 29-39.
- Wolters-Arts, A. M. C. & Sassen, M. M. A. (1991) Deposition and reorientation of cellulose microfibrils in elongating cells of *Petunia* stylar tissue. *Planta*, **185**, 179-189.

Chapter 5

General discussion: Aspects of the mechanism behind the highly ordered textures of cellulose microfibrils in plant cell walls

Miriam Akkerman, Tijs Ketelaar, Anne Mie C. Emons

*Laboratory of Cell Biology, Department of Plant Sciences, Wageningen
University, Droevendaalsesteeg 1, 6708 PB Wageningen, The Netherlands*

Cellulose microfibril textures are highly ordered

Cellulose microfibrils (CMFs) in the cell wall are deposited in highly organized textures. Among different species, cell types, and developmental stages a diversity of textures exist. In *Arabidopsis* roots CMFs in elongating cells are present in an orientation transverse to the cell's elongation direction (see chapter 3 of this thesis). Around fully-grown root cells additional layers of CMFs are present with different orientations, from oblique to longitudinal (see for example root hair cell walls, Akkerman et al. (2012) chapter 4 in this thesis). The wall textures of epidermal cells in *Arabidopsis* hypocotyls resemble those in roots except for the outer wall. This outer epidermal wall in light-grown growing hypocotyl cells, consists of multiple layers with each subsequent layer having another CMF orientation. The CMF orientation changes stepwise and cycles from transverse via oblique to longitudinal and back to transverse again (Chan et al. 2010). The layers form a thick polylamellated wall texture. Such wall textures have also been found in for instance collenchyma cells (Roland and Vian 1979) and root hairs of *Equisetum* and mainly aquatic plants (Emons and van Maaren 1987).

Different textures have different physical and mechanical properties and functions. It is generally thought that the orientation of CMFs determines the cell elongation direction, which is perpendicular to the orientation of the CMFs (Baskin 2005). In hypocotyl epidermal cells it is the inner cell wall that exerts this task (Dark-grown: Crowell et al. 2011, Light-grown: Chan et al. 2011). In the outer wall of light-grown hypocotyl epidermal cells, where CMF orientations change in a rotary pattern (Chan et al. 2011), the transverse orientation is thought to gain a high elongation rate (Chan 2011). Thick walls with longitudinal or helical CMFs provide strength and those with multiple CMF orientations, like the outer hypocotyl epidermal walls, are thought to provide strength in multiple (bend) directions (Anderson et al. 2010, Chan et al. 2011, Crowell et al. 2011). In the *Arabidopsis* root cells both the outer and the inner face of growing epidermal cells have transverse CMFs (see chapter 3 of this thesis).

The main question that follows from the above is: How are these orientations created? During stretching of the wall it is possible that already deposited CMFs change their orientation more towards longitudinal (multinet growth

hypothesis: Roelofsen and Houwink 1953) shown to be the case in styles of *Petunia* (Wolters-Arts and Sassen 1991) and more recently in *Arabidopsis* dark-grown hypocotyl cells (Anderson et al. 2010). This kind of reorientation, however, cannot explain the highly organized polylamellated walls as seen in for instance the outer epidermal wall of light-grown *Arabidopsis* hypocotyls (Chan et al. 2010), since in these walls the orientations of CMFs also change from longitudinal back to transverse.

Since CMF textures are produced by organized cellulose synthase (CESA) complexes, we here discuss the complete pathway of these nanomachines through the cell from their synthesis to their movement in the plasma membrane, including the role of the actin cytoskeleton and the cortical microtubule (CMT) array, to understand the mechanisms behind the highly ordered CMF textures.

Global distribution of CESA complexes via Golgi bodies over bundles of actin filaments

Let us start at the beginning of the pathway that a CESA complex follows from assembly in the ER to active movement in the plasma membrane. It is thought that subunits are assembled to a CESA complex in the ER (Rudolph 1987) and are transported to Golgi bodies via mobile secretory units (DaSilva 2004). Golgi bodies have been shown to contain rosettes (Haigler and Brown 1986), which are the CESA complexes (Kimura et al. 1999). Golgi bodies distribute glycosides and glycoproteins through the cell. They travel over actin filaments by class XI myosin activity, like mitochondria and peroxisomes (Nebenführ et al. 1999, Sparkes et al. 2008, Avisar et al. 2008, Avisar et al. 2009).

In this thesis it is shown that Golgi body movement in the cell cortex depends on the structure of the actin cytoskeleton. In cortical areas with thick bundles of actin filaments they show fast directed movement, like in trans-vacuolar cytoplasmic strands, with velocities of up to 7 $\mu\text{m}/\text{sec}$. From earlier research it is known that disruption of actin filaments reduces *Arabidopsis* root cell elongation and induces radial swelling in a dose-dependent manner (Baskin and Bivens 1995, Collings et al. 2006), in onion (Thomas et al. 1973) and

maize roots (Blancaflor 2000, Baluska et al. 2001). In accordance with these results, mutations in some actin-binding proteins that disrupt actin organization affect cell elongation (Ramachandran et al. 2000, Dong et al. 2001, Barrero et al. 2002, Nishimura et al. 2003, Ketelaar et al. 2004). Crowell et al. (2009) and Gutierrez et al. (2009) observed that, after the use of actin depolymerizing agents, Golgi bodies aggregated. CESA complex density increased in the plasma membrane above Golgi aggregates, while it was largely reduced in other areas of the plasma membrane.

Fine-scale positioning of Golgi bodies in the cell cortex: Golgi bodies wiggle on fine F-actin and pause on CMTs near exocytosis sites

In this thesis it is shown that in cortical areas with a fine F-actin network, i.e. thin bundles of actin filaments and/or single actin filaments, Golgi bodies show random 'wiggling'. During wiggling they remain at approximately the same location and probably release secretory vesicles in close vicinity of exocytosis sites. Crowell et al. (2009) and Gutierrez et al. (2009) analyzed the motility of GFP-CESA3 labeled Golgi bodies in combination with insertion events of GFP-CESA3 containing CESA complexes into the plasma membrane. Both groups noticed that insertion events correlate with the presence of Golgi bodies just beneath the plasma membrane. Crowell et al (2009) conclude that CESA complex insertions are preceded by a 'pausing' Golgi body just beneath the plasma membrane and that pausing occurs on a CMT. This is in accordance with the observation of Nebenführ et al. (1999) that after CMT depolymerization the average velocity of Golgi bodies is slightly higher. Golgi bodies might pause on a CMT via kinesin-13A. Lu et al. (2005) showed that the Arabidopsis kinesin-13A localizes to Golgi bodies. They demonstrated association of Golgi bodies with CMTs using confocal laser scanning microscopy and transmission electron microscopy. Kinesin-13A is a suitable candidate for linking Golgi bodies to CMTs, as in trichomes of Arabidopsis kinesin-13a mutants Golgi bodies aggregated and morphogenesis was affected (Lu et al. 2005).

Many but not all insertions take place above a CMT. Gutierrez et al. (2009) measured a coincidence of insertion events with CMTs in 78% of the observed insertions.

It can be concluded that in the secretory pathway the positioning of secretion is globally determined by the actin cytoskeleton whereas the CMT array positions individual insertion events. Sampathkumar et al. (2011) showed transient co-localization of CMTs and actin filaments and actin nucleation events scaffolded by CMTs. This suggests physical interaction of actin filaments and CMTs.

Insertion of CESA complexes into the plasma membrane

While wiggling and pausing, a Golgi body probably releases Golgi vesicles, which fuse with the plasma membrane during the process of exocytosis. During exocytosis the content of a vesicle is released into the cell wall and its membrane, including integral membrane proteins, becomes part of the plasma membrane. It is thought that CESA complexes enter the plasma membrane in this way. Exocytosis requires the interplay of the vesicle membrane, the plasma membrane and cytoplasmic actors, proteins and ions (exocyst: Hála et al. 2008, Chong et al. 2010, Wang et al. 2010, SNAREs: Uemura et al. 2004, Ca²⁺: Batty et al. 1999, Yamazaki et al. 2008). For budding off from a Golgi body, for movement to the plasma membrane and for fusion with the plasma membrane, neither actin filaments nor CMTs are necessary since both latrunculin B and oryzalin treatment, drugs that respectively depolymerize F-actin and microtubules, did not prevent the insertion of CESA complexes into the plasma membrane (Crowell et al. 2009, Gutierrez et al. 2009).

Insertion of CESA complexes can take place via Small CESA Containing compartments (SmaCCs). SmaCCs may well be single Golgi derived vesicles or groups of vesicles. Also Golgi bodies have been observed to associate with SmaCCs (Gutierrez et al. 2009). SmaCCs occur especially during osmotic stress and other treatments that reduce CESA complex density in the plasma membrane (Gutierrez et al. 2009). During osmotic stress CESA complexes disappear from the plasma membrane while SmaCCs (Gutierrez et al. 2009)

and Microtubule-Associated cellulose Synthase Compartments (MASCs) (Crowell et al. 2009), probably the same structures, accumulate on CMTs. Gutierrez et al. (2009) present evidence that CESA complexes, in SmaCCs, accumulate on CMTs because their insertion into the plasma membrane is blocked, while Crowell et al. (2009) suggest that the complexes, in MASCs, are internalized back into the cell. Also in electron micrographs of freeze fractured preparations rosettes, the CESA complexes, are absent from the plasma membrane when the cell has lost turgor pressure (Emons 1985). During recovery from osmotic stress CESA complexes were observed to be inserted into the plasma membrane above CMT tethered SmaCCs (Gutierrez et al. 2009). They show that during fusion of a SmaCC with the plasma membrane in most cases one CESA particle is inserted and that during some insertion events two CESA particles are inserted at the same spot. SmaCCs move by end-tracking depolymerizing microtubules, both plus and minus ends (Crowell et al. 2009, Gutierrez et al. 2009). Both Crowell et al. (2009) and Gutierrez et al. (2009) reason that it is unlikely that SmaCCs move by kinesins. This does not mean that kinesins could not play a role. Wei et al. (2009) showed, by using immunogold labeling for transmission electron microscopy, that Kinesin-13A is present on Golgi associated secretory vesicles in Arabidopsis root cap peripheral cells and kinesins of the KinI/Kinesin-13 family are thought to have a regulatory role in the depolymerization at both ends of microtubules in *Drosophila* (Wu et al. 2006). Therefore, it is well possible that SmaCCs end track CMTs with Kinesin-13A and probably play a role in the regulation of CMT dynamics .

Direction of CESA complexes, orientation of CMTs and CMFs

For decades, it is thought that cortical microtubules (CMTs) orient the nascent CMFs (Baskin 2001, Lloyd 2011). Many observations of correlations between CMT and CMF orientation were done (reviewed by Baskin 2001). However, not in all cells CMTs and CMFs are thought to be in parallel alignment (reviewed in Emons et al. 1992, Baskin 2001 and Wasteneys 2004) and experiments in which drugs and mutants were used are not always in agreement with the hypothesis that CMTs orient nascent CMFs (Sugimoto et

al. 2000, 2003). However, in these last articles outer wall CMTs were compared to inner wall CMFs.

A geometrical model was formulated (Emons 1994) which shows that in theory all textures can be produced by modulating the number of cellulose synthase (CESA) complexes active in the plasma membrane without guiding tracks from within the cell (Emons and Mulder 1998, 2000; Mulder and Emons 2001).

In 2006 work by Paredez et al. caused a breakthrough in the CMT-CMF debate by live imaging of CESA complexes with an YFP-CESA6 fusion protein in combination with CFP-TUA1 labeled CMTs in growing *Arabidopsis* hypocotyls (dark-grown). They showed that CESA complexes move bidirectionally along CMTs with an average velocity of about 350 nm/min (Paredez et al. 2006). Later research using fluorescently tagged CESA3 or CESA6 showed the same movement pattern in the plasma membrane and approximately the same velocity in *Arabidopsis* hypocotyls (Debolt et al. 2007, Persson et al. 2007, Desprez et al. 2007, Crowell et al. 2009, 2011, Gutierrez et al. 2009, Gu et al. 2010, Chan et al. 2010, 2011, Li et al. 2011, Bringmann et al. 2012). As CESA complex velocity is temperature dependent also lower and higher velocities of CESA complexes have been measured (Fujita et al. 2011).

In this thesis we show that the movement of CESA complexes in plasma membranes of growing *Arabidopsis* root epidermal cells also coincides with underlying CMTs (90% of the CESA complexes) and that CESA complex velocities are in the same range as in hypocotyls. Throughout the root elongation zone CESA tracks and CMTs are transverse to the growth axis. Above the growth zone both CESA tracks and CMTs become more oblique, as was shown before for CMTs and CMFs in these cells (Sugimoto et al. 2000). Taken together, the currently available data show that (1) A large majority of CESA complexes in *Arabidopsis* epidermal cells in roots and hypocotyls move bidirectionally along CMTs (2) CESA insertion events occur in most cases above underlying CMTs (3) CMTs appear not to be required for insertion of CESA complexes (Gutierrez et al. 2009) and (4) CMTs appear not to be required for production of an ordered cell wall texture, since in the absence of CMTs ordered textures are being formed (Paredez et al. 2006, Emons et al. 2007b).

We conclude that CMTs are required to produce a specific CMF orientation, such as the transverse orientation in elongating cells and the rotating orientations in the multilayered outer wall in light-grown *Arabidopsis* hypocotyls, since after oryzalin treatment CESA tracks did not change direction anymore and a thick inner layer was present in which CMFs showed the same longitudinal orientation (Chan et al. 2010).

Since, at least in epidermal cells of *Arabidopsis* roots and hypocotyls, CMFs are oriented by CMTs, the next question to answer is: What orients CMTs? Theoretical studies have shown that, when taking into account the actual parameters of microtubule (de)polymerization and the known actions of microtubule binding proteins, CMTs in growing plant cells tend to align (Tindemans et al. 2010). Also in vitro, in small glass cuvettes, confined geometries, microtubules align depending on their density (Cosentino Lagomarsino et al. 2006). Concerning the orientation of CMTs, it has been concluded that CMTs modify their orientation according to major tensile stress lines generated by growth in the *Arabidopsis* shoot apical meristem and that this orientation is largely dependent on the tissue shape (Hamant et al. 2008, Hamant et al. 2010, Heisler et al. 2010).

Another finding related to the question “What orients CMTs?” has been that CMTs require active CESA complexes to achieve a proper organization (Paredez et al. 2008). It has been shown that the cellulose synthesis inhibiting agent isoxaben, probably working by direct interaction with CESA3 and CESA6 (Scheible et al. 2001), causes depletion of plasma membrane localized CESA complexes (Paredez et al. 2006) and causes alteration of CMT organization (Paredez et al. 2008). Moreover Bringmann et al. (2012) showed that the *csi1* mutant, mutated in *CELLULOSE SYNTHASE INTERACTING1*, shows defects in CMT organization. CSI1 is a putative linker protein that associates a CESA complex with a CMT (Gu et al. 2010, Bringmann et al. 2012, Li et al. 2012). A possibility could be that interaction between CESA complexes and CMTs, mediated by CSI1, causes a reaction that gives mechano-reactivity, so that both CMTs and CESA complexes orient in the direction of mechanical stress lines.

Constant repositioning of CMTs allows the production of an even layer of CMFs

In this thesis we measured densities of CESA rows, CMTs and CMFs in root epidermis cells. The densities of CESA rows and CMTs correspond to each other but there is a large difference in density of CMFs in the innermost layer (42.0 to 48.9 per μm .) and the density of rows of CESA complexes (max 1.79 per μm), and concomitant distance between CMTs. This can be understood if a CMF layer is made consecutively by CESA complexes moving in orientations between already existing CMFs. However, during live cell imaging multiple CESA complexes are seen to track individual CMTs in a row. How can CESA complexes that move in rows produce a layer of uniformly distributed and oriented CMFs as seen in the CMF preparations obtained with electron microscopy techniques, instead of producing local wall thickenings of several CMFs on top of each other? Since, as mentioned above, over 90% of the CESA complexes track CMTs, we hypothesized that nascent CMFs are deposited next to older ones in a parallel alignment due to constant CMT reorganization over time. In support of this hypothesis, time lapse imaging experiments show that CMTs indeed reposition over 10 minute intervals, supporting our hypothesis (chapter 3). The distance between CMFs probably is kept constant by linker-proteins and/or hemicelluloses which contribute to the proper alignment of the CMFs.

Future perspectives

Over the last years, rapid progress in understanding the regulation of CMF deposition has been made using fluorescently tagged CESA complexes. Nevertheless, many questions remain unanswered. The main upcoming challenges relate to understanding CMT reorganization, the relation with mechanical stress, and the positioning of CESA complex insertion into the plasma membrane. If this research area remains as vibrant as over the last 6 years, these challenges should be tackled in the near future.

References

- Anderson CT, Carroll A, Akhmetova L, Somerville C (2010) Real-Time Imaging of Cellulose Reorientation during Cell Wall Expansion in Arabidopsis Roots. *Plant Physiol.* 152: 787–796.
- Avisar D, Prokhnovsky AI, Makarova KS, Koonin EV, Dolja VV (2008) Myosin XI-K is required for rapid trafficking of Golgi stacks, peroxisomes, and mitochondria in leaf cells of *Nicotiana benthamiana*. *Plant Physiol.* 146: 1098-1108.
- Avisar D, Abu-Abied M, Belausov E, Sadot E, Hawes C, Sparkes IA (2009) A comparative study of the involvement of 17 Arabidopsis myosin family members on the motility of Golgi and other organelles. *Plant Physiol.* 150: 700-709.
- Baluska F, Jasik J, Edelmann HG, Salajová T, Volkmann D (2001) Latrunculin B-induced plant dwarfism: Plant cell elongation is F-actin-dependent. *Dev. Biol.* 231: 113-124.
- Barrero RA, Umeda M, Yamamura S, Uchimiya H (2002) Arabidopsis CAP regulates the actin cytoskeleton necessary for plant cell elongation and division. *Plant Cell* 14: 149-163.
- Baskin TI (2001) On the alignment of cellulose microfibrils by cortical microtubules: a review and a model. *Protoplasma* 215: 150-171.
- Baskin TI (2005) Anisotropic Expansion of the Plant CellWall. *Annu. Rev. Cell. Dev. Biol.* 21:203-222.
- Baskin TI and Bivens NJ (1995) Stimulation of radial expansion in Arabidopsis roots by inhibitors of actomyosin and vesicle secretion but not by various inhibitors of metabolism. *Planta* 197: 514-521.
- Batley NH, James NC, Greenland AJ, Brownlee C (1999) Exocytosis and Endocytosis. *The Plant Cell* 11: 643–659.
- Blancaflor EB (2000) Cortical actin filaments potentially interact with cortical microtubules in regulating polarity of cell expansion in primary roots of maize (*Zea mays* L.). *J. Plant Growth Regulation* 19: 406-414.
- Bringmann M, Li E, Sampathkumar A, Kocabek T, Hauser MT, Persson S (2012) POM-POM2/CELLULOSE SYNTHASE INTERACTING1 Is Essential for the Functional Association of Cellulose Synthase and Microtubules in Arabidopsis. *Plant Cell* 24: 163–177
- Chan J, Crowell E, Eder M, Calder G, Bunnewell S, Findlay K, Vernhettes S, Höfte H, Lloyd C (2010) The rotation of cellulose synthase trajectories is microtubule dependent and influences the texture of epidermal cell walls in Arabidopsis hypocotyls. *J Cell Sci.* 123: 3490-3495
- Chan J (2011) Microtubule and cellulose microfibril orientation during plant cell and organ growth. *Journal of Microscopy* doi: 10.1111/j.1365-2818.2011.03585.x
- Chan J, Eder M, Crowell EF, Hampson J, Calder G, Lloyd C (2011) Microtubules and CESA tracks at the inner epidermal wall align independently of those on the outer wall of light-grown Arabidopsis hypocotyls. *J. Cell Sci.* 124: 1088-1094

- Chong YT, Gidda SK, Sanford C, Parkinson J, Mullen RT, Goring DR (2010) Characterization of the *Arabidopsis thaliana* exocyst complex gene families by phylogenetic, expression profiling, and subcellular localization studies. *New Phytologist* 185: 401–419.
- Collings DA, Lill AW, Himmelspach R and Wasteneys GO (2006) Hypersensitivity to cytoskeletal antagonists demonstrates microtubule–microfilament cross-talk in the control of root elongation in *Arabidopsis thaliana*. *New Phytologist* 170: 275–290
- Cosentino Lagomarsino M, Tanase C, Vos JW, Emons AMC, Mulder BM, Dogterom M (2007) Microtubule Organization in Three-Dimensional Confined Geometries: Evaluating the Role of Elasticity Through a Combined In Vitro and Modeling Approach. *Biophysical Journal* 92: 1046–1057.
- Crowell EF, Bischoff V, Desprez T, Rolland A, Stierhof YD, Schumacher K, Gonneau M, Höfte H, Vernhettes S (2009) Pausing of Golgi bodies on microtubules regulates secretion of cellulose synthase complexes in *Arabidopsis*. *Plant Cell* 21: 1141–1154
- Crowell EF, Timpano H, Desprez T, Franssen-Verheijen T, Emons AM, Höfte H, Vernhettes S (2011) Differential regulation of cellulose orientation at the inner and outer face of epidermal cells in the *Arabidopsis* hypocotyl. *Plant Cell* 23: 2592–2605
- DaSilva LLP, Snapp EL, Denecke J, Lippincott-Schwartz J, Hawes C and Brandizzi F (2004) Endoplasmic Reticulum Export Sites and Golgi Bodies Behave as Single Mobile Secretory Units in Plant Cells. *Plant Cell* 16: 1753–1771
- DeBolt S, Gutierrez R, Ehrhardt DW, Melo CV, Ross L, Cutler SR, Somerville C, Bonetta D (2007) Morlin, an inhibitor of cortical microtubule dynamics and cellulose synthase movement. *Proc. Natl. Acad. Sci. USA* 104: 5854–5859
- Desprez T, Juraniec M, Crowell EF, Jouy H, Pochylova Z, Parcy F, Höfte H, Gonneau M, Vernhettes S (2007) Organization of cellulose synthase complexes involved in primary cell wall synthesis in *Arabidopsis thaliana*. *Proc. Natl. Acad. Sci. USA* 104: 15572–15577
- Dong CH, Xia GX, Hong Y, Ramachandran S, Kost B and Chua NH (2001) ADF proteins are involved in the control of flowering and regulate F-actin organization, cell expansion, and organ growth in *Arabidopsis*. *Plant Cell* 13: 1333–1346.
- Emons AMC (1985) Plasma membrane rosettes in root hairs of *Equisetum hyemale*. *Planta* 163: 350–359.
- Emons AMC, Derksen J, Sassen MMA (1992) Do microtubules orient plant cell wall microfibrils? *Physiol. Plant.* 84: 486–493.
- Emons AMC (1994) Winding threads around plant cells: a geometrical model for microfibril deposition. *Plant, Cell Environ.* 17 (1994) 3–14.
- Emons AMC, Akkerman M, Ebskamp MJM, Schel JHN, Mulder B (2007) How cellulose synthase density in the plasma membrane may dictate cell wall texture. In: *Cellulose: Molecular and Structural Biology* / Brown RM, Saxena IM, Dordrecht: Springer.
- Emons AMC, Höfte H, Mulder B (2007b) Microtubules and cellulose microfibrils: how intimate is their relationship? *Trends in Plant Science* 12: 279 - 281.
- Emons AMC and Van Maaren N (1987) Helicoidal cell wall texture in root hairs. *Planta* 170: 145–151
- Emons AMC, Mulder BM (1998) The making of the architecture of the plant cell wall: how cells exploit geometry. *Proc. Natl. Acad. Sci. USA* 95:7215–19

- Emons AMC, Mulder BM (2000) How the deposition of cellulose microfibrils builds cell wall architecture. *Trends in Plant Science* 5: 35-40.
- Fujita M, Himmelspach R, Hocart CH, Williamson RE, Mansfield SD, Wasteneys GO (2011) Cortical microtubules optimize cell-wall crystallinity to drive unidirectional growth in *Arabidopsis*. *Plant J.* 66: 915-928
- Gu Y, Kaplinsky N, Bringmann M, Cobb A, Carrola A, Sampathkumar A, Baskin TI, Persson S, Somerville CR (2010) Identification of a cellulose synthase-associated protein required for cellulose biosynthesis. *PNAS* 107: 12866–12871
- Gutierrez R, Lindeboom JJ, Paredes AR, Emons AM, Ehrhardt DW (2009) *Arabidopsis* cortical microtubules position cellulose synthase delivery to the plasma membrane and interact with cellulose synthase trafficking compartments. *Nat. Cell Biol.* 11: 797-806
- Haigler CH, Brown RM (1986) Transport of rosettes from the Golgi apparatus to the plasma membrane in isolated mesophyll cells of *Zinnia elegans* during differentiation to tracheary elements in suspension culture. *Protoplasma* 134: 111–20
- Hála M, Cole R, Synek L, Drdova E, Pecenkova T, Nordheim A, Lamkemeyer T, Madlung J, Hochholdinger F, Fowler JE, Zarsky V (2008) An Exocyst Complex Functions in Plant Cell Growth in *Arabidopsis* and Tobacco. *The Plant Cell* 20: 1330–1345.
- Hamant O, Heisler MG, Jönsson H, Krupinski P, Uyttewaal M, Bokov P, Corson F, Sahlin P, Boudaoud A, Meyerowitz EM, Couder Y, Traas J (2008) Developmental patterning by mechanical signals in *Arabidopsis*. *Science* 322: 1650-1655
- Hamant O, Traas J, Boudaoud A (2010) Regulation of shape and patterning in plant development. *Curr. Opin. Genet. Dev.* 20: 454-459
- Heisler MG, Hamant O, Krupinski P, Uyttewaal M, Ohno C, Jonsson H, Traas J, Meyerowitz EM (2010) Alignment between PIN1 Polarity and Microtubule Orientation in the Shoot Apical Meristem Reveals a Tight Coupling between Morphogenesis and Auxin Transport. *PLoS Biology* 8: e1000516.
- Ketelaar T, Allwood EG, Anthony R, Voigt B, Menzel D, Hussey PJ (2004) The actin-interacting protein AIP1 is essential for actin organization and plant development. *Curr. Biol.* 14: 145-149.
- Kimura S, Laosinchai W, Itoh T, Cui X, Linder CR, Brown Jr MR (1999) Immunogold Labeling of Rosette Terminal Cellulose-Synthesizing Complexes in the Vascular Plant *Vigna angularis*. *The plant cell* 11: 2075–2085.
- Li S, Lei L, Somerville CR, Gu Y (2011) Cellulose synthase interactive protein 1 (CSI1) links microtubules and cellulose synthase complexes. *PNAS* 109: 185–190.
- Lloyd C (2011) Dynamic Microtubules and the Texture of Plant Cell Walls. Chapter 7 in *International Review of Cell and Molecular Biology* 287: 287-322.
- Lu L, Lee YRJ, Pan R, Maloof JN, Liu B (2005) An Internal Motor Kinesin Is Associated with the Golgi Apparatus and Plays a Role in Trichome Morphogenesis in *Arabidopsis*. *Molecular Biology of the Cell* 16: 811–823.
- Mulder B, Emons AMC (2001) A dynamical model for plant cell wall architecture formation. *J. Math. Biol.* 42: 261-289.

- Nebenführ A, Gallagher LA, Dunahay TG, Frohlick JA, Mazurkiewicz AM, Meehl JB, Staehelin LA (1999) Stop-and-go movements of plant Golgi stacks are mediated by the acto-myosin system. *Plant Physiol.* 121: 1127-1141
- Nishimura T, Yokota E, Wada T, Shimmen T, Okada K (2003) An Arabidopsis ACT2 dominant-negative mutation, which disturbs F-actin polymerization, reveals its distinctive function in root development. *Plant Cell Physiol.* 44: 1131-1140.
- Paradez AR, Somerville CR, Ehrhardt DW (2006) Visualization of cellulose synthase demonstrates functional association with microtubules. *Science* 312: 1491-1495
- Paradez AR, Persson S, Ehrhardt DW Somerville CR (2008) Genetic Evidence That Cellulose Synthase Activity Influences Microtubule Cortical Array Organization. *Plant Physiology* 147: 1723-1734
- Persson S, Paradez A, Carroll A, Palsdottir H, Doblin M, Poindexter P, Khitrov N, Auer M, Somerville CR (2007) Genetic evidence for three unique components in primary cell-wall cellulose synthase complexes in Arabidopsis. *Proc. Natl. Acad. Sci. USA* 104: 15566-15571
- Ramachandran S, Christensen HEM, Ishimaru Y, Dong C, Chao-Ming W, Cleary AL, Chua N (2000) Profilin plays a role in cell elongation, cell shape maintenance, and flowering in Arabidopsis. *Plant Physiol.* 124: 1637-1647.
- Roelofsen PA and Houwink AL (1953) Architecture and growth of the primary cell wall in some plant hairs and in the *Phycomyces* sporangiophore. *Acta Bot. Neer.* 2: 218.
- Roland JC, Vian B (1979) The wall of the growing plant cell: its three-dimensional organization. *Int. Rev. Cytol.* 61: 129-166.
- Rudolph U (1987) Occurrence of rosettes in the ER membrane of young *Funaria hygrometrica* protonemata. *Naturwissenschaften* 74: 439.
- Sampathkumar A, Lindeboom JJ, Debolt S, Gutierrez R, Ehrhardt DW, Ketelaar T, Persson S (2011) Live Cell Imaging Reveals Structural Associations between the Actin and Microtubule Cytoskeleton in Arabidopsis. *Plant Cell* 23: 2302-2313.
- Scheible WR, Eshed R, Richmond T, Delmer D, Somerville CR (2001) Modifications of cellulose synthase confer resistance to isoxaben and thiazolidinone herbicides in Arabidopsis *Ixr1* mutants. *PNAS* 98: 10079-10084.
- Sugimoto K, Williamson RE, Wasteneys GO (2000) New techniques enable comparative analysis of microtubule orientation, wall texture, and growth rate in intact roots of Arabidopsis. *Plant Physiol.* 124: 1493-1506
- Sugimoto K, Himmelspach R, Williamson RE, Wasteneys GO (2003) Mutation or Drug-Dependent Microtubule Disruption Causes Radial Swelling without Altering Parallel Cellulose Microfibril Deposition in Arabidopsis Root Cells. *Plant Cell* 15: 1414-1429.
- Sparkes IA, Teanby NA, Hawes C (2008) Truncated myosin XI tail fusions inhibit peroxisome, Golgi, and mitochondrial movement in tobacco leaf epidermal cells: a genetic tool for the next generation. *J. Exp. Botany* 59: 2499-2512.
- Tindemans SH, Hawkins RJ, Mulder BM (2010) Survival of the Aligned: Ordering of the Plant Cortical Microtubule Array. *Physical review letters* 104: 058103
- Thomas DDS, Lager NM, Manavathu EK (1973) Cytochalasin B: effects on root morphogenesis in *Allium cepa*. *Can. J. Botany* 51: 2269-2273.

- Uemura T, Ueda T, Ohniwa RL, Nakano A, Takeyasu K, Sato MH (2004) Systematic analysis of SNARE molecules in Arabidopsis: Dissection of the post-Golgi network in plant cells. *Cell structure and function* 29: 49-65.
- Wang J, Ding Y, Wang J, Hillmer S, Miao Y, Wan Lo S, Wang X, Robinson DG, Jianga L (2010) EXPO, an Exocyst-Positive Organelle Distinct from Multivesicular Endosomes and Autophagosomes, Mediates Cytosol to Cell Wall Exocytosis in Arabidopsis and Tobacco Cells. *Plant Cell* 22: 4009–4030
- Wasteneys GO (2004) Progress in understanding the role of microtubules in plant cells. *Current opinion in plant biology* 7: 651-660.
- Wei L, Zhang W, Liu Z, LiWei Y (2009) AtKinesin-13A is located on Golgi-associated vesicle and involved in vesicle formation/budding in Arabidopsis root-cap peripheral cells. *BMC Plant Biology* 2009, 9:138
- Wolters-Arts AMC and Sassen MMA (1991) Deposition and reorientation of cellulose microfibrils in elongating cells of *Petunia stular* tissue. *Planta* 185: 179-189.
- Wu X, Xiang X, Hammer JA (2006) Motor proteins at the microtubule plus-end. *TRENDS in Cell Biology* 16: 135-143
- Yamazaki T, Kawamura Y, Minami A, Uemura M (2008) Calcium-Dependent Freezing Tolerance in Arabidopsis Involves Membrane Resealing via Synaptotagmin SYT1. *Plant Cell* 20: 3389–3404.

Summaries and acknowledgements

Summary, samenvatting, dankwoord/acknowledgements

Summary

The shape and strength of plant cells is determined by a combination of turgor pressure and constraining cell wall. The main load bearing structures in the cell wall, cellulose microfibrils (CMFs), are deposited in highly organized textures. For more than 50 years scientists have tried to elucidate how the organized CMF textures are being generated and what role cortical microtubules (CMTs) play in CMF deposition. In 2006 Paredez et al. caused a breakthrough by live imaging of cellulose synthase (CESA) complexes that move along CMTs. However, the mechanism by which CMTs guide CESA complexes is still unknown at the moment of writing this thesis and many questions related to the CMF organization still are unanswered.

This thesis illuminates the mechanism behind the highly organized CMF textures. To analyze the positioning and patterning of CESA complexes in the cell we studied the following three aspects: (1) the distribution and delivery (close) to the plasma membrane of CESA complexes via Golgi bodies, (2) the distribution and movement of CESA complexes inside the plasma membrane while producing CMFs and finally (3) their product, the CMF texture of the cell wall. We chose epidermal root cells of *Arabidopsis thaliana* and compared cells of different growth stages.

Chapter 1 is an introduction into cellulose deposition and an outline of this thesis.

In chapter 2 the movement and distribution of Golgi bodies is studied in the cortex of cells of different growth stages, early elongation zone compared to late elongation zone, in relation to the configuration of the actin cytoskeleton. Golgi bodies in the cortex of cells in the early elongation zone, where growth accelerates to rapid growth, show slow random oriented movement, called wiggling. In the cortex of cells in the late elongation zone, where cell elongation ceases, they also show a second kind of motility, fast directed movement with velocities of up to $7 \mu\text{m}\cdot\text{s}^{-1}$, like in cytoplasmic strands in the same cells. The cortical areas where Golgi body movement is slow and random co-localize with fine F-actin, a configuration of single or thin bundles of filaments. On the other hand, areas where Golgi body movement is fast and

directed co-localize with thick actin filament bundles. When Golgi bodies enter an area with a different actin cytoskeleton configuration they change their type of motility concomitantly. We conclude that Golgi body dynamics correlate with the actin cytoskeleton organization.

CESA complexes are known to run in rows along CMTs in *Arabidopsis* hypocotyl cells. In chapter 3 we studied the orientation, density, alignment and movement of CMTs and CESA complexes using immunocytochemistry and live cell imaging. Furthermore we studied the orientation and density of the product of the CESA complexes, the CMFs, in the innermost wall layer with Field Emission Scanning Electron Microscopy (FESEM). The CMTs, the tracks of CESA complexes and the innermost CMFs lay in the same orientation, approximately transverse to the elongation axis in both the inner and outer periclinal cell face in the elongation zone and root hair zone, where cell elongation ceases. CESA complexes predominantly move in rows along CMTs in both directions. While the CMFs form a uniform cell wall layer, CESA complexes run one after the other along CMTs that are wider spread from each other than the CMFs and only few CESA complexes move in between the CMTs. To understand how CESA complexes can produce a uniform layer of CMFs, instead of local CMF thickenings, we studied whether the CMTs change position during CMF production. Time lapse movies of CMTs show that CMTs reposition over time, so that CESA complexes produce an even CMF layer. In this way we can understand how the density of CMFs in the nascent cell wall can be higher than that of the CMTs and the moving rows of CMFs in the plasma membrane. CMFs are deposited consecutively next to earlier deposited ones in the same orientation.

In chapter 4 we used several different electron microscopy techniques to visualize CMF texture: transmission Electron Microscopy (TEM) of ultrathin sections after mild or complete matrix extraction, TEM of surface preparations and FESEM of surface preparations. We used root hairs of three different species; *Arabidopsis thaliana*, *Medicago truncatula* and *Vicia sativa*. We compare and discuss the results of the techniques for the capacity to measure orientation, density, length and width of the CMFs. In ultrathin sections and surface preparations we observed that the three species studied have root

hairs with an axial/helical wall texture. Surface preparations are best suitable for density and orientation measurements of CMFs within the most inner cell wall layer. Ultrathin sections showed that the thickness of CMFs in *Arabidopsis* is approximately 3 nm, which indicates that these CMFs are produced by single CESA complexes.

Chapter 5 is a general discussion of our work in relation to the field. It describes the role of the actin cytoskeleton, Golgi body motility and CMTs in the deposition of an organized texture of CMFs.

Samenvatting

De vorm en de sterkte van plantencellen wordt bepaald door een combinatie van turgordruk en tegendruk van de celwand. De voornaamste krachtdragende structuren in de celwand, de cellulose microfibrillen (CMF), worden afgezet in zeer georganiseerde texturen. Al meer dan 50 jaar proberen wetenschappers op te helderen hoe de georganiseerde CMF-texturen gemaakt worden en welke rol corticale microtubuli (CMT) spelen bij CMF-afzetting. In 2006 zorgden Paredez et al. voor een doorbraak door het afbeelden van cellulose synthase (CESA) complexen die langs CMT bewegen in levende cellen. Het mechanisme waarmee CMT deze CESA-complexen leiden is echter nog steeds onbekend op het moment dat dit proefschrift wordt geschreven en veel vragen met betrekking tot de CMF-organisatie zijn nog onbeantwoord. Dit proefschrift belicht het mechanisme achter de georganiseerde CMF-texturen. Om de positionering en het patroon van CESA-complexen in de cel te analyseren hebben we de volgende drie aspecten bestudeerd: (1) de distributie en bezorging (vlakbij) de plasmamembraan van CESA-complexen via Golgi-lichaampjes, (2) de distributie en beweging van CESA-complexen in de plasmamembraan terwijl ze CMF produceren en tenslotte (3) hun product, de CMF-textuur van de celwand. We hebben wortelepidermiscellen gekozen van *Arabidopsis thaliana* en hebben cellen van verschillende groeistadia met elkaar vergeleken.

Hoofdstuk 1 is een introductie in aspecten van de cellulose-afzetting zoals beschreven in dit proefschrift.

In hoofdstuk 2 wordt de beweging en de distributie van Golgi-lichaampjes bestudeerd in de cortex van cellen van verschillende groeistadia, namelijk de vroege strekkingszone waar groei versnelt naar snelle groei en de late strekkingszone waar groei bijna stopt, in relatie tot de configuratie van het actinecytoskelet. Golgi-lichaampjes in de cortex van cellen in de vroege strekkingszone laten langzame willekeurig georiënteerde bewegingen zien, 'wiggling' genoemd. In de cortex van cellen in de late strekkingszone laten ze ook een tweede type beweging zien, snelle gerichte beweging met snelheden tot $7 \mu\text{m}\cdot\text{s}^{-1}$, zoals in cytoplasmadraden in dezelfde cellen. De corticale

gebieden waar de beweging van Golgi-lichaampjes langzaam en willekeurig is, overlapt met fijn F-actine, een configuratie van losse actinefilamenten en/of dunne bundels van filamenten. Anderzijds overlappen gebieden waar de beweging van Golgi-lichaampjes snel en gericht is met dikke bundels van actinefilamenten. Zodra Golgi-lichaampjes een gebied ingaan met een andere actinecytoskeletconfiguratie verandert hun type beweging overeenkomstig. We concluderen dat de dynamiek van Golgi-lichaampjes correleert met de organisatie van het actinecytoskelet.

Het is bekend dat CESA-complexen in rijen langs CMT bewegen in *Arabidopsis* hypocotylcellen. In hoofdstuk 3 bestuderen we de oriëntatie, dichtheid, opstelling en beweging van CMT en CESA-complexen in *Arabidopsis* wortelepidermiscellen door gebruik te maken van immunocytochemie en 'live cell imaging'. Verder hebben we de oriëntatie en dichtheid van het product van de CESA-complexen, de CMF, in de binnenste celwandlaag bestudeerd met 'Field Emission Scanning Electron Microscopy' (FESEM). De CMT, de banen van CESA-complexen en de binnenste CMF liggen in dezelfde oriëntatie, ongeveer dwars op de strekkingsas, aan zowel de binnen als de buitenzijde van de cel in de strekkingszone en in de wortelhaarzone, waar celgroei stopt. CESA-complexen bewegen voornamelijk in rijen in beide richtingen langs CMT. Terwijl de CMF een uniforme celwandlaag vormen, bewegen de CESA-complexen achter elkaar aan langs CMT die wijder verspreid liggen van elkaar dan de CMF en slechts een paar CESA-complexen bewegen tussen de CMT. Om te begrijpen hoe CESA-complexen een uniforme laag van CMF kunnen produceren in plaats van plaatselijke CMF-verdikkingen, bestudeerden we of the CMT hun positie veranderen tijdens CMF-productie. Tijd-verloop filmpjes van CMT laten zien dat CMT constant repositioneren, zodat CESA-complexen een vlakke CMF-laag produceren. Op deze manier wordt duidelijk hoe de dichtheid van CMF in de laatst gevormde celwandlaag hoger kan zijn dan die van de CMT en de rijen van bewegende CESA-complexen in de plasmamembraan. CMF worden opeenvolgend afgezet naast eerder afgezette CMF in dezelfde oriëntatie.

In hoofdstuk 4 hebben we verschillende electronen microscopische technieken gebruikt om de CMF textuur te visualiseren: Transmissie

Electronen Microscopie (TEM) van ultra-dunne coupes na milde of volledige matrix extractie, TEM van oppervlakte preparaties en FESEM van oppervlakte preparaties. We hebben wortelharen van drie verschillende soorten gebruikt; *Arabidopsis thaliana*, *Medicago truncatula* and *Vicia sativa*. We vergelijken en bediscussiëren de resultaten van de technieken met betrekking tot de capaciteit om oriëntatie, dichtheid, lengte en dikte van de CMF te meten. In ultra-dunne coupes en oppervlakte preparaties observeerden we dat de drie bestudeerde soorten wortelharen hebben met een axiale/helicale celwand textuur. Oppervlakte preparaties zijn het meest geschikt voor dichtheid en oriëntatie metingen van CMF in de binnenste celwand laag. Ultra-dunne coupes laten zien dat de dikte van CMF in *Arabidopsis* ongeveer 3 nm is, wat aangeeft dat deze CMF geproduceerd zijn door individuele CESA complexen.

Hoofdstuk 5 is een algemene discussie van ons werk in relatie tot het vakgebied. Het beschrijft de rol van het actine cytoskelet, van de beweging van Golgi-lichaampjes en van CMT in het afzetten van een georganiseerde textuur van CMF.

Dankwoord/acknowledgements

Allereerst wil ik Anne Mie Emons hartelijk bedanken voor de kans die ze mij gegeven heeft om als AIO dit onderzoek te doen, dat een essentieel fundamenteel vraagstuk behandelt in de Plantencelbiologie en dat op dit moment nog steeds zeer actueel is. Ik wil haar ook bedanken voor haar enthousiasme en vertrouwen in mij en voor de kans om dit proefschrift na vele jaren te kunnen volbrengen. Tijs Ketelaar wil ik graag bedanken voor zijn begeleiding, positieve aanmoedigingen en hulp met name bij het Golgi-actine werk en het CESA werk. Verder wil ik veel collega's bedanken voor hun bijdrage in discussies en hulp in het lab en achter de microscoop: Carolina Cifuentes, Bela Mulder, Michel Ebskamp, Jan Vos, Norbert de Ruijter, Björn Sieberer, Agnieska Esseling-Ozdoba, John Esseling, André van Lammeren, Peter Twumasi, Hannie van der Honing, Jelmer Lindeboom en daarbij ook voor hun bijdrage aan het cellulose microfibril werk: Tiny Franssen-Verheijen, Lianne den Hollander, Peter Immerzeel, Jan Schel, Adriaan van Aelst, voor haar bijdrage aan het CESA-CMT werk: Ying Zhang, en voor haar bijdrage aan het Golgi werk: Elysa Overdijk.

Herman Höfte en Stephanie Robert van het INRA in Versailles wil ik bedanken voor hun gastvrijheid en samenwerking tijdens mijn uitwisseling.

Mijn broers Marko en Wijnand, mijn zus Linda, vriendinnen Reina, Monique, Marije, Annemiek, Brenda en Ineke, en mijn schoonfamilie, heel hartelijk bedankt voor jullie belangstelling.

Mijn lieve ouders, Henk en Lucienne, veel dank voor jullie interesse, onuitputtelijke ondersteuning en vertrouwen.

Ten slotte mijn man Sijtze voor het altijd bereid zijn mee te denken en te helpen en voor de gelegenheid die je mij gegeven hebt om dit werk te kunnen afmaken. Onze kinderen Reinder, Mare en Ruurd voor hun belangstelling in wat mij bezig hield zo lang achter de computer, het prachtig uitspreken van het woord proefschrift en het blije dansje.

About the author

Curriculum vitae, list of publications, education statement

Curriculum vitae



Miriam Akkerman, geboren op 21 november 1973 te Amersfoort, behaalde in 1992 haar Gymnasium diploma aan het Gymnasium te Apeldoorn. Zij studeerde vervolgens ruim 2 jaar Industrieel Ontwerpen aan de Technische Universiteit Delft waar zij haar propedeuse en tweede jaars vakken behaalde. Vanuit haar belangstelling naar levende systemen startte ze eind 1994 met de studie Biologie aan de Wageningen Universiteit. Ze behaalde haar propedeuse cum laude en specialiseerde zich in de richting plantorganisme. Daarnaast deed ze vakken op de gebieden Bodemkunde, Vegetatietypen van Nederland, Biologische landbouw en Natuur en Milieu Educatie. Ze studeerde af in 1998. Aansluitend, in 1999, heeft ze bij het IVLOS aan de Universiteit Utrecht haar eerste graads lesbevoegdheid voor Biologie behaald. Tijdens haar studie gaf ze bijles, met name in scheikunde, aan scholieren en studenten. Na de leraaropleiding koos ze ervoor te gaan werken als onderzoeker, voor de uitdaging om nieuwe kennis te vinden en vraagstukken op te lossen. Vanwege haar interesse in het visueel-microscopisch volgen en analyseren van celbiologische processen begon ze in 2001 met het onderzoek beschreven in dit proefschrift bij de leerstoelgroep Plantencelbiologie van prof. dr. Anne Mie Emons. Naast het doen van onderzoek begeleidde ze met plezier studenten bij het vak Celbiologie. In de periode 2006 – 2009 kreeg ze drie kinderen. In 2012 promoveerde ze op dit onderzoek.

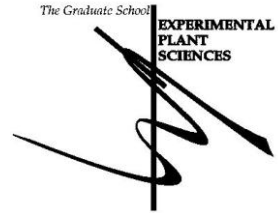
List of publications

Emons AMC, **Akkerman M**, Ebskamp MJM, Schel JHN, Mulder B (2007) How cellulose synthase density in the plasma membrane may dictate cell wall texture. In: Cellulose: Molecular and Structural Biology / Brown RM, Saxena IM, Dordrecht: Springer.

Akkerman M, Overdijk O, Schel JHN, Emons AMC, Ketelaar T (2011) Golgi body motility in the plant cell cortex correlates with actin cytoskeleton organization. *Plant and Cell Physiology* 52: 1844 - 1855.

Akkerman M, Franssen-Verheijen T, Immerzeel P, Den Hollander L, Schel JHN, Emons AMC (2012) Texture of Cellulose Microfibrils of Root Hair Cell Walls of *Arabidopsis thaliana*, *Medicago truncatula*, and *Vicia sativa*. *Journal of Microscopy*. doi: 10.1111/j.1365-2818.2012.03611.x.

Education Statement of the Graduate School Experimental Plant Sciences



Issued to: Miriam Akkerman
Date: 17 September 2012
Group: Plant Cell Biology, Wageningen University & Research Centre

1) Start-up phase	date
<ul style="list-style-type: none"> • First presentation of your project Planning and first results on Golgi body dynamics 	Feb 15, 2002
<ul style="list-style-type: none"> • Writing or rewriting a project proposal 	
<ul style="list-style-type: none"> • Writing a review or book chapter Emons AMC, Akkerman M, Ebskamp MJM, Schel JHN, Mulder B(2007) How cellulose synthase density in the plasma membrane may dictate cell wall texture. In: Cellulose: Molecular and Structural Biology. Bronw RM, Saxena IM. Dordrecht, Springer. 	2007
<ul style="list-style-type: none"> • MSc courses • Laboratory use of isotopes 	
<i>Subtotal Start-up phase</i>	<i>3,5 credits*</i>

2) Scientific Exposure	
<ul style="list-style-type: none"> • EPS PhD Student Days EPS PhD student day, Wageningen University EPS PhD student day, University Utrecht EPS PhD student day, Vrije Universiteit Amsterdam EPS PhD student day, Radboud University Nijmegen 	Jan 24, 2002 Mar 27, 2003 Jun 03, 2004 Jun 02, 2005
<ul style="list-style-type: none"> • EPS Theme Symposia Theme 1 symposium 'Developmental Biology of Plants', Wageningen Theme 1 symposium 'Developmental Biology of Plants', Leiden Theme 1 symposium 'Developmental Biology of Plants', Wageningen Theme 1 symposium 'Developmental Biology of Plants', Wageningen 	Feb 18, 2002 Feb 07, 2003 Feb 17, 2004 Apr 26, 2005
<ul style="list-style-type: none"> • NWO Lunteren days and other national Platforms NWO-ALW Lunteren meeting ALW/FOM/VvBBMT meeting on molecular and cellular biophysics, Lunteren NWO-ALW Lunteren meeting ALW/FOM/VvBBMT meeting on molecular and cellular biophysics, Lunteren NWO-ALW Lunteren meeting ALW/FOM/VvBBMT meeting on molecular and cellular biophysics, Lunteren NWO-ALW Lunteren meeting ALW/FOM/VvBBMT meeting on molecular and cellular biophysics, Lunteren 	Apr 15-16, 2002 Oct 07-08, 2002 Apr 07-08, 2003 Sept 29-30, 2003 Apr 05-06, 2004 Sept 27-28, 2004 Apr 04-05, 2005 Oct 10-11, 2005
<ul style="list-style-type: none"> • Seminars (series), workshops and symposia Seminars (Casper Vroemen, Molendijk, Geoff Wasteney, Herman Hofte, Patrick Hussey) Flying seminars (Chris Somerville, Mark Estelle) Seminars (Millar, Yang, J. Dangl, Dirk Bosch, Cytoskelet, Marileen Dogterom) Flying seminar Natasha Raikhel 	Feb-Dec 2002 May 28 & Oct 22, 2002 Jan-Dec, 2003 Sept 23, 2003

NVVM meeting, Papendal Arnhem	Dec 11-12, 2003
Workhop on molecular systems biology, Schoorl	Jan 20-21, 2004
Seminars (PCB, Jiri Friml, PCB)	Apr-Oct, 2004
Symposium systems biology	Nov 04, 2004
Seminars Maths & Plantcellbiology	2005
Seminars (I. Lichtscheidl, B. Mulder, DNA, H. Schiessel, M. Dogterom)	May-Nov, 2005
Cell biophysics meeting, AMC Amsterdam	May 28, 2005
Flying seminars (Joseph Ecker, Phil Benfey)	Oct 02 & 24, 2005
Seminars Mathematics and biochemical networks	Dec 02, 2005
• Seminar plus	
Natasha Raikhel	Sept 23, 2003
• International symposia and congresses	
COST meeting, Reims, France	May 30-Jun 02, 2002
RMS Botancial microscopy meeting, Lisbon, Portugal	Apr 12-17, 2003
COST meeting, Helsinki, Finland	Sep 04-06, 2003
RMS Botanical microscopy meeting, Wageningen	Apr 16-21, 2011
• Presentations	
Oral presentation at NVVM meting at Papendal, Arnhem	Dec 11-12, 2003
Oral presentation at EPS theme 1 symposium, Leiden	Feb 07, 2003
Oral presentation at Lunteren	Apr 07-08, 2003
Oral/poster presentation at COST meeting Helsinki	Sep 04-06, 2003
Oral presentation at Cell biophysics meeting, AMC Amsterdam	May 28, 2004
Poster at COST meeting Reims	May 30 – Jun 02, 2002
Poster at meeting on molecular and cellular biophysics, Lunteren	Oct 07-08, 2002
Poster at NWO-ALW Lunteren meeting	Apr 07-08, 2003
Poster at NWO-ALW Lunteren meeting	Apr 04-05, 2005
Poster at RMS Botanical microscopy meeting, Wageningen	Apr 16-21, 2011
• IAB interview	Jun 04, 2004
• Excursions	
Amolf Amsterdam	Jan 28, 2003
<u>EMSA University Utrecht, Tomography</u>	<u>Jul 26, 2002</u>
<i>Subtotal Scientific Exposure</i>	<i>27,6 credits*</i>

3) In-Depth Studies

• EPS courses or other PhD courses	
EMBO course Plant cell Biology, Wageningen	Jun 16-26, 2002
FEBS course Microspectroscopy: Monitoring Molecular Interactions and Reactions in Living Cells, Wageningen	Sep 30 – Oct 05, 2002
• Journal club	
Participation in literature discussion group at Plant Cell Biology	2002-2005
• Individual research training	
COST exchange to laboratory H. Hofte, INRA Versailles. Colaboration on cellulose synthesis.	Feb 16 – Mar 07, 2004
<i>Subtotal In-Depth Studies</i>	<i>7,8 credits*</i>

4) Personal development

• Skill training courses	
PhD course "Guide to digital scientific artwork", Wageningen	Apr 04-05, 2002
Course Endnote, library Wageningen	2003
Career perspectives Meyer&Meyard	Dec 2005 – Jan 2006

-
- **Organisation of PhD students day, course or conference**
 - **Membership of Board, Committee or PhD council**

<u>Membership of PhD council</u>	<u>2004-2005</u>
<i>Subtotal Personal Development</i>	<i>2,8 credits*</i>
TOTAL NUMBER OF CREDIT POINTS*	41,7

Herewith the graduate School declares that the PhD candidate has complied with the educational requirements set by the Educational Committee of EPS which comprises of a minimum total of 30 ECTS credits.

** A credit represents a normative study load of 28 hours of study.*

Cover: Section of a cryo-fixed *Arabidopsis thaliana* root immunolabeled with anti-CESA3. The picture shows Golgi bodies transporting CESA3 containing cellulose synthase complexes to the plasma membrane. (We thank H. Höfte for the CESA3 antibody.)

Print: GVO Ede